Biomolecular modeling

Marcus Elstner and Tomáš Kubař

Theoretical Chemical Biology, Karlsruhe Institute of Technology

(Dated: February 11, 2014)

Contents

I. MOLECULAR MECHANICS: A CLASSICAL DESCRIPTION OF MOLECULES

A. The conceptual and chemical basis

Chemical bonding is a genuinely quantum effect, which cannot be understood on the grounds of classical physics. However, the solution of the Schrödinger equation is numerically very expensive, and only small molecules can be treated quantum mechanically (up to ≈100 atoms). To be able to treat larger molecules, it is necessary to find further approximations.

Two fundamental simplifications often made in quantum chemistry are the so called Born-Oppenheimer approximation (BO) and the classical treatment of the nuclei. BO requires the electron motion to be much faster than the motion of the nuclei (atoms), so that the electrons follow instantaneously the motion of the nuclei (being somehow 'fixed' to the nuclei).[1] The other approximation is the neglect of nuclear quantum effects, like tunneling effects (hydrogen) or zero-point vibrations.

With these simplifications, we have the picture of N electrons moving in the electrostatic potential of M nuclei. Then, we have to solve the Schrödinger equation for these N electrons, which can be a formidable task. Or, vice versa, we have the M nuclei 'sitting' within the 'sea' of N electrons! What is a chemical bond in such a case? What causes the attraction between two nuclei? In many cases, we do *not* have a large electron delocalization, thus there is nothing like a sea of electrons (which is the case in a metal). In organic molecules, we have two electrons in every bonding orbital, and that is how covalent bonding is explained. The main idea behind the empirical models of chemical bond is that the strength of, say, a C–H bond mediated through the bonding orbitals is similar in *all* C–H bonds. In other words, we have a localized/local phenomenon to deal with.

So, how can we model a covalent bond? Is it possible to use simple springs to approximate a bond? Consider the molecules H_2, O_2 or N_2: If we model the interaction between two atoms with a harmonic spring with the energy $E(x)$ given as a function of the interatomic

[1] This means that the electrons never leave those orbitals that they have been 'assigned' to in the electronic ground state. But there are cases, when they 'leave' these ground state orbitals, e.g. in high-energy collisions of nuclei. The electrons are excited then – a process not treated within the BO framework.

distance x

$$E(x) = \frac{1}{2}k(x - x_0)^2 \tag{I.1}$$

then there are two parameters k and x_0. The values of these parameters may be derived from spectroscopic measurements (bond length and vibrational frequency).[2]

In equilibrium, the force between the atoms

$$F(x) = -\frac{\partial E(x)}{\partial x} = k(x - x_0) \tag{I.2}$$

vanishes for $x = x_0$, thus $x = x_0$ is the equilibrium geometry.

A diatomic molecule is a one-dimensional system, and thus it is equivalent to one particle with mass m connected to a spring with spring constant k.[3] The force on the particle is due to Hooke's law proportional to $x - x_0$, and using Newton's second law, we have

$$F = ma = m\frac{\mathrm{d}^2x}{\mathrm{d}t^2} = -k(x - x_0) \tag{I.3}$$

This ordinary differential equation has a solution

$$x(t) - x_0 = c_1 \cdot \sin\left[\sqrt{\frac{k}{m}}\,t\right] + c_2 \cdot \cos\left[\sqrt{\frac{k}{m}}\,t\right] \tag{I.4}$$

The comparison with the known equation for harmonic motion

$$x(t) = c \cdot \sin(\omega t) \tag{I.5}$$

provides the relation of the frequency with the force constant k and mass m:

$$\omega = \sqrt{\frac{k}{m}} \tag{I.6}$$

From another point of view, we obtain k directly from the second derivative of the energy:

$$k = \frac{\mathrm{d}^2E(x)}{\mathrm{d}x^2} \tag{I.7}$$

This will hold in more complex molecules as well: the second derivatives of the energy with respect to the atomic coordinates determine the frequencies of (harmonic) motion of the atoms in a molecule.

[2] In addition, there is also the information about the heat of formation. However, a harmonic spring does not allow the bond to dissociate, therefore this information cannot be used until a 'better' force field is used, like a Morse potential.

[3] The strict derivation introduces the reduced mass of the system.

Therefore, we can parametrize a simple force field from experiment, once we know the equilibrium distances and the vibrational frequencies. Alternatively, we can obtain these values from quantum-chemical calculations.

Does this mean that we can take a protein molecule and put springs between all the atoms? If yes, does every bond need different values of k and x_0, because every bond is in a different chemical environment? If this is the case, we would not obtain any benefit. The essence of empirical modeling of chemical bonding is that the number of necessary parameters is much smaller than the number of bonds. In other words, we will use several (not many) 'types' of chemical bonds with assigned parameters to represent any bond in our molecules.

In the other extreme, can we assign (for instance) each C–H bond the same k and x_0 value? It is not quite simple, but let us see:

1. Spectroscopy

Molecules consist of units/groups that have similar properties in every molecule. For instance, every C–H has a length of $r = 1.06$–1.11 Å and a vibrational frequency $\tilde{\nu} \approx 3100\ \mathrm{cm}^{-1}$, whatever its environment in the molecule is.

2. Thermochemistry

Molecular enthalpies of formation are approximately additive, so that:
$CH_4 \cong 4$ C–H
$C_2H_6 \cong 6$ C–H + C–C
This illustrates that the C–H potential looks like the Morse potential for every C–H unit in any chemical environment. The depth of the minimum is adjusted to fit the enthalpies of formation.

3. The concept of atom type

These points indicate that bonds between atoms can be modeled by universal potentials, if one tries to identify *atom types* in similar chemical environments (groups):

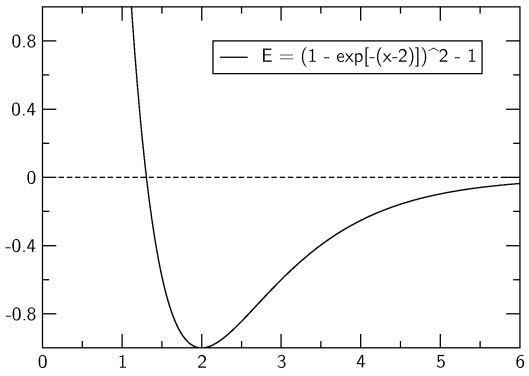

FIG. 1: Morse's potential

- Hybridization: clearly, an sp^3 carbon with four single bonds differs from an sp^2 carbon with a double bond or even an sp carbon with a triple bond. So, we need different potentials for the C–C, C=C and C≡C bonds. Also, there will be various different C atom types as well, like an aromatic carbon etc. Therefore, we introduce different carbons and determine the parameters (k, x_0) using some selected molecules which are typical for this chemical environment. For carbon, we use C_2H_6, C_2H_4, C_2H_2 and benzene to determine the parameters (k, x_0) for these four different carbons.

- A carbon atom bonded to an oxygen is electron deficient and this directly affects its bonding to other atoms. If we have a situation like in O=CH–C…, the C–C bond will be affected and it is thus desirable to introduce an additional C type – a carbonyl carbon, which uses different force constants for the adjacent C–C bond.

Biomolecular force fields typically use about 20 different C, 10 N and 5 O and H atom types.

4. Localization of the wavefunction

The quantum mechanical basis of these findings is that the electron wave function is localized. It can be localized in a bond, or localized on a fragment of a molecule. Such a fragments may constitute of functional groups or larger pieces like amino acids, DNA bases, sugars etc. The localization is crucial in at least two respects:

- Definition of the atom types: Electron delocalization can lead to different properties of the atomic fragments, like the different carbons in the carbonyl group, benzene etc.

- Electrostatic interactions. In the force fields, atomic charges are defined — i.e. every atom is assigned a point charge and interacts with other atoms according to Coulomb's law

$$E_{\mathrm{QQ}} \propto \frac{Q_1 Q_2}{R_{12}} \tag{I.8}$$

These charges have to be estimated carefully, and it is very helpful to use the rule of *group neutrality*: Every functional group or molecular fragment has an integer charge.

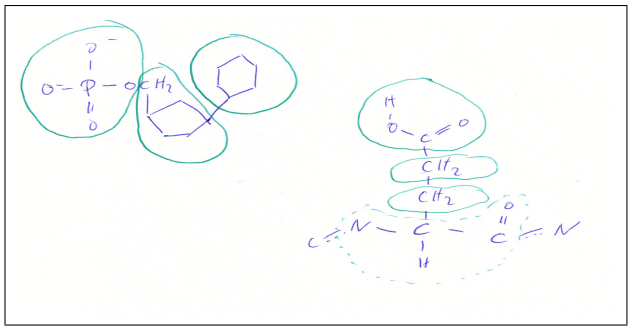

5. *Bonded and non-bonded interactions*

Then, there are two distinct types of interactions between atoms in an extended molecule:

- interactions mediated by, and resulting directly from the presence of a covalent bond between the atoms. We usually put springs between the atoms and have to care about bond and dihedral angles. With this treatment, we describe all the quantum-mechanical phenomena like exchange and correlation using an effective potential between two atoms (like discussed above for a diatomic molecule).

- classical Coulomb interactions and van der Waals (vdW) forces between atoms, which are both long-range. For bonded atoms, these interactions are already effectively treated through the bonded parameters. These interactions are thus excluded between atoms which are neighbors (up to the fourth neighbor).[4]

[4] Usually, the non-bonded interaction between an atom and its third neighbor, so called 1–4 interaction, is taken into account but scaled down by a multiplicative ('fudge') factor.

B. Determination of the non-bonding parameters: Coulomb and vdW forces

The Coulomb interaction consists of three contributions: the nucleus–nucleus repulsion

$$\frac{1}{2}\sum_{ij}\frac{Z_i \cdot Z_j}{R_{ij}} \tag{I.9}$$

the nucleus–electron attraction,

$$-\sum_{i}\int\frac{Z_i \cdot \rho(r)}{|R_i - r|}\mathrm{d}r \rightarrow -\sum_{ij}\frac{Z_i \cdot Q_j}{R_{ij}} \tag{I.10}$$

(the electron charge density $\rho(r) \rightarrow \sum_j Q_j$ is approximated by the sum of atomic point charges Q_j),
and the classical (Hartree) electron–electron interaction term is approximated as interaction of point charges sitting on the atoms

$$\frac{1}{2}\iint\frac{\rho(r)\cdot\rho(r')}{|r-r'|} \rightarrow \frac{1}{2}\sum_{ij}\frac{Q_i \cdot Q_j}{R_{ij}} \tag{I.11}$$

If we define an *effective atomic net charge* as $q_i = -Q_i + Z_i$, we can write the total Coulomb energy as:

$$E_{QQ} = \frac{1}{2}\sum_{ij}\frac{q_i \cdot q_j}{R_{ij}} \tag{I.12}$$

Thus, we have to determine the effective atomic charge for every atom type (or atom).[5] This may be conveniently done by performing quantum-chemical calculations. Making use of the localization of the wave function, we can calculate the typical molecular fragments and try to determine the charges from there. These fragments are individual amino acid residues for proteins and the bases (e.g. uracil in Fig. 2), sugars and phosphates for DNA. In the uracil example, we can see that there are three different hydrogen atom types, one nitrogen, one oxygen and two carbons. However, there are two issues associated with this procedure:

First, atomic charges are difficult to define at all; there are several schemes to calculate them and it might be difficult to judge which is the best. Nowadays, Mulliken charges are no longer used because their drawbacks have become evident. A popular strategy is to use the

[5] The term 'atom type' is used with respect to bonded and vdW interaction. Usually, the atomic charges must be determined for more specifically defined atoms.

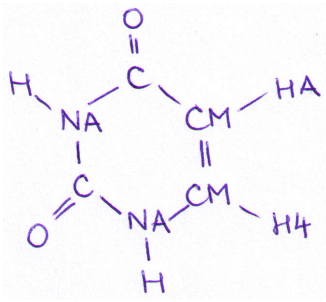

FIG. 2:

so-called *potential-derived charges*. Here, one calculates the *electrostatic potential* (ESP) of the molecule at its surface (see Fig. 3) and then fits the atomic charges in order to reproduce ESP for a set of points one the surface. The fitting constitutes in minimizing the error R:

$$R = \sum_i (\phi_i - \phi_i^0)^2 \tag{I.13}$$

with ϕ_i being ESP induced by the system of point charges at the reference point i and ϕ_i^0 being the ESP obtained previously in the quantum-chemical calculation.

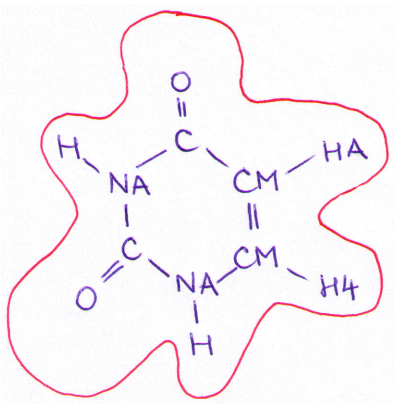

FIG. 3:

Second, charges are calculated in the gas phase (i.e. for an isolated molecule), while the electrostatic situation in an aqueous solution is different — molecules are more polar. As an example, the water molecule has a dipole of about 1.8 D in the gas phase, while it is about 2.4 D in solution. To account for that, charges may be taken to be larger than the gas phase values. A widely used strategy has been to use a small basis sets in the QM calculations, as it is known that such calculations overestimate molecular dipole moments.

These force fields use static atomic charges and, therefore, neglect the effects of polarization and charge transfer between the atoms. Presently, *polarizable force fields* are becoming more and more popular. Here, *atomic polarizability* α_i is assigned to every atom i. In a linear response approach, an external electric field induces a dipole at the atom:

$$\overrightarrow{\mu_i} = \overleftrightarrow{\alpha_i} \cdot \overrightarrow{E} \tag{I.14}$$

Of course, the external electric field is generated by all other atoms present in the system. This phenomenon will be discussed later on.

A further important non-bonded contribution is the repulsion driven by Pauli exclusion principle. In contrast to the classical Coulomb interaction, it is of a purely quantum-mechanical origin. Two electrons with same spin try to avoid a large spatial overlap. A typical example is the interaction of two neutral, closed-shell systems like two He atoms.[6] If the electron densities of both He atoms start to overlap as in Fig. 4, the Pauli repulsion sets in. This interaction is an *exchange effect* and decays exponentially with the spatial overlap. Despite its pure quantum-mechanical character, we can model this effect conveniently by an exponential term

$$E_{\text{ex}} \propto \exp\left[-a \cdot R_{ij}\right] \tag{I.15}$$

The exponential function is not quite computationally efficient, and most empirical force fields use a R^{-12} decay.

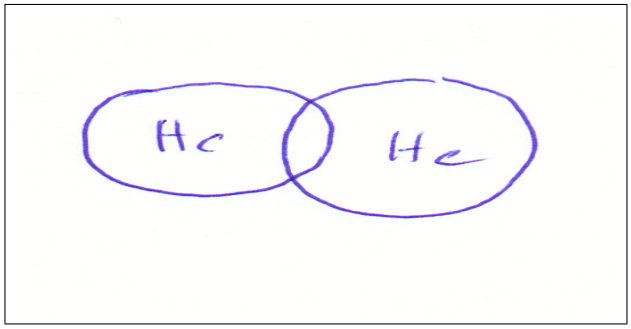

FIG. 4:

The Pauli repulsion relates to the motion of electrons with the same spin, on short intermolecular distances. In addition, we also have a correlation of electrons irrespective

[6] ... being the crudest approximation of two benzene molecules :-)

of their spin, which is retained on longer distances. Two electrons repel each other due to the Coulomb interaction, trying to move away from each other. Consider now two atomic fragments with no overlap as in Fig. 5. Due to the zero-point energy, no quantum particle is ever at rest. If an electron in the neutral fragment A fluctuates in such a way that it creates a dipole in A, then this dipole will induce another dipole in the opposite direction in the fragment B. Thus, the fluctuations of dipoles will be correlated due to the Coulomb interaction. This correlated fluctuation of dipoles in the two fragments leads to an effective

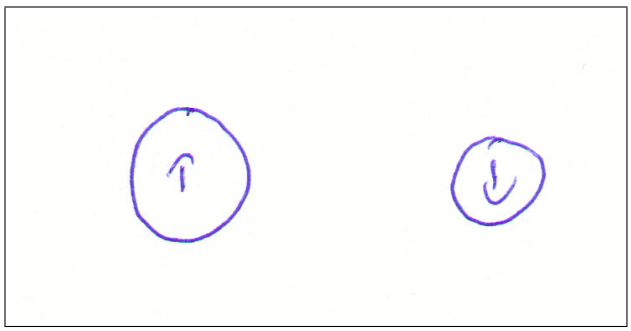

FIG. 5:

attractive interaction of the fragments, because of the opposite orientation of the interacting dipoles.[7]

A simple model in Fig. 6 describes this qualitatively. Two systems of one negative and one positive charge each are connected with a spring at a distance r. The negative and positive charge in every pair can be separated by z_1 and z_2, if some force acts on them. The complex system has a force constant k and (reduced) mass m with $\omega = \sqrt{k/m}$. The separation of charges in small systems brings on dipole moments of $\mu_1 = z_1 q$ and $\mu_2 = z_2 q$. The Schrödinger equation for one oscillator

[7] This effect is not described at the Hartree–Fock level of quantum chemistry, and is also missing in density-functional theory. MP2 or CI would cover it.

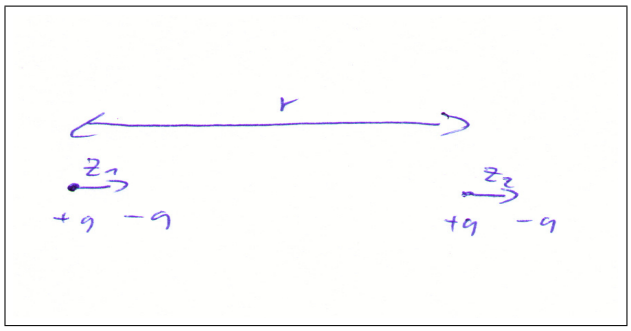

FIG. 6:

$$-\frac{\hbar^2}{2m}\nabla_1^2\psi + \frac{1}{2}kz_1^2\psi = E\psi \tag{I.16}$$

has a zero-point solution

$$E = \frac{1}{2}\hbar\omega \tag{I.17}$$

Let us couple the oscillators with the dipole–dipole interaction:

$$V(r) = -\frac{1}{4\pi\varepsilon_0}\frac{2\mu_1\mu_2}{r^3} \tag{I.18}$$

Inserting $V(r)$ into the Schrödinger equation of the large system, we find

$$E(r) = \frac{1}{2}\hbar\omega\left(2 - \frac{1}{4\pi\varepsilon_0}\frac{q^4}{k^2r^6}\right) \tag{I.19}$$

Now, the force on a point charge may be related to (i) its magnitude q and the intensity of electric field E, and (ii) the displacement z, giving the below equality:

$$\begin{aligned} F &= qE \\ F &= kz \\ z &= qE/k \end{aligned} \tag{I.20}$$

So, two relations for the induced dipole moment of such an oscillator in the electric field E are available, making it possible to eliminate μ_{ind}:

$$\mu_{\text{ind}} = qz = q^2E/k \tag{I.21}$$

$$\mu_{\text{ind}} = \alpha E \tag{I.22}$$

$$\alpha = q^2/k \tag{I.23}$$

Therefore, relation I.19 may be rearranged to

$$E(r) - \hbar\omega = -\frac{1}{2}\hbar\omega \cdot \frac{1}{(4\pi\varepsilon_0)^2}\frac{\alpha^2}{r^6} \tag{I.24}$$

This is the well-known expression for the dispersive interaction, which is attractive with the dependence of R^{-6} and dependent on the polarizabilities of the interaction partners.

The most common function which combines the Pauli repulsion and the dispersive interaction is the Lennard-Jones 12-6 potential

$$V(r) = 4\varepsilon\left(\left(\frac{\sigma}{r}\right)^{12} - \left(\frac{\sigma}{r}\right)^{6}\right) \tag{I.25}$$

which is shown in Fig. 7. The minimum lies at $r_m = 2^{1/6}\sigma$ and the well depth is $-\varepsilon$, and σ and ε are treated as empirical parameters.

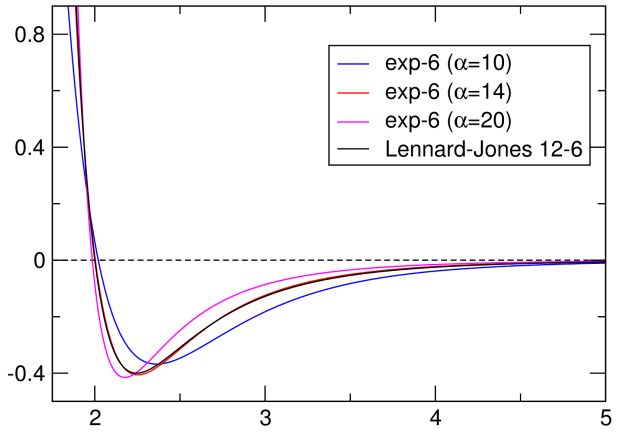

FIG. 7: The Lennard-Jones potential with $\varepsilon = 0.4$ and $\sigma = 2$, and several similar exp-6 potentials with various values of α.

The R^{-12}-component of LJ potential may be inappropriate for some applications, so that another function should be used to describe the repulsive component. Exponential function is such an alternative, giving together with the R^{-6}-term the so-called exp-6 potential:

$$V(r) = \frac{\varepsilon}{1 - 6/\alpha} \cdot \left(\frac{6}{\alpha} \cdot \exp\left[\alpha\left(1 - \frac{r}{\sigma}\right)\right] - \left(\frac{\sigma}{r}\right)^{6}\right) \tag{I.26}$$

where the parameter α controls the steepness of the repulsive component.[8] The exp-6

[8] Note that unlike the LJ potential, this function does not grow without bound when approaching $r = 0$ from the positive side. Rather, it passes a maximum at a certain distance r_0; however, this numerical problem occurs only at quite short distances that cannot normaly be reached in simulations of realistic molecular systems. Still, the definition of the function may be modified to $V(r) = +\infty$ for $r < r_0$, to correct for this undesired behavior.

potential has been used in studies of phase transitions like freezing; the LJ potential has been notorious for failing to describe phase transitions.

To find the vdW parameters for heteronuclear interactions, several 'mixing rules' have been proposed, the simplest being:

$$\begin{aligned} \sigma_{\mathrm{AB}} &= \frac{\sigma_{\mathrm{AA}} + \sigma_{\mathrm{BB}}}{2} \\ \varepsilon_{\mathrm{AB}} &= \sqrt{\varepsilon_{\mathrm{AA}} \cdot \varepsilon_{\mathrm{BB}}} \end{aligned} \tag{I.27}$$

To find a good set of non-bonded parameters is a challenging task, and force fields are constantly being improved, meaning that new sets of parameters are proposed. A crucial test and calibration of a force field is the density and the heat of vaporization of organic liquids, since these properites depend critically on the magnitude of non-bonded parameters — the charges and vdW parameters.

C. Hydrogen bonding

Early force fields contained special potentials to describe hydrogen bonding. Hydrogen bond is the attractive interaction between a hydrogen atom and an electronegative atom like oxygen or nitrogen. The hydrogen must be covalently bonded to another electronegative atom, so that this covalent bond is polarized and the hydrogen bears a partial positive charge. A typical example is the hydrogen bond between two water molecules in Fig. 8 left. Typical binding energies are around 20 kJ/mol but may reach higher values if the binding partners are strongly polarized or even charged, or if there are several hydrogen bonds between them, like in the GC base pair in DNA, see Fig. 8 right.

FIG. 8: Water dimer (left) and the guanine:cytosine nucleobase pair (right).

Clearly, Coulomb interaction is the dominant contribution to the hydrogen bond, but vdW interaction can become important also, especially in weakly bound systems. It has

been shown that they become crucial especially to describe the angular dependence of the interaction energy in complexes like $H_2CO \ldots H_2O$ and similar.

Thus, force fields have everything in place to describe these phenomena (Coulomb and vdW terms), and most modern force fields do not require a special treatment for this bonding type. However, a third contribution, the *charge transfer* (Fig. 9), is not captured by force fields at all. It may be included in the other terms in an effective way.

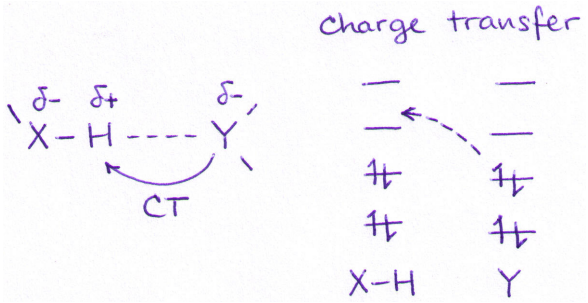

FIG. 9: Charge transfer between the charge donor (Y) and acceptor(X–H).

D. Determination of the bonded parameters: harmonic springs

1. *Bonds*

A bond dissociation curve typically looks like that in Fig. 1, and is well reproduced by the Morse potential with the functional form

$$E(r) = D\left(1 - \exp\left[-\alpha(r - r_0)\right]\right)^2 \tag{I.28}$$

In principle, the Morse potential allows for a quite good representation of the potential, in a broad range of distances. However, it is computationally quite inefficient, because of the presence of the exponential, and the Morse potential is rarely used in molecular mechanics studies.

A way to approximate virtually any function is to apply the Taylor expansion

$$E(r) = E(r_0) + \frac{\mathrm{d}E}{\mathrm{d}r}(r_0) \cdot (r - r_0) + \frac{1}{2}\frac{\mathrm{d}^2E}{\mathrm{d}r^2}(r_0) \cdot (r - r_0)^2 + \ldots \tag{I.29}$$

Most force fields use a harmonic approximation, i.e. the Taylor expansion cut after the second-order term. $E(r_0)$ is a constant which we set to zero, and the first derivative $\frac{\mathrm{d}E}{\mathrm{d}r}(r_0)$

vanishes if the function has a minimum in r_0. Therefore, with the definition of the force constant k we have, in the second order:

$$E(r) = \frac{1}{2}k(r - r_0)^2 \tag{I.30}$$

We can immediately see in Fig. 10 that the approximation of the true potential with a quadratic function is quite crude and holds only in a quite narrow interval of distances around the minimum. Importantly, the vibrations of covalent bonds exhibit quite a small magnitude (of several tenths of ångström) and so we actually never need to describe the potential beyond this narrow interval.[9] The application of harmonic approximation is then justified. To parametrize such a force field, we need two parameters per bond: the force constant k and the equilibrium distance r_0.

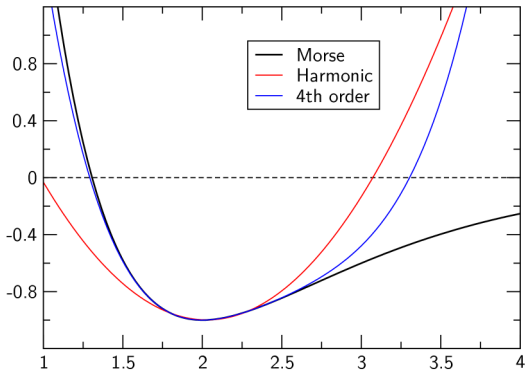

FIG. 10: Comparison of the harmonic and quartic functions with the Morse potential

To be able to compute accurate vibration frequencies, terms up to fourth order can be important to describe the curvature of the potential energy dependence; Fig. 10 compares the Morse potential with the harmonic and fourth-order functions. Also, the quartic function approximates the Morse potential a wider interval of distances.

2. Angles

As for the bonds, we apply a harmonic approximation for the angle deformation and get the potential

$$E_{\text{bend}}(\vartheta) = \frac{1}{2}k_\vartheta(\vartheta - \vartheta_0)^2 \tag{I.31}$$

[9] of course, if we do not aim at studying chemical reactions, i.e. having covalent bonds created of broken

Again, we can obtain the parameters from experiment. For instance, let us consider a

water molecule, which has an equilibrium bond angle of $\vartheta_0 = 104°$ and a bending vibration frequency of about 1700 cm^{-1}.

3. Dihedrals

Dihedral angles describe the rotation around covalent bonds. Four atoms are needed to define this angle (ω):

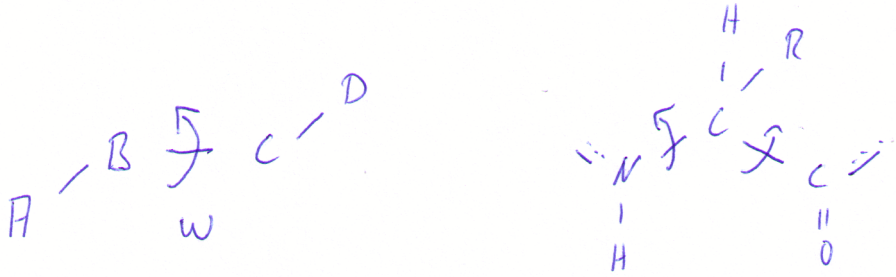

Clearly, the dependence of potential energy on the dihedral angle will be described with a periodic function, and a usual way to express this is a sum of several cosine functions:

$$E(\omega) = \sum_{n=1,2,3,4,6} V_n \cos\left[n \cdot \omega - \gamma_n\right] \tag{I.32}$$

with V_n being the height of the torsional barrier, n giving the periodicity ($n = 1$: 360°, $n = 2$: 180°, $n = 3$: 120°) and phase offsets γ_n.

Now, consider the C–C single and the C=C double bonds as examples. The single bond has a periodicity of 120°, i.e. we have three minima for one full rotation of 360°, and the potential energy is described as

$$E_{\mathrm{C-C}}(\omega) = V \cdot \cos 3\omega \tag{I.33}$$

The C=C double bond has a 180°-periodicity and thus only two minima for the full rotation. The energy is given by

$$E_{\mathrm{C=C}}(\omega) = V \cdot \cos\left[2\omega - 90°\right] \tag{I.34}$$

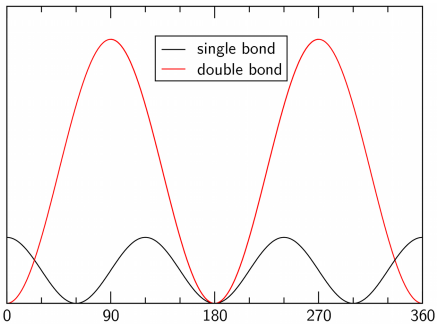

E. The complete equation

Adding up all contributions, the total energy of a typical biomolecular force field reads

$$\begin{aligned} E(R^N) \;=\; & \frac{1}{2}\sum_i k_i(r_i - r_i^0)^2 + \frac{1}{2}\sum_j k_j^\vartheta(\vartheta_j - \vartheta_j^0)^2 + \frac{1}{2}\sum_n V_n \cdot \cos\left[n\omega - \gamma_n\right] \\ & + \sum_i^N \sum_{j=i+1}^N \left\{ 4\varepsilon_{ij}\left(\left(\frac{\sigma_{ij}}{r_{ij}}\right)^{12} - \left(\frac{\sigma_{ij}}{r_{ij}}\right)^{6}\right) + \frac{1}{4\pi\varepsilon_0}\frac{q_i q_j}{r_{ij}} \right\} \end{aligned} \tag{I.35}$$

F. Exercises

1. Show for the Lennard-Jones potential (Eq. I.25) that the minimum is at $r_m = 2^{1/6}\sigma$ and the well depth is $-\varepsilon$.

2. Calculate the first and second derivative of the general force field (Eq. I.35). Only the terms dependent on r_i and r_{ij} are required.

II. GEOMETRY OPTIMIZATION AND NORMAL MODES OF VIBRATION

Consider again a diatomic molecule. The total force-field energy

$$E(x) = \frac{1}{2}k(x - x_0)^2 \tag{II.1}$$

is positive if the distance between the atoms x does not equal the reference bond length x_0.

Consider the case, that we obtain the dimer in a geometry with the bond distance of $x_1 \neq x_0$. Now, how can we determine the optimal geometry in that case, i.e. the geometry (distance) with the lowest energy? We calculate the force F acting upon both atoms, as the negative of the gradient g of energy:

$$F(x) = -g(x) = -\frac{\partial E(x)}{\partial x} = -k(x - x_0) \tag{II.2}$$

To approach towards the minimum, we calculate the force at the actual distance x_1

$$F(x_1) = -k(x_1 - x_0) \tag{II.3}$$

If we move the atoms in direction of the force until the force is zero, we will reach a stationary point.

Once there, we have to check if it is indeed a minimum (and not a saddle point, for instance). We can do this by evaluating the second derivative

$$k = \frac{\partial^2 E(x)}{\partial x^2} \tag{II.4}$$

If this is positive (corresponding to a real vibrational frequency $\omega = \sqrt{k/m}$), then we are in a minimum. Otherwise, the frequency is imaginary and the coordinates correspond to a saddle point on the potential energy surface (which cannot happen with just one harmonic potential). The second derivative of energy describes the curvature of the potential energy function and is directly related to the vibrational frequency.

This procedure is what we call *energy minimization* or *geometry optimization.*

Generally, our energy function depends on $3N$ atomic coordinates (x, y, z for each of N atoms). It is convenient to write all the coordinates in one vector

$$\vec{r} = (x_1, y_1, z_1, x_2, \ldots z_N) \tag{II.5}$$

In three dimensions (corresponding to one atom), the gradient reads[10]

$$\vec{g} = \nabla E(\vec{r}) = \left(\frac{\partial E}{\partial x}, \frac{\partial E}{\partial y}, \frac{\partial E}{\partial z} \right) \tag{II.6}$$

For N atoms, $\vec{g}$ and $\vec{F}$ are $3N$-dimensional vectors:

$$\vec{g} = \left(\frac{\partial E}{\partial x_1}, \frac{\partial E}{\partial y_1}, \frac{\partial E}{\partial z_1}, \frac{\partial E}{\partial x_2}, \dots \frac{\partial E}{\partial z_N}, \right) \tag{II.7}$$

The unit vector in the direction of the gradient is given by

$$\vec{e} = \frac{\vec{g}}{|\vec{g}|} \tag{II.8}$$

A. Steepest-descent minimization (SD)

Within the method of steepest descent, the optimizer moves *iteratively* – in steps $\vec{h}$ along the direction of the force

$$\vec{h} = \alpha \cdot \vec{e} \tag{II.9}$$

The critical point here is the choice of the step size α. If the step is too long, we follow the gradient down the potential though but may miss the minimum along the gradient and go up the valley on the opposite side. If the step is too short, we may need to perform too many steps, which in turn means too many (costly) evaluations of energy and forces.

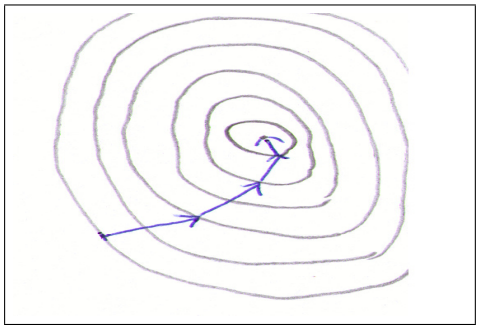

FIG. 11: Steepest descent minimization

One way to overcome this problem is to perform a *line search* along the direction $\vec{e}$, and find a minimum on this line. In other words, we are looking for a value of α_k such that r_{k+1}

[10] using *nabla* — the formal vector of partial derivatives $\nabla \equiv \left(\frac{\partial}{\partial x}, \frac{\partial}{\partial y}, \frac{\partial}{\partial z} \right)$

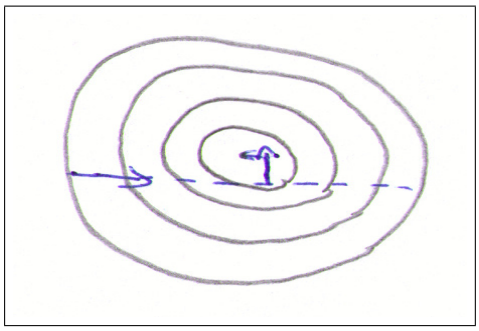

FIG. 12: Line search

is the minimum along the search direction e_k:

$$\vec{r}_{k+1} = \vec{r}_k + \alpha_k \vec{e}_k \tag{II.10}$$

The interesting and important point is that two successive search directions (steps) are *orthogonal* to each other:

$$\vec{h}_{k-1} \cdot \vec{h}_k = 0 \tag{II.11}$$

A problem may arise if the energy function forms a narrow valley. In such a case, the second next search direction will be similar. Therefore, an efficient strategy attempts to avoid this double work and looks for search directions that are orthogonal to *all* previous ones.

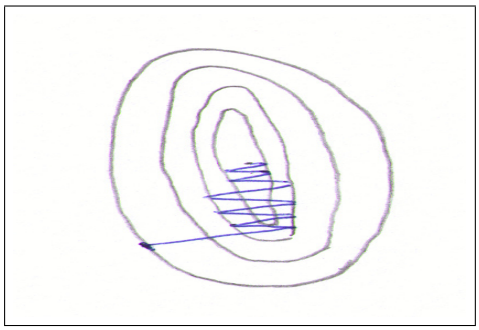

FIG. 13: Problem of SD in a narrow valley

B. Conjugate gradient minimization

Consider the Taylor series of a $3N$-dimensional function up to the second order:

$$\begin{aligned} E(\vec{r}) &= E(\vec{o}) + \sum_i \frac{\partial E}{\partial r_i}(\vec{o}) \cdot r_i + \frac{1}{2} \sum_{ij} \frac{\partial^2 E}{\partial r_i \partial r_j}(\vec{o}) \cdot r_i r_j \\ &= c - \vec{b} \cdot \vec{r} + \frac{1}{2} \cdot \vec{r} \cdot \mathbf{A} \cdot \vec{r} \end{aligned} \tag{II.12}$$

with the constants c, $\vec{b}$ and $\mathbf{A}$ given as

$$c = E(\vec{o}), \qquad \vec{b} = -\nabla E(\vec{o}), \qquad \mathbf{A}_{ij} = \frac{\partial^2 E}{\partial x_i \partial x_j}(\vec{o}) \tag{II.13}$$

If we express the derivative of E in a point $\vec{r}$, we obtain

$$\nabla E(\vec{r}) = \mathbf{A} \cdot \vec{r} - \vec{b} \tag{II.14}$$

To minimize the function E now means to find the point $\vec{r}_{min}$ where the derivative vanishes: $\nabla E(\vec{r}_{min}) = 0$. This task corresponds to the solution of this set of linear equations:

$$\mathbf{A} \cdot \vec{r} = \vec{b} \tag{II.15}$$

To do this, we could calculate the first ($\vec{b}$) and second ($\mathbf{A}$ – Hessian) energy derivative and solve the set of equations.

With that, we would directly obtain the minimum $\vec{r}_{min}$, but

- To evaluate the second derivatives is computationally very expensive. If possible, we try to avoid such a calculation whenever we can (to calculate the gradient, we need $3N$ derivatives, while for the Hessian we need $(3N)^2$).
- Usually, the potentials of interest are not simple harmonic potentials, i.e. we only make a *local* harmonic approximation. Thus, the obtained solution $\vec{r}_{min}$ is not the minimum we are looking for, but only a step towards the true minimum. Practically, we would have to perform such calculations iteratively, which would become very time-consuming.

Therefore, we look for methods which use information in the form of gradients *only*. As we have seen on the example of the SD method, successive gradients can have similar directions, which leads to a lot of double work. The conjugate gradient method constructs successive search directions, which are conjugate to each other in a certain way.

Practically, we perform the first step $\vec{h}_1$ along the gradient $\vec{g}$:

$$\vec{h}_1 = -\vec{g}_1 \tag{II.16}$$

The second step should be 'conjugate' to the first step, i.e. it should not go in the same direction.

Now, how does the gradient of E change if we move along a certain direction $\vec{h}_k$? Let us consider two successive steps k and $k+1$. We have:

$$\begin{aligned} \vec{g}_k &= \mathbf{A} \cdot \vec{r}_k - \vec{b} \\ \vec{g}_{k+1} &= \mathbf{A} \cdot \vec{r}_{k+1} - \vec{b} \\ \vec{g}_{k+1} - \vec{g}_k &= \mathbf{A} \cdot (\vec{r}_{k+1} - \vec{r}_k) \end{aligned} \tag{II.17}$$

This means that going along the search direction $\vec{h}_k = -\vec{g}_k$, we obtain the change of the gradient $\Delta_k \vec{g} = \vec{g}_{k+1} - \vec{g}_k$. This is the effect of the search direction $-\vec{g}_k$. Now, when moving along the next search direction $\vec{h}_{k+1}$, we do not want to lose the fruit of the work done so far, i.e. we wish to keep the change of gradient that has already been made ($\Delta_k \vec{g}$). Therefore, the gradient shall remain *orthogonal*[11] to $\vec{h}_k$. This can be achieved if the change of gradient along $\vec{h}_{k+1}$ is orthogonal to $\vec{h}_k$:

$$\begin{aligned} \vec{h}_k \cdot \Delta_{k+1} \vec{g} &= 0 \\ \vec{h}_k \cdot (\vec{g}_{k+2} - \vec{g}_{k+1}) &= \vec{h}_k \cdot \mathbf{A} \cdot (\vec{r}_{k+2} - \vec{r}_{k+1}) = \vec{h}_k \cdot \mathbf{A} \cdot \vec{h}_{k+1} = 0 \end{aligned} \tag{II.18}$$

This condition is a generalization of the concept of orthogonality, and the two vectors $\vec{h}_{k+1}$ and $\vec{h}_k$ are denoted as *conjugate* (with respect to $\mathbf{A}$). They are orthogonal if the matrix $\mathbf{A}$ is a unit matrix.

Now, we want to perform sequential steps as with the line search algorithm,

$$\begin{aligned} \vec{r}_{k+1} &= \vec{r}_k - \alpha_k \cdot \vec{g}_k \\ \mathbf{A} \cdot (\vec{r}_{k+1} - \vec{r}_k) &= -\alpha_k \cdot \mathbf{A} \cdot \vec{g}_k = \vec{g}_{k+1} - \vec{g}_k \end{aligned} \tag{II.19}$$

If we choose α_k such that $\vec{r}_{k+1}$ is the minimum along the search direction $\vec{g}_k$, we know that the two successive gradients are orthogonal. We can multiply the last equation with $\vec{g}_k$ to get:

$$\alpha_k = \frac{\vec{g}_k \cdot \vec{g}_k}{\vec{g}_k \cdot \mathbf{A} \cdot \vec{g}_k} \tag{II.20}$$

This equation assures the orthogonality of $\vec{g}_k$ and $\vec{g}_{k+1}$, so that every search direction is orthogonal to the previous one, and determines the step size. For that, we need the gradient and the Hessian.

[11] or *perpendicular* in our simple 2D drawings

However, the calculation of the Hessian is often too costly, and the step should thus be determined in another way. Several algorithms to do so have been developed, and we will briefly describe the Fletcher–Reeves method here: The new search direction at $\vec{r}_{k+1}$ is calculated as (without proof)

$$\vec{h}_{k+1} = -\vec{g}_{k+1} + \gamma_k \cdot \vec{h}_k \tag{II.21}$$

with

$$\gamma_k = \frac{\vec{g}_{k+1} \cdot \vec{g}_{k+1}}{\vec{g}_k \cdot \vec{g}_k} \tag{II.22}$$

assuring

$$\begin{aligned} \vec{g}_k \cdot \vec{g}_l &= 0 \\ \vec{g}_k \cdot \vec{h}_l &= 0 \\ \vec{h}_k \cdot \mathbf{A} \cdot \vec{h}_l &= 0 \end{aligned} \tag{II.23}$$

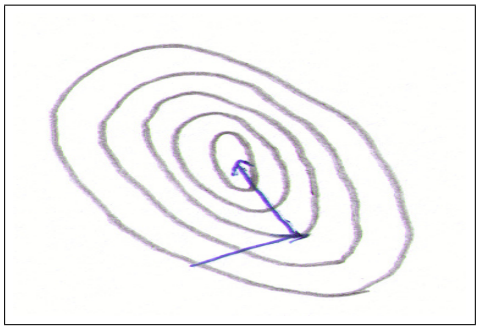

FIG. 14: Conjugate gradients

- This has to be compared with the steepest descent method. In SD, the search directions $-\vec{g}_{k+1}$ and $-\vec{g}_k$ are generally not orthogonal to each other, which can lead to the case that successive steps spoil the efforts of each other. The conjugate-gradient directions $\vec{h}_k$ are not constructed to be orthogonal, either; however, it is their property of being conjugate ($\vec{h}_k \cdot \mathbf{A} \cdot \vec{h}_l = 0$) that increases the efficiency of the minimization significantly.

- In principle, CG determines the minimum of a N-dimensional quadratic potential in N steps. Every vector in an N-dimensional space can be constructed from N basis vectors. In many cases, these are chosen to be orthogonal. It can be shown, that the

vectors $\vec{h}_k$ form a linearly independent set of vectors, and so they represent an optimal set of search directions to find the minimum in N steps. The vector determining the path from the initial point $\vec{r}_1$ to the minimum $\vec{r}^*$ can then be written as

$$\vec{r}^* - \vec{r}_1 = \sum_k \alpha_k \cdot \vec{h}_k \tag{II.24}$$

C. Hessian-update based methods: Newton–Raphson and quasi-Newton–Raphson

Now, consider the vector

$$\vec{r} = \vec{r}^* - \vec{r}_1 \tag{II.25}$$

where $\vec{r}^*$ is the global minimum and $\vec{r}_1$ an arbitrary starting point. Since the gradient vanishes in the minimum, we find from

$$\mathbf{A} \cdot \vec{r} = \vec{b} \tag{II.26}$$

that

$$\begin{aligned} \vec{r} &= \mathbf{A}^{-1} \cdot \vec{b} \\ \vec{r}^* &= \vec{r}_1 + \mathbf{A}^{-1} \cdot \vec{b} \end{aligned} \tag{II.27}$$

so that we are able to find the minimum of a quadratic potential in one step, simply by inverting the Hessian $\mathbf{A}$. This is a very favorable property, because in CG we would have needed around N steps (N – dimensionality of the problem). The Hessian contains the information about the curvature of the function, with large curvature giving large eigenvalues. Therefore, the inverse of the Hessian leads to large steps in regions of low curvature and vice versa This property will speed up the convergence for shallow potentials, where it would be very slow just to follow the gradient.

A trivial example is the parabola $f(x) = x^2$. For this function, the so called Newton–Raphson (NR) method as described in Eq. II.27 gives:

$$0 = r_1 - \frac{1}{2} \cdot 2 \cdot r_1 \tag{II.28}$$

(with $f''(r) = 2$ and $f'(r) = 2r$). Compare this with a flat potential like $f(r) = 0.1 \cdot r^2$. The inverse of the second derivative $f''(r) = 0.2$ is $[f''(x)]^{-1} = 5$, giving a large step size.

Practically, there are some issues:

- to evaluate the Hessian and to invert it (an $\mathcal{O}(N^3)$-operation) can be very costly, co that the CG method becomes computationally cheaper, in particular if
- the potential is not harmonic. Then, NR may even fail (converge to a saddle point, proceed in a wrong direction etc.) and it may not be the method of choice.

Therefore, one usually starts the optimization (when forces are large) with SD and CG, and NR is invoked only later – close to the minimum, where the harmonic approximation works better.

Very efficient are so-called *Hessian-update methods*, where the inverse Hessian is not calculated, but rather updated during the optimization.

$$\vec{r}_{k+1} = \vec{r}_k - \mathbf{A}_k^{-1} \cdot \vec{g}_k \tag{II.29}$$

One starts with $\mathbf{A}_1^{-1} = \mathbf{I}$ (unit matrix) and the matrix is 'updated' in every step, so that it is identical to the inverse Hessian for large k. This means that in the beginning, one follows the gradient, and the information about the curvature is collected along the way.

All optimization techniques require a criterion to stop the procedure. Common practice is to stop if the gradient and the change of energy between two steps become small (smaller than a preset threshold).

D. Harmonic approximation of molecular vibrations: the normal modes

The displacement from equilibrium of a harmonic oscillator $r(t)$ is given by the solution of the ordinary differential equation

$$m \cdot \ddot{r} = -k \cdot r \tag{II.30}$$

with k being the second derivative of the potential with respect to the displacement r. If we insert $r(t) = A \cdot \sin(\omega t)$, we immediately obtain

$$-m \cdot \omega^2 = -k \tag{II.31}$$

and the vibrational frequency $\omega = \sqrt{k/m}$.

If we think of large molecules like proteins with N atoms, the problem becomes quite complicated. Every atom interacts with each other, so we have to deal with N^2 interactions,

which are usually not harmonic (Coulomb and vdW interactions, many-body interactions, although the bonded terms are harmonic).

In the *harmonic approximation*, we take the force-field energy I.35 and apply the Taylor approximation around the equlibrium positions of the atoms, with r_i being the deviations from the equilibrium (the first derivative vanishes at equilibrium):

$$E(\vec{r}) = E(\vec{r}_0) + \frac{1}{2}\sum_{i,j}^{N} \frac{\partial^2 E}{\partial r_i \, \partial r_j} \cdot r_i \cdot r_j \tag{II.32}$$

With

$$k_{ij} = \frac{\partial^2 E}{\partial r_i \, \partial r_j} \tag{II.33}$$

and setting $E(\vec{r}_0) = 0$ we have

$$E(\vec{r}) = \frac{1}{2}\sum_{i,j}^{N} k_{ij} \cdot r_i \cdot r_j \tag{II.34}$$

Note that the k_{ij} introduced here are different form the force constants in the force field!

The force on atom i is now the (negative of the) derivative of the energy with respect to the atomic coordinate r_i:

$$F_i = -\frac{\partial E}{\partial r_i} = -\sum_{j}^{N} k_{ij} \cdot r_j \tag{II.35}$$

Looking at atom i, we have

$$m_i \cdot \ddot{r}_i = F_i = -\sum_{j}^{N} k_{ij} \cdot r_j \tag{II.36}$$

Since we have E, we know how to calculate the second derivatives, once we have located the minimum. The movement of atom i is now coupled to all other atoms, and the equations we have to solve become quite complicated. In case of a diagonal matrix $k_{ij} = k_{ii}\delta_{ij}$, we would have

$$m_i \cdot \ddot{r}_i = k_{ii} \cdot r_i \tag{II.37}$$

for which we know the solution

$$r_i(t) = a_i \cdot \sin[\omega t] \tag{II.38}$$

where we have a system of uncoupled oscillators. We can use this as an ansatz to solve the system of coupled oscillators, to obtain

$$m_i \cdot \omega^2 \cdot a_i = -\sum_j^N k_{ij} \cdot a_j \tag{II.39}$$

The vector $\vec{a} = (a_1, a_2 \dots a_{3N})$ gives the amplitude of the motion, i.e. determines how much an atom is involved in the motion. We define $\lambda = \omega^2$ and the (diagonal) mass matrix $\mathbf{M}_{ii} = m_i$. With that, we can write:

$$\lambda \cdot \mathbf{M} \cdot \vec{a} = \mathbf{k} \cdot \vec{a} \tag{II.40}$$

Multiplying from the left with $\mathbf{M}^{-1}$, we get

$$\lambda \cdot \vec{a} = \mathbf{M}^{-1} \cdot \mathbf{k} \cdot \vec{a} \tag{II.41}$$

This is an eigenvalue problem for the matrix $\mathbf{M}^{-1} \cdot \mathbf{k}$, which we know how to solve. The only problem is that this matrix is not symmetric, which makes the numerical solution more difficult. Therefore, we look how to get an eigenvalue problem for a symmetric matrix.

This can be done if we define

$$\vec{b} = \mathbf{M}^{1/2} \cdot \vec{a} \qquad \text{i.e.} \qquad \vec{a} = \mathbf{M}^{-1/2} \cdot \vec{b} \tag{II.42}$$

and get instead of II.40 this problem:

$$\lambda \cdot \mathbf{M}^{1/2} \cdot \vec{b} = \mathbf{k} \cdot \mathbf{M}^{-1/2} \cdot \vec{b} \tag{II.43}$$

Now, we multiply from the left with $\mathbf{M}^{-1/2}$ and obtain

$$\begin{aligned} \mathbf{M}^{-1/2} \cdot \lambda \cdot \mathbf{M}^{1/2} \cdot \vec{b} &= \mathbf{M}^{-1/2} \cdot \mathbf{k} \cdot \mathbf{M}^{-1/2} \cdot \vec{b} \\ \lambda \cdot \vec{b} &= \widetilde{\mathbf{k}} \cdot \vec{b} \end{aligned} \tag{II.44}$$

with a symmetric matrix $\widetilde{\mathbf{k}}$ given as

$$\widetilde{\mathbf{k}}_{ij} = \frac{k_{ij}}{\sqrt{m_i}\sqrt{m_j}} \tag{II.45}$$

Now, we can solve a standard eigenvalue problem

$$\left(\widetilde{\mathbf{k}} - \lambda \cdot \mathbf{I}\right) \cdot \vec{b} = 0 \tag{II.46}$$

to get the eigenvalues λ_ν and eigenvectors $\vec{b}_\nu$. The $N \times N$ matrix $\widetilde{\mathbf{k}}$ has N eigenvalues λ_ν and eigenvectors $\vec{b}_\nu$, which correspond to the *normal modes* of the system. These represent the independent modes of motion of the molecule. Every eigenvector $\vec{b}_\nu$ contains the amplitudes of every atom in the system (in the directions x, y and z), contributing to the particular normal mode ν: $\vec{b}_\nu = (b_1^\nu, b_2^\nu, ...b_N^\nu)$.

For example, think of the three modes of vibration of a water molecule:

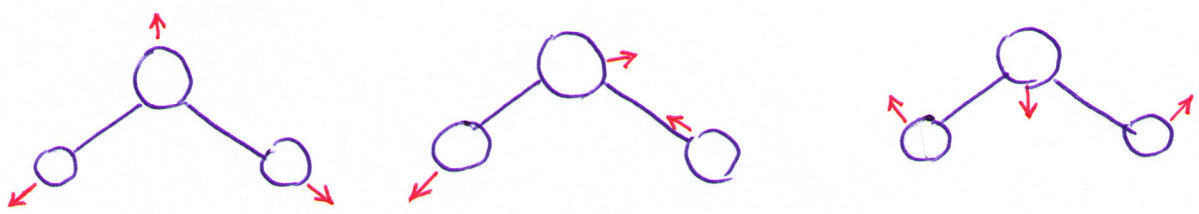

Example:

Consider a fictitious linear triatomic molecule, with two equal bond lengths and force constants, atom masses m_1, m_2 and $m_3 = m_1$, and harmonic springs only between atoms 1–2 and 2–3. The potential energy E then reads

$$E = \frac{1}{2}k \cdot (x_1 - x_2)^2 + \frac{1}{2}k \cdot (x_2 - x_3)^2 \tag{II.47}$$

with x_i being the displacements from the equilibrium positions.

We have the Hessian

$$\mathbf{k} = \begin{pmatrix} k & -k & 0 \\ -k & 2k & -k \\ 0 & -k & k \end{pmatrix} \tag{II.48}$$

the mass matrix

$$\mathbf{M} = \begin{pmatrix} m_1 & 0 & 0 \\ 0 & m_2 & 0 \\ 0 & 0 & m_1 \end{pmatrix} \tag{II.49}$$

and the mass-weighted Hessian

$$\mathbf{k} = \begin{pmatrix} \frac{k}{m_1} & -\frac{k}{\sqrt{m_1 m_2}} & 0 \\ -\frac{k}{\sqrt{m_1 m_2}} & 2\frac{k}{m_2} & -\frac{k}{\sqrt{m_1 m_2}} \\ 0 & -\frac{k}{\sqrt{m_1 m_2}} & \frac{k}{m_1} \end{pmatrix} \tag{II.50}$$

The solution of the eigenproblem leads to three normal modes:

$$\begin{aligned} \lambda = \tfrac{k}{\sqrt{m_1}}: &\qquad b_1 = -b_3,\ b_2 = 0 \\ \lambda = 0: &\qquad b_1 = b_3,\ b_2 = \sqrt{m_2/m_1}\cdot b_1 \\ \lambda = k\cdot\tfrac{m_2+2m_1}{m_1 m_2}: &\qquad b_1 = b_3,\ b_2 = -2\sqrt{m_1/m_2}\cdot b_1 \end{aligned} \tag{II.51}$$

The first mode describes a motion with the central atom at rest, and m_1 and m_3 vibrating with opposite amplitudes – symmetric stretch. The second mode corresponds to pure translation of the whole molecule along the x axis. Since $a_1 = a_3 = \frac{b_1}{\sqrt{m_1}}$, we find that $a_2 = a_1$. In the third mode, the central atom moves in the opposite direction to the outer atoms – asymmetric stretch.

E. Exercises

1. Consider the function $f(x, y) = x^2 + 2y^2$. Calculate the gradient in the point (2,2) and the Hessian in (0,0). Would you reach the minimum when moving along that gradient? What are the eigenvalues of the Hessian in (0,0)? Start in the point (0,1) and move along the gradient with the step size of 1. Where do you arrive at?

2. Starting in the point (9,9), a line search in the first step finds the point (4,−1). Show that the new search direction constructed in this point with CG directly reaches (0,0).

3. Show that you arrive in the minimum in one step if you use the Newton–Raphson method.

4. Consider the function $f(x, y) = x^4+4x^2y^2-2x^2+2y^2$. Plot this function and determine the eigenvalues of the Hessian in the minimum (1,0) and in the saddle point (0,0). What are the eigenvectors?

5. Derive the Hessian of the artificial linear triatomic system (Eq. II.50).

III. MOLECULAR DYNAMICS SIMULATIONS

Consider a chemical reaction in solution. The molecules of solute are surrounded by many water molecules, which fluctuate and thereby assume different hydrogen bonding interactions with the solute. The different orientations of water molecules induce different dipole moments on the solute. As a result

- the energy of the system will fluctuate a lot;
- since there are a multitude of local minima close in energy, the search for a global minimum will become extremely difficult if not meaningless;
- even if a global minimum is found, the product state may have a very different global minimum than the reactant state with respect to the conformation of the water molecules. In this case, we do not know how to compare the energies at all!

The **(micro)state** of a system is completely determined, if we know the positions $\vec{r}_i$ and the momenta $\vec{p}_i$ of all the particles. We call the $6N$-dimensional space spanned by the coordinates and the momenta the **phase space**, $\{\vec{r}_i, \vec{p}_i\}$. A **trajectory** in the phase space is the sequence of points $\{\vec{r}_i(t), \vec{p}_i(t)\}$ passed by during the dynamics of the system.

For an example, let us consider the harmonic oscillator. We can plot the time dependence of the coordinate

$$r(t) = a \cdot \cos\left[\omega t\right] \tag{III.1}$$

as well as the time dependence of the velocity

$$v(t) = -a\,\omega \cdot \sin\left[\omega t\right] \tag{III.2}$$

On the other hand, we can also plot the velocities versus the coordinates in the 2-dimensional phase space, and we see easily that the trajectory in the phase space is elliptic:

$$\left(\frac{x(t)}{a}\right)^2 + \left(\frac{v(t)}{a \cdot \omega}\right)^2 = 1 \tag{III.3}$$

The total energy of the harmonic oscillator is

$$E = T + V = \frac{1}{2} m\omega^2 a^2 \tag{III.4}$$

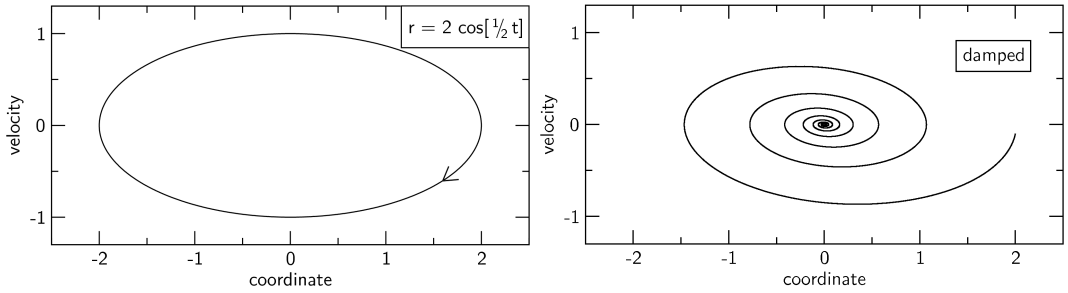

Therefore, different values of a and ω correspond to different energies. The trajectories in phase space never cross for such so-called **conservative systems** (systems conserving the total energy). If we have *friction* or some other *damping*, the oscillator is losing energy (non-conservative system) and the motion will look like spirals ending in the origin. Here, different trajectories may cross.

Now, let us return to the molecule in solution. It does not make much sense to look at a single structure; rather, we may wish to average the property of interest over all available structures. For example, we follow the trajectory in phase space for some time and evaluate the energy for many **snapshots** $\{\vec{r}_i(t_k), \vec{p}_i(t_k)\}$ along the trajectory. So, we obtain values of energy E_k in time instants $t_k\,(k = 1, \ldots, M)$ and calculate the average:

$$\langle E \rangle = \frac{1}{M} \sum_{k=1}^{M} E_k \tag{III.5}$$

We do this for the product and for the reactant, obtain average energies for both states, and thus the energy difference. In principle, this is a very good idea, but there are a few issues:

- How can we assure that we have enough points (snapshots) to represent all possible (or at least relevant) conformations of the molecular system?
- How do we obtain the trajectory? $\rightarrow$ perform MD! Then, how to consider the temperature?
- Suppose we know the structure of the reactant, then how do we get the structure of the product and, if desired, the whole reaction path? This is a difficult problem and we will have to spent some time on that.
- What about entropy? Does the average of energy provide sufficient information? This is another difficulty, so we will have to look deeper into thermodynamics and statistics.

Here, we are at the core of biomolecular simulations: It is easy to understand the total energy of the force field, and how geometry optimization works. The main issue is to make proper use of the energy function to get the *thermodynamic properties* right. Biomolecular simulations are all about thermodynamics, in possible contrast to quantum chemistry, where people look at small molecules with quite simple structures and with a focus just on total energies. At the moment, we will concentrate on the former two points. The latter two points will be discussed in next chapters.

If we have a trajectory, we can calculate so-called **time averages** for the properties of interest, like structural properties or velocities. For any property $A(t)$, this works the same way as for energy, so that we may generalize the Eq. III.5:

$$\langle A(t) \rangle_t = \frac{1}{t_1 - t_0} \int_{t_0}^{t_1} A(t) \, \mathrm{d}t \tag{III.6}$$

On the other hand, an experimental sample contains a huge number of molecules. This number is so large that we can assume all relevant conformations of molecule and solvent to be present. Think of a large number of harmonic oscillators, then for every point in the phase space $\vec{r}_i, \vec{p}_i$, there will be for every point (on the ellipse) an oscillator, which is at that point. Such a collection of systems is called an **ensemble**.

Now, let us count how many molecules (oscillators) in the ensemble are found in a phase-space point $\vec{r}_i, \vec{p}_i$ as well as in all the other points. Doing this, we obtain the **phase space density**, i.e. the number of realizations of each point in the phase space (per volume unit):

$$\rho(\vec{r}, \vec{p}) \tag{III.7}$$

If we integrate ρ over the entire phase space, we obtain the total number of systems (oscillators or molecules):

$$Z = \int \rho(\vec{r}, \vec{p}) \, \mathrm{d}\vec{r} \, \mathrm{d}\vec{p} \tag{III.8}$$

We can use this phase space density to calculate the **ensemble average**:

$$\langle A \rangle_e = \frac{1}{Z} \int A \cdot \rho(\vec{r}, \vec{p}) \, \mathrm{d}\vec{r} \, \mathrm{d}\vec{p} \tag{III.9}$$

Experimentally, we always measure ensemble averages; however, in a simulation, we always have a single system for which we calculate time averages. To be able to compare both, we always assume that the systems we study are **ergodic**. This means that the system

passes through all points of the phase space constituting the real ensemble during the MD, if the simulation is long enough. If the system is indeed ergodic, these averages are equal:

$$\langle A \rangle_e = \langle A \rangle_t \tag{III.10}$$

A. Integration of the equations of motion

We leave the statistics and look how we can get the trajectories in computer simulations. The total energy $E = T + V$ is often termed *Hamilton function* H, or Hamiltonian in quantum mechanics. The Hamilton formalism is a practical way to derive equations of motion, once we know the total energy:

$$\dot{r_i} = \frac{\partial H}{\partial p_i} \qquad \dot{p_i} = -\frac{\partial H}{\partial r_i} \tag{III.11}$$

We cannot prove these equations here, but give an example (momentum $p = m \cdot v$):

$$\begin{aligned} H &= \frac{1}{2}\frac{p^2}{m} + \frac{1}{2}kr^2 \\ \dot{r} &= \frac{\partial H}{\partial p} = \frac{p}{m} \\ \dot{p} &= -\frac{\partial H}{\partial r} = -k \cdot r \end{aligned} \tag{III.12}$$

which, if put together ($\dot{p} = m \cdot \ddot{r}$ from the eqn for $\dot{r}$), give the well-known equation of motion of the harmonic oscillator. These are **ordinary differential equations** (ODE) of 1st and 2nd order.

A 1st-order differential equation may look like this: $\dot{x} = -k \cdot x$. Such an equation has a solution $x(t) = A \cdot \exp[-k \cdot t]$. Examples of natural phenomena following this exponential law are radioactive decay or the dynamics of populations. More generally, we can write these ODEs as

$$\dot{x} = f(x, t) \tag{III.13}$$

A 2nd-order ODE then follows as

$$\ddot{x} = f(x, \dot{x}, t) \tag{III.14}$$

An example is the equation of motion of a harmonic oscillator $\ddot{x} = -\frac{k}{m} \cdot x$, or, when we introduce damping proportional to velocity (which is often the case):

$$\ddot{x} = -\zeta \cdot \dot{x} - \frac{k}{m} \cdot x \tag{III.15}$$

We can reduce the 2nd-order ODE to two 1st-order ODEs by introducing v:

$$\begin{aligned} \dot{x} &= v \\ \dot{v} &= -\zeta \cdot v - \frac{k}{m} \cdot x \end{aligned} \tag{III.16}$$

Now, we have to solve these ODEs numerically. There are several methods available, which we will briefly discuss.

B. Simple numerical solution – the Euler method

To solve a 1st-order ODE

$$\dot{r} = f(r, t) \tag{III.17}$$

we proceed by a Taylor expansion ($\Delta t = t - t_0$):

$$r(t) = r(t_0) + \dot{r}(t_0) \cdot \Delta t + \frac{1}{2}\ddot{r}(t_0) \cdot \Delta t^2 + \dots \tag{III.18}$$

The **Euler approximation** is a first-order approximation, so that we neglect the second and higher orders:

$$r(t) \approx r(t_0) + \dot{r}(t_0) \cdot \Delta t \tag{III.19}$$

We start the numerical integration at time t_0, take a time step Δt and get the value of r and v in the time $t = t_0 + \Delta t$. For our MD simulation, we have

$$\begin{aligned} r(t_0 + \Delta t) &= r(t_0) + v(t_0) \cdot \Delta t \\ v(t_0 + \Delta t) &= v(t_0) + a(t_0) \cdot \Delta t \\ a(t_0) &= -\frac{1}{m}\frac{\partial H}{\partial r} = -\frac{F}{m} \end{aligned} \tag{III.20}$$

where H is the Hamilton function. Instead, we can use the potential energy V only, and the derivative of V is the force upon the atom.

To start the MD, we have to specify the *initial conditions* – the positions r_0 and the velocities v_0, and calculate the force at the positions r_0 to get the accelerations a_0. Then, we can use the Euler equations to get the positions and velocities at the time $t_0 + \Delta t$.

This means, to obtain a trajectory over a time interval T, we have to evaluate the forces on all atoms $M = T/\Delta t$ times, i.e. to perform M steps. Therefore, the computational cost of the calculation of forces determines how many steps we can afford to make.

C. The Verlet method

The numerical error of the Euler method is too large to allow for time steps of 1 fs. Therefore, methods with errors in $\mathcal{O}(\Delta t^3)$ have to be used. A popular one is the Verlet method. Here, we make a virtual step in positive time and in 'negative' time, and expand up to second order:

$$\begin{aligned} r(t+\Delta t) &= r(t) + \dot{r}(t)\cdot\Delta t + \frac{1}{2}\ddot{r}(t)\cdot\Delta t^2 \\ r(t-\Delta t) &= r(t) - \dot{r}(t)\cdot\Delta t + \frac{1}{2}\ddot{r}(t)\cdot\Delta t^2 \end{aligned} \tag{III.21}$$

We may add both equations to eliminate the velocity $\dot{r}$:

$$\begin{aligned} r(t+\Delta t) &= 2\cdot r(t) - r(t-\Delta t) + \ddot{r}(t)\Delta t^2 \\ \ddot{r}(t) &= a(t) = \frac{F(t)}{m} = -\frac{1}{m}\frac{\partial V}{\partial r}(t) \end{aligned} \tag{III.22}$$

This equation seems to be a little strange, as it requires not only the positions $r(t)$ and the accelerations $a(t)$, but in addition the positions one step back $r(t-\Delta t)$! This may look like a problem, because at the start of a MD, we know only $r(t_0)$, $v(t_0)$ (and $a(t_0)$ via forces) but not $r(t_0-\Delta t)$. This would mean that Verlet could not be started. We have to use the initial velocities to calculate the positions an imaginary step back $r(t_0-\Delta t)$ to start Verlet:

$$r(t_0-\Delta t) = r(t_0) - v(t_0)\cdot\Delta t \tag{III.23}$$

The algorithm does not contain velocities explicitly; if these are of interest, they may be obtained as

$$\dot{r}(t) = v(t) = \frac{r(t+\Delta t) - r(t-\Delta t)}{2\cdot\Delta t} \tag{III.24}$$

This form of the algorithm is called the Verlet normal form. An excerpt of the computer program used to generate the 'astronomic' trajectories (below in this chapter) is shown in Fig. 15. Note that there are two main parts of the program: (i) the calculation of force(s), and (ii) the propagation of coordinates of the particle(s). This is the case in programs for biomolecular simulations, too.

Several equivalent variations of the algorithm have been developed, like the **velocity Verlet**. Here are new positions calculated first

$$r(t+\Delta t) = r(t) + v(t)\cdot\Delta t + \frac{1}{2}a(t)\cdot\Delta t^2 \tag{III.25}$$

```
/* initial "old" positions from initial velocities */
for (k=0; k<DIM; k++)
    r_old[k] = r[k] - v[k] * dt;

for (t=0.; t < CYCLES*PERIOD; t+=dt) {
    /* distance (from the Sun) */
    rnorm = sqrt(NORM2(r));
    /* gravitation force (on the comet)
     * f = -1 / r^2
     * multiply this by the unit vector in the direction of r
     * f = -1 / r^2 * vector(r) / r
     */
    for (k=0; k<DIM; k++)
        f[k] =  - r[k] / CUB(rnorm);
    /* Verlet integrator */
    for (k=0; k<DIM; k++) {
        r_new = 2 * r[k] - r_old[k] + f[k] * SQR(dt);
        r_old[k] = r[k];
        r[k] = r_new;
    }
}
```

FIG. 15: Snippet of the code for the simulation of a comet orbiting around the Sun. The force acting on the comet is the gravitational $\vec{F} = -1/r^2 \cdot \vec{r}/r$, where r is the distance from the Sun.

followed by the evaluation of forces (and thus accelerations) in the new positions. New velocities are then obtained as

$$v(t + \Delta t) = v(t) + \frac{1}{2}\left(a(t) + a(t + \Delta t)\right) \cdot \Delta t \tag{III.26}$$

which are used in the next calculation of positions r. Here, MD can be started with the knowledge of r_0 and v_0; however, in every next step, new positions $r(t + \Delta t)$ must be calculated first so that accelerations may be updated in order to obtain $v(t + \Delta t)$.

Although both mentioned forms of the Verlet algorithm are equivalent, the velocity Verlet exhibits better numerical precision. It is interesting to note why: The numerical problem of normal Verlet is that it adds a small but important term $\ddot{r}(t_0)\Delta t^2$ to a large term calculated as a difference $2r(t) - r(t - \Delta t)$. This is a critical point in a calculation running on a computer, which has a limited numerical precision: A small number that is obtained as a difference of two similar large numbers is burdened with large relative uncertainty. In such a case, it is desirable to use an algorithm which is mathematically equivalent but does not require to perform such a potentially problematic calculation.

Leap-frog is another flavor of Verlet-type integrators, particularly similar to the velocity Verlet. Its characteristic feature is that the positions and velocities are evaluated in an alternating fashion: $r(t)$, $v(t + \frac{1}{2}\Delta t)$, $r(t + \Delta t)$, $v(t + \frac{3}{2}\Delta t)$, $r(t + 2\Delta t)$, $v(t + \frac{5}{2}\Delta t)\ldots$ The name of the method comes from the leap-frog exercise popular with children. Starting at t,

the velocities at $t + \frac{1}{2}\Delta t$ are obtained first

$$v(t + \frac{1}{2}\Delta t) = v(t - \frac{1}{2}\Delta t) + a(t) \cdot \Delta t \tag{III.27}$$

and the second step of a leap-frog iteration is the calculation of positions:

$$r(t + \Delta t) = r(t) + v(t + \frac{1}{2}\Delta t) \cdot \Delta t \tag{III.28}$$

So, the accelerations have to be obtained at t, $t + \Delta t$, $t + 2\Delta t \ldots$ They are calculated from forces, and positions are needed to compute forces – therefore it is actually necessary that positions be known at the same points in time that accelerations shall be obtained.

D. Time step in Verlet integration

The length of the time step is a crucial parameter in the simulation. There is a numerical and a chemical constraint on the step size:

- Numerical: Since we neglect the contributions in Δt^3 and higher orders, we introduce an error in the order of Δt^3 ($\mathcal{O}(\Delta t^3)$). A possibility is to make the step very short, so that the error is small. But then, we need to perform too many steps to simulate a certain time T. on the other hand, if we make the step too long, we introduce an error in the integration. Aside from a dynamics that will deviate from the exact one, the momentum may not be conserved, as a consequence of this error.

- Chemical: The fastest motion in biological systems is the movement of hydrogen atoms, with the period of around 10 fs. A rule of thumb recommends the step size to be at least an order of magnitude smaller than the period of the fastest motion.[12] Practically, this leads to a step size of 1 fs.

The step size (of typically 1 or several fs) is the fundamental time unit in MD. This means, we need 1 million calculations of energy and forces to get a trajectory in a total length of 1 ns. For large systems, multi-nanoseconds simulations can be routinely done, and even microsecond regime may be reached for smaller ones.

[12] Note that compared to the 'astronomic' simulations used here to illustrate the properties of various integrators, this requirement is several orders of magnitude weaker.

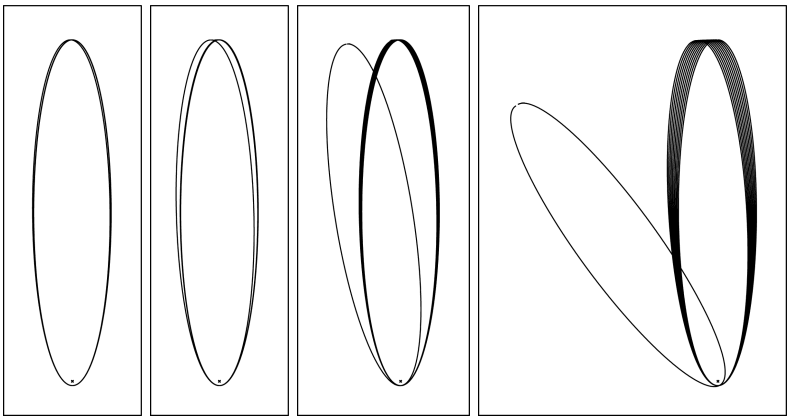

FIG. 16: Simulation of the motion of a comet orbiting around the Sun (small cross at the bottom) using the Verlet integrator with various time steps, from the left: 1×10^{-5}, 2×10^{-5}, 5×10^{-5} and 10×10^{-5} of the period of motion. First ten orbits are shown, the following 89 not shown and the 100th shown again.

The error caused by a too long time step is illustrated in Fig. 16. We have a test system composed of one static heavy object (a star) and one moving light object (a comet), and we simulate the dynamics of this system with the Verlet integrator considering gravitation force between the objects. Note that gravitation observes the same inverse-square-law as Coulomb interaction, which is relevant in molecular systems. In this 'astronomic' toy system, the exact trajectory would be an ellipse with the star in one focus, and the comet would orbit around along this ellipse periodically. We perform the simulation with four different values of the time step and plot the trajectory.

Apparently, we obtain a reasonable trajectory with the shortest time step, although we observe a small deviation from a single ellipse already. The error becomes more evident with the second-longest time step, while it is very large for the longest time step considered. It is important to note here that the trajectory is precessing (the axis of the ellipse is 'rotating') but it remains elliptic whatever the time step is. Also, the total energy remains constant and so does the orbital period (interval of time needed to complete one orbit). This is a consequence of the *reversibility* of Verlet integration: if we reverse the course of time at a certain point in the simulation (taking the time step of $-\Delta t$), we would end up in the initial point of the simulation eventually. So, the energy in a Verlet simulation may fluctuate (this happens when we make the time step longer), but around a constant value throughout the simulation.

E. More advanced methods

The Verlet method (with the error of $\mathcal{O}(\Delta t^3)$) is a very approximative one though, but still it is routinely used in MD simulations. What makes Verlet so efficient? It (i) requires the forces on atoms (to yield second derivatives of positions – accelerations) to be calculated only once per time step, and (ii) involves no higher derivatives of positions. More accurate methods to solve ODEs have been developed, too, and some of them are used in MD simulations if the accuracy of the integration is a concern.

1. Gear integration: predictor–corrector

A straightforward way to improve the quality of integrator would be to involve several extra terms from the Taylor expansion, i.e. to cut the expansion at some further point. This is hardly ever done; instead, other ways to improve the accuracy have been taken. Gear's predictor–corrector family of methods provides solutions correct to an order of choice. Here, new position etc. are calculated ('predicted') from the Taylor expansion as usually. Then, the forces are calculated in the new positions to give accelerations. These are then used to 'correct' the new positions, and new positions are then calculated finally. This method is rarely used due to the considerable computational requirements, although it may provide quite accurate solutions of equations of motion as well as make a longer time step possible.

In a simulation with nth-order Gear integrator, we work with the coordinates of all atoms (written together as $\vec{r}$) and their time derivatives up to the order of $n-1$. In a compact way, these data may be written as

$$R = \begin{pmatrix} \vec{r} \\ \dot{\vec{r}} \cdot \Delta t \\ \ddot{\vec{r}} \cdot \frac{1}{2}\Delta t^2 \\ \dddot{\vec{r}} \cdot \frac{1}{6}\Delta t^3 \end{pmatrix} \tag{III.29}$$

for the 4th-order method. For higher-order methods, higher derivatives come in as $\frac{\mathrm{d}^k \vec{r}}{\mathrm{d}t^k} \cdot \frac{1}{k!}\Delta t^k$. At the start of the simulation, the positions $\vec{r}$ and velocities $\dot{\vec{r}}$ have to be initialized, and the accelerations $\ddot{\vec{r}}$ have to be calculated from forces, so one calculation of forces is required at start. The higher derivatives may be set to zero.

An integration step at time t starts with a *prediction* of the coordinates (and their derivatives) at time $t + \Delta t$ as follows:

$$R_{\mathrm{p}}(t + \Delta t) = \begin{pmatrix} 1 & 1 & 1 & 1 \\ 0 & 1 & 2 & 3 \\ 0 & 0 & 1 & 3 \\ 0 & 0 & 0 & 1 \end{pmatrix} \cdot R(t) \tag{III.30}$$

where the matrix contains binomial coefficients. What does such a prediction mean? In fact, this calculation is the same as passing a polynomial of order $n-1$ through the previous n points of the trajectory (at times t, $t - \Delta t$,... $t - (n-1)\Delta t$) and assuming that the next point lies on this polynomial, too. For continuous force functions, a prediction based on this approximation may be a good one. Note that no calculation of force has been required in the algorithm so far!

Then, we estimate the *error* of the prediction. For this, we calculate the force at the predicted position, and compare it with the predicted force. The difference of these gives the error:

$$E = \frac{1}{2}\frac{\vec{f}(\vec{r}_{\mathrm{p}})}{m}\Delta t^2 - \frac{1}{2}\ddot{\vec{r}}_{\mathrm{p}}\Delta t^2 \tag{III.31}$$

This is a vector with as many components as the vector of coordinates has (so that every coordinate with its derivatives has 'its own' error).

Finally, using the error E, we calculate the *corrected* coordinates and derivatives as

$$R(t + \Delta t) = R_{\mathrm{p}}(t + \Delta t) + E \cdot \begin{pmatrix} a_0 \\ a_1 \\ a_2 \\ a_3 \end{pmatrix} \tag{III.32}$$

The necessary coefficients a_0, $a_1 \ldots a_{n-1}$ were estimated to prevent the integration errors from accumulating in the course of propagation, and may be looked up in tables. For the 4th-order method for 2nd-order ODE with forces not depending on velocities, they take values of $\frac{1}{6}$, $\frac{5}{6}$, 1 and $\frac{1}{3}$, respectively.

The Gear integration may provide trajectories that are more accurate than those obtained with the Verlet method using the same time step. Trajectories from test simulations with Gear integration are shown in Fig. 17. With the two shortest time steps, we obtain perfect

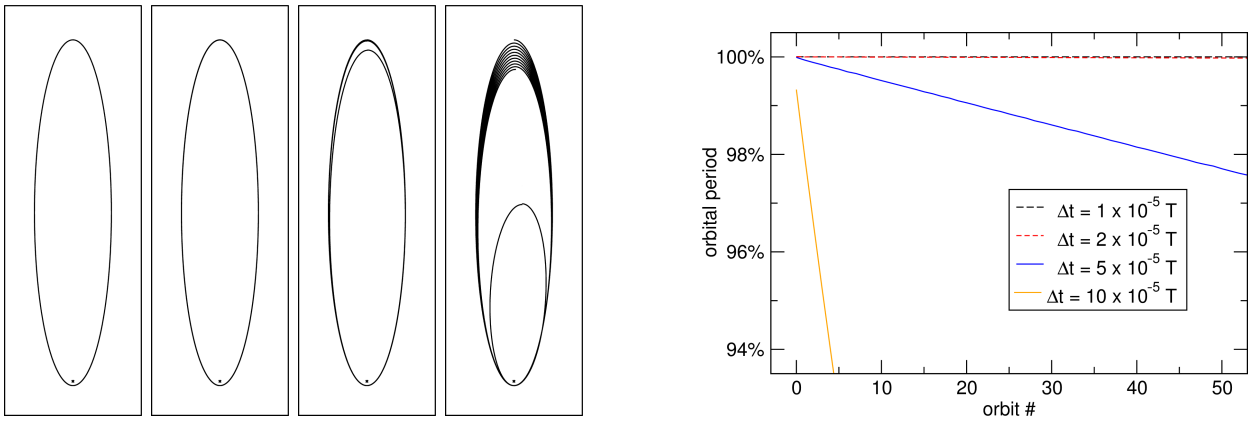

FIG. 17: Simulation of the motion of a comet orbiting around the Sun (small cross at the bottom) using the 4th-order Gear integrator with various time steps. *Left:* Trajectories obtained (from left to right) with $\Delta t = 1 \times 10^{-5}$, 2×10^{-5}, 5×10^{-5} and 10×10^{-5} of the correct period of motion. First ten orbits are shown, the following 89 not shown and the 100th shown again. *Right:* The orbital period – time needed to pass one complete orbit. This effect correlates with the decreasing total energy in the system and is negligible for time step up to 2×10^{-5} of the correct period.

trajectories, with no visible deviations even after 100 orbits. Note that we saw a certain deviation in the Verlet simulation even with the shortest time step. We see incorrect behavior of the simulation with the second-largest time step, and it is just wrong with the longest one. It is important to note that the character of the deviation (error) is different from what we saw in Verlet simulations: Rather than rotating around the star, the elliptic trajectory of the comet is getting 'shorter' in the course of time. At the same time, the orbital period is becoming shorter, and the total energy of the system is decreasing.[13] This is a general observation: the energy will decrease or increase (*drift*) in the simulation. With a longer time step and/or higher-order Gear integration, this deviation may be negligible. Still, the Gear integrators are not reversible and do not conserve energy.

Further, we analyze higher-order Gear integrators briefly. We simulate the same system with 5th-order and 6th-order method, and compare the trajectories to the previous ones. To see possible deviations clearly, we perform the simulations with the long time step of 10×10^{-5} of the correct period; the trajectories are shown in Fig. 18. Two leftmost trajectories are known already – these are the Verlet trajectory (Verlet corresponds to 3th-order Gear

[13] This means that the comet would land (or collapse) onto/into the star eventually.

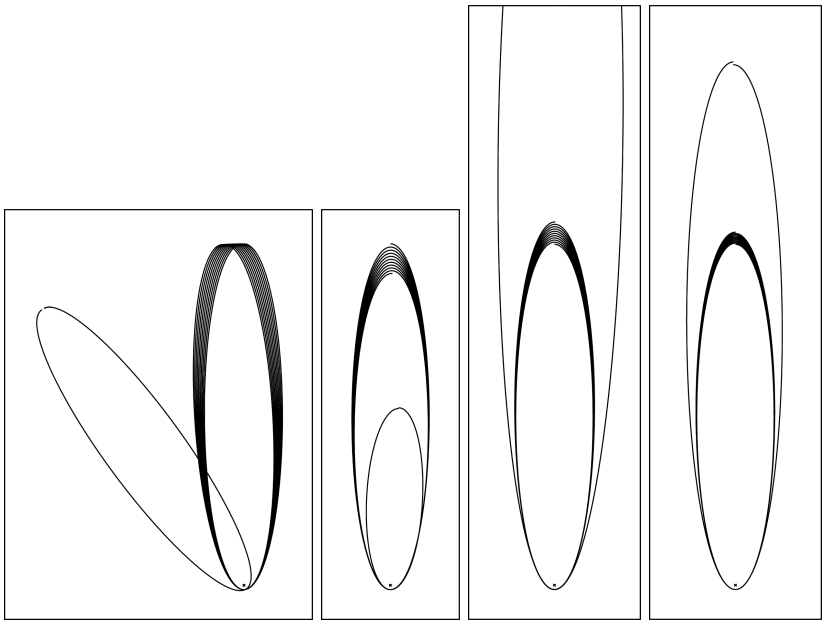

FIG. 18: Simulation of the motion of a comet orbiting around the Sun (small cross at the bottom) using several Gear integrators the time step of 10×10^{-5} of the correct period of motion. From the left: Verlet integrator, 4th-order, 5th-order and 6th-order Gear integrator. First ten orbits are shown, the following 89 not shown and the 100th shown again.

formally) and that obtained with 4th-order Gear. Evidently, including the higher derivatives in the calculation did not bring any large improvement of the accuracy of the integration in this case. The relative error, expressed as the relative rate of energy drift, is smaller though, but the result is still unsatisfactory.

A general observation would be that when taking the time step shorter, the results of higher-order methods will improve faster. However, when taking the time step longer, higher-order methods will be more prone to a complete failure while lower-order methods are more robust. An appropriate conclusion is that higher-order integrators are a good choice if accurate trajectories are desired, and lower-order or Verlet integration is sufficient for applications with 'weaker' requirements. Usually, the latter is the case with molecular simulations.

2. Runge–Kutta integration

The group of Runge–Kutta methods are numerical integrators of 1st-order ODEs. The classical Runge–Kutta method[14] evaluates the first derivative four times in every step, giving four values g_0, g_1, g_2 and g_3. The points at which we need to calculate the derivative are chosen depending on the previous calculations, and the first calculation is done at the start of (the integration step starts at time t when the position is $r(t)$):

$$\begin{aligned} g_0 &= \dot{r}\left(r(t)\right) \\ g_1 &= \dot{r}\left(r(t) + \tfrac{1}{2} g_0 \Delta t\right) \\ g_2 &= \dot{r}\left(r(t) + \tfrac{1}{2} g_1 \Delta t\right) \\ g_3 &= \dot{r}\left(r(t) + g_2 \Delta t\right) \end{aligned} \tag{III.33}$$

The value of the function at time $t + \Delta t$ is the integrated using a weighted average of the obtained values of the derivative:

$$r_{n+1} = r_n + \tfrac{1}{6}\left(g_0 + 2g_1 + 2g_2 + g_3\right) \cdot \Delta t \tag{III.34}$$

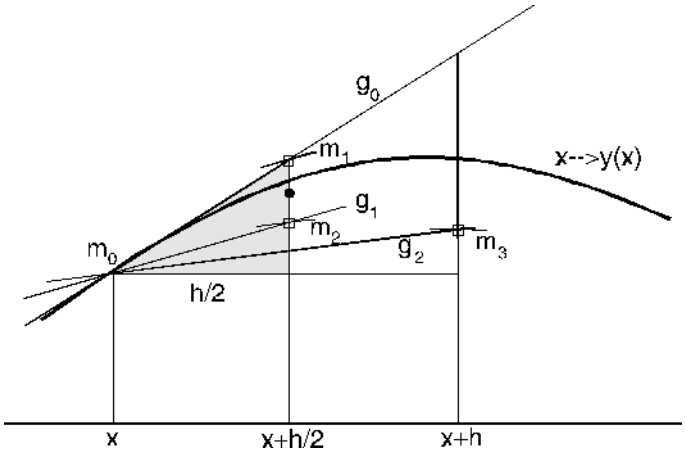

FIG. 19: Principle of the RK4 method. The derivative of function y is calculated four times per time step, at points m_0 (which is the point resulting from the previous time step), m_1, m_2 and m_3. The calculated derivatives g_0,... g_3 are shown as arrows, and each of them determines the point at which the next calculation of derivative will be done. The resulting point is obtained using a weighted average of all four values g_0,... g_3. (Image downloaded from www.hsg-kl.de)

[14] So classical that it is sometimes termed simply RK4.

We can say that RK4 is a predictor–corrector algorithm using four predictor calculations per step, requiring four calculations of the derivative. This increased computational effort reduces the order of the error per step to $\mathcal{O}(\Delta t^5)$ – fourth-order method. We should further note that the purpose of RK4 is to solve a 1st-order problem, much like the simple Euler method is. However, the Newton equations of motion, which we have to solve in classical MD simulations, constitute 2nd-order differential equations, and so RK4 cannot be used to integrate them directly. If we wish to use RK4 for this purpose, we need to convert the equation of motion to the system of two 1st-order equations. Here, the positions and the velocities of atoms would constitute the functions to be propagated with the algorithm:

$$\begin{aligned} \dot{\vec{r}} &= \vec{v} \\ \dot{\vec{v}} &= \frac{\vec{f}}{m} \end{aligned} \tag{III.35}$$

An application in computational chemistry where RK4 can be used directly is the integration of time-dependent Schrödinger equation as a 1st-order ODE for the wave function Ψ of the system:

$$\frac{\partial \Psi}{\partial t} = -\frac{i}{\hbar}\hat{H}\Psi \tag{III.36}$$

Having expanded Ψ in a suitable basis set, we could obtain the necessary derivative using the matrix representation of Hamiltonian, in a straightforward way.

F. Exercises

1. Derive the equations of motion for the linear triatomic system with Hamiltonian

$$H = \frac{1}{2}\sum_{i=1}^{3} m_i v_i^2 + \frac{1}{2}k(x_1 - x_2)^2 + \frac{1}{2}k(x_2 - x_3)^2 \tag{III.37}$$

2. Derive the equations of motion for the particle i (r_i and p_i) using the Hamilton formalism for

$$H = \frac{1}{2}\sum_{i} m_i v_i^2 + \frac{1}{2}\sum_{ij} V_{ij} \tag{III.38}$$

V_{ij} is given by the Lennard-Jones potential discussed in Chapter 1. These are the equations we have to solve when doing real MD for a system of uncharged particles without covalent bonds, like argon atoms.

IV. THERMODYNAMIC ENSEMBLES

A system of classical particles interacting with a potential V is a **deterministic system**. Knowing the **initial conditions**, which consist of the positions and velocities of all particles at the initial time, we can calculate the **trajectory** of the system, i.e. the positions $r(t)$ and velocities $v(t)$ at all future times t. We can have **analytic** solutions, as in the case of the harmonic oscillator, where we have the trajectories in a closed form:

$$x(t) = x_0 \cdot \cos[\omega t] \qquad v(t) = -v_0 \cdot \sin[\omega t] \tag{IV.1}$$

or, if the system becomes too complicated, we have to compute the trajectories **numerically**, for instance using the Verlet method.

Note that so-called **chaotic** systems are also strictly deterministic. For completely specified initial conditions, the system is perfectly predictable. The point here is that two trajectories which are initially close in phase space, may depart exponentially from each other, while they would stay close in non-chaotic systems (e.g. harmonic oscillator). We say that the solution of the underlying differential equations is unstable. This may happen already for seemingly simple systems like a double pendulum!

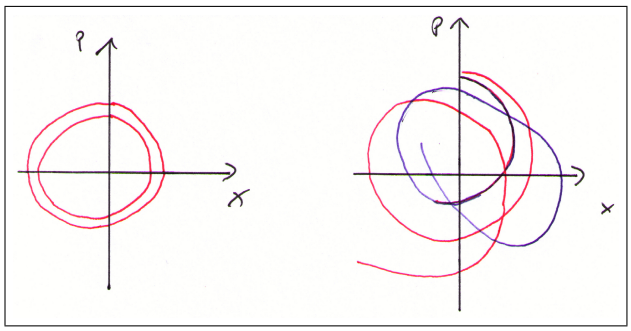

FIG. 20: For a 'chaotic' system, two initially close trajectories depart exponentially. Therefore, small differences in the initial conditions may lead to very different behavior of the system, despite being completely deterministic.

A motion becomes **stochastic**, if we do not have the information about all degrees of freedom, like for a dust particle moving in an erratic fashion. If we could keep track about the movements of all air molecules, the particle motion would be completely deterministic for us. We have to describe systems using **statistical mechanics**, if we cannot keep track of all degrees of freedom.

We are now interested to find simulation techniques, where we can control the temperature. The temperature is a crucial parameter, which determines if a certain part of the phase space is to be reached during the MD. The phase space will be sampled differently at high temperatures than at low ones, and different ensembles will be generated. In particular, we have to find a way to model the system, that we simulate the right phase space density.

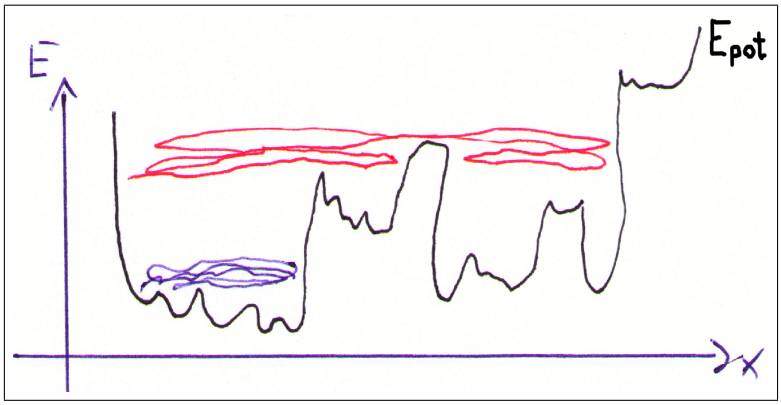

FIG. 21: A high energy $E = E_{\text{kin}} + E_{\text{pot}}$ allows to sample more different parts of the phase space. The difference $E - E_{\text{pot}}$ corresponds to the kinetic energy E_{kin}.

A. Microcanonical (NVE) ensemble: isolated system

A system is called **isolated** if it exchanges neither energy (in the form of heat or work) nor matter (particles) with the environment. In this case, the total energy of the system is constant and given by the sum of the kinetic energy E_{kin} and the potential energy E_{pot}

$$E = E_{\text{kin}} + E_{\text{pot}} \tag{IV.2}$$

Like for the harmonic oscillator, the kinetic and potential energies fluctuate in time as they are being transformed into each other all the time, keeping the total energy constant. This is what we describe when using the plain Verlet method for a large molecule after specifying the initial conditions. Looking into different regions of the molecule, the kinetic energy can be very different locally.

It is known from kinetic theory of gases that the kinetic energy is related to the temperature T

$$\langle E_{\text{kin}} \rangle = \frac{3}{2} NkT \tag{IV.3}$$

with $\langle E_{\text{kin}} \rangle = \frac{1}{2} \sum_i m_i \langle v_i^2 \rangle$. So, if we stuck a thermometer into various regions of the entire system (with N particles), we would measure different temperatures, fluctuating in time.

This is not quite the situation we normally have in the experimental setup (a test tube with a sample). Usually, our systems are in **thermodynamic equilibrium** with the environment, so that they have the same temperature (and optionally pressure) as the environment.

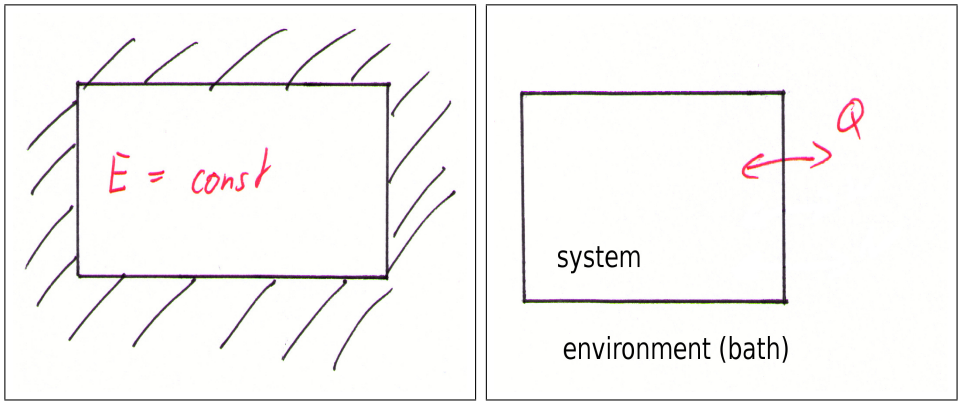

FIG. 22: Left: Isolated system. Right: Closed system; exchange of heat in the canonical ensemble.

The canonical ensembles allow for the exchange of heat and work, but not matter (particles).[15] If we keep the volume, temperature and number of particles constant, we call the system an **NVT ensemble**. If we keep pressure, temperature and the number of particles constant, allowing the volume to change, it is called an **NPT ensemble**.

B. Canonical (NVT) ensemble: closed system

In the **canonical ensemble**, the thermal contact of the system with the environment leads to an exchange of energy in the form of heat, until the same temperature T as in the environment is reached. Strictly spoken, temperature is only defined if there is such a thermal contact, and therefore not applicable to the closed systems as discussed above.

For a classical system in thermal equilibrium is the velocity of a particle/atom (its component in any direction) and the speed[16] given by the **Maxwell–Boltzmann distribution**

[15] There is another thermodynamic ensemble with constant volume, temperature and chemical potential, allowing the number of particles to change = exchange of matter with the environment (grand canonical ensemble).

[16] *Velocity* is the vector $\vec{v}$ and its magnitude is denoted as the scalar *speed* (v).

$$p(v_{x,i}) = \sqrt{\frac{m_i}{2\pi kT}} \cdot \exp\left[-\frac{m_i v_{x,i}^2}{2kT}\right] \tag{IV.4}$$

$$p(v_i) = 4\pi \left(\frac{m_i}{2\pi kT}\right)^{3/2} \cdot v_i^2 \cdot \exp\left[-\frac{m_i v_i^2}{2kT}\right] \tag{IV.5}$$

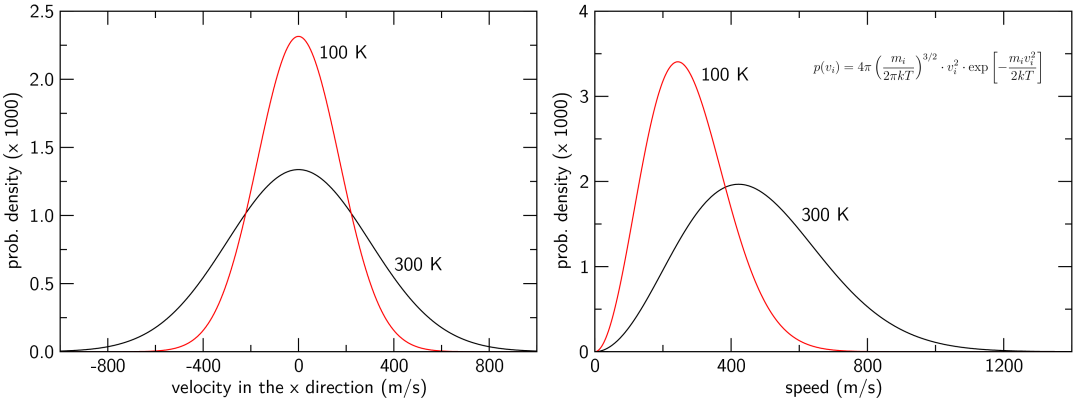

FIG. 23: The distribution of velocity in the x direction (left) and speed (right) of a N_2 molecule (ideal gas approximation).

With this, the **equipartition theorem** (Gleichverteilungssatz) can be derived, which ascribes every degree of freedom the same amount of kinetic energy of

$$\left\langle \frac{1}{2} m_i v_{x,i}^2 \right\rangle = \frac{1}{2} kT \tag{IV.6}$$

Since every atom i has three degrees of freedom x_i, y_i and z_i (and $v_i^2 = v_{x,i}^2 + v_{y,i}^2 + v_{z,i}^2$), we find for the total kinetic energy of the system

$$\langle E_{\text{kin}} \rangle = \left\langle \sum_i \frac{1}{2} m_i v_i^2 \right\rangle = \left\langle \sum_i \frac{1}{2} m_i v_{x,i}^2 + \frac{1}{2} m_i v_{y,i}^2 + \frac{1}{2} m_i v_{z,i}^2 \right\rangle = \frac{3}{2} NkT \tag{IV.7}$$

The point is that this special velocity distribution is a property of systems in contact with a heat reservoir, which is not the case for the microcanonical ensemble.

We can use this formula to control the temperature in our system in a very simple way. An algorithm that allows to control the temperature during an MD simulation is called a **thermostat**.

1. Scaling of velocities

We start the simulation using one of the variants of the Verlet integrator, having specified the initial positions and velocities. Usually, we know the positions from (experimental struc-

ture etc.), and velocities can be drawn randomly from the Maxwell–Boltzmann distribution corresponding to a desired temperature (using a random number generator).

In the course of the simulation, the actual temperature will deviate from the target temperature, which may be understood as the temperature of the heat bath in equilibrium with the simulated molecular system:

$$T(t) = \frac{2}{3}\frac{E_{\mathrm{kin}}(t)}{Nk} \neq T_{\mathrm{ref}} \tag{IV.8}$$

Note a discrepancy with the previous definition of thermodynamic temperature (Eq. IV.3) — temperature should correspond to the *average* of kinetic energy over time. However, Eq. IV.8 presents some sort of 'instantaneous temperature,' i.e. 'temperature' in a certain time t. This quantity will fluctuate in the course of simulation, whereas the true thermodynamic temperature is an average over this simulation.

The instantaneous temperature is just another name for the mean kinetic energy (Eq. IV.3), which is in turn determined by the velocities of the atoms. Now then, a simple idea how to bring the instantaneous temperature to the target is to *scale* the velocities of all atoms by a certain multiplicative factor λ. The required magnitude of this factor may be estimated by casting the 'new' velocities $\lambda \cdot v_i$ into the expression for the temperature and making this equal to T_{ref}:

$$\begin{aligned} T_{\mathrm{ref}} &= \frac{1}{\frac{3}{2}Nk} \cdot \frac{1}{2}\sum_i m_i \left(\lambda \cdot v_i\right)^2 = \\ &= \lambda^2 \cdot \frac{1}{\frac{3}{2}Nk} \cdot \frac{1}{2}\sum_i m_i v_i^2 = \\ &= \lambda^2 \cdot T \end{aligned} \tag{IV.9}$$

From this, the value of λ follows simply as

$$\lambda = \sqrt{\frac{T_{\mathrm{ref}}}{T}} \tag{IV.10}$$

So, we have to scale the velocities of all atoms by this factor, in order to obtain the target temperature T_{ref} exactly.

This is a very crude way of controlling the temperature. From time to time, we knock the system by rescaling the velocities, affecting the 'natural' way of evolution of the system. This is quite drastic and can lead to artifacts. More importantly, the system does not represent any canonical ensemble, i.e. its **phase space density** ρ is not that of a canonical

ensemble. As for the velocities, we never make sure that their distribution is correct (the Maxwell–Boltzmann distribution). This is very important because we calculate all properties of interest as averages:

$$\langle A \rangle = \frac{1}{Z} \int \rho \cdot A \, \mathrm{d}\vec{r} \, \mathrm{d}\vec{p} \tag{IV.11}$$

With the velocity scaling method, it could happen that our system would **sample** the phase space incorrectly, leading to wrong averages.

2. Berendsen thermostat

A way to avoid the severe turns in the dynamics is to adjust the velocities more smoothly, resigning on the target temperature to be recovered in every step (like it is done with simple scaling).

With the Berendsen coupling scheme, the simulated system is considered as coupled to an infinite thermal bath with temperature T_{ref}. We ask the temperature to change between two time steps according to:

$$\frac{\mathrm{d}T}{\mathrm{d}t} = \frac{1}{\tau} \left(T_{\mathrm{ref}} - T \right) \tag{IV.12}$$

so that the rate of change of temperature (due to the change of velocities) is proportional to the deviation of the actual temperature from the target. The constant of proportionality is the relaxation time τ, and this 1st-order differential equation corresponds to an exponential decay of temperature towards the target. Thus, we want to change the temperature by

$$\Delta T = \frac{\Delta t}{\tau} \left(T_{\mathrm{ref}} - T \right) \tag{IV.13}$$

which will be achieved by scaling the velocities by a factor λ as above:

$$\Delta T = T_{\mathrm{ref}} - T = \left(\lambda^2 - 1 \right) \cdot T \tag{IV.14}$$

$$\lambda = \sqrt{1 + \frac{\Delta t}{\tau} \left(\frac{T_{\mathrm{ref}}}{T} - 1 \right)} \tag{IV.15}$$

For $\tau = \Delta t$, we get the simple velocity scaling; for the usually applied larger values ($\tau = 0.1 - 1$ ps), the temperature of system is fluctuating around the target temperature (of the imaginary external bath).

This **fluctuation** of temperature is a desired property. For the canonical ensemble, we can calculate the *variance* of 'instantaneous temperature' T:

$$\sigma_T^2 = \left\langle (T - \langle T \rangle)^2 \right\rangle = \left\langle T^2 \right\rangle - \langle T \rangle^2 \tag{IV.16}$$

and obtain the relative variance

$$\frac{\sigma_T^2}{\langle T \rangle^2} = \frac{2}{3N} \tag{IV.17}$$

For large number of particles (atoms) N, the magnitude of fluctuations approaches zero. However, for finite-sized systems, we observe a visible fluctuation of temperature, which is indeed a feature of the canonic ensemble. So, if we kept the kinetic energy (and thus the instantaneous temperature) constant by means of the simple velocity scaling, we would not obtain the correct fluctuations.

There are several drawback with the velocity rescaling algorithms:

- It does not generate a rigorous canonical ensemble.
- Various parts of the system (different individual molecules, or solute × solvent) may exhibit different temperatures, while the temperature of the entire system is correct. This discrepancy may be maintained for extended periods of time.
- It gradually moves the energy from the fastest modes of motion to the slowest/weakest ones, violating the equipartition theorem. The bond stretching and angle bending modes are usually the fastest modes, and the loss of energy of these modes manifests itself as a 'freezing' of the molecules. On the other hand, the three translations (and, for aperiodic systems, the three rotations) of the entire system are the slowest modes, and thus those that actually gain the energy. This problem is known as the 'flying (or spinning) ice cube.'

3. Andersen thermostat

The Andersen thermostat has an entirely different working principle. From time to time, some particles (atoms) are selected to undergo a 'collision' with the particles of a heat bath, which changes their velocities suddenly. Such an algorithm exhibits a certain stochastic character.

This thermostat works as follows:

- Start the MD with a standard integrator (Verlet...)
- Select randomly the particles (atoms) that shall undergo a collision with the heat bath.
- For these particles, assign new velocities by a draw from the correct Maxwell–Boltzmann distribution. All other particles remain unaffected.

The advantage of the Andersen thermostat is that if correctly implemented, it really generates a canonical ensemble. However, for this to come true, the rate of collisions with imaginary particles must be neither too low (insufficient) nor too high (in that case, the collisions would dominate the dynamics of the system over the equations of motion).

4. Nosé–Hoover thermostat

The Nosé–Hoover thermostat rigorously represents a canonical ensemble and is thus usually the method of choice. However, it is conceptionally and mathematically slightly difficult to understand. We present the fundamental ideas here.

The heat reservoir is treated as a part of the system and is assigned an extra degree of freedom s, with which a fictitious mass Q is associated. The equations of motion are then derived for this *extended system* with $3N + 1$ degrees of freedom.

The equations of motion for the atoms are modified to

$$\ddot{r}_i = \frac{F_i}{m_i} - s \cdot \dot{r}_i \tag{IV.18}$$

with the second term formally corresponding to a kind of 'friction' due to the bath. Further, there is another equation of motion for the bath parameter s:

$$\dot{s} = \frac{1}{Q}\left(T - T_{\mathrm{ref}}\right) \tag{IV.19}$$

The strength of coupling of the real system to the bath is determined by the 'mass' parameter Q. This may be made more intuitive by introducing a time parameter τ:

$$Q = \frac{\tau^2 \cdot T_{\mathrm{ref}}}{4\pi^2} \tag{IV.20}$$

This parameter has the meaning of a *period of oscillation* of the kinetic energy between the real system and the bath. Here, it is important to note the difference between the τ in the Berendsen and in the Nosé–Hoover coupligs: The Berendsen method consists in

the exponential damping of temperature difference, with coefficient τ. In the Nosé–Hoover framework, an oscillatory relaxation of temperature is achieved, with period τ.

This way, the prerequisities of the thermostat are incorporated in the equations of motion, and the thermostat thus constitutes an integral part of the integrator, rather than an *a posteriori* correction, as is the case of all previosly mentioned ones. The Nosé–Hoover thermostat is used frequently and it can be shown that the ensemble average taken with the Nosé–Hoover ensemble is identical to that of the canonical ensemble.

C. Canonical NPT ensemble

Rather than under the condition of constant volume, chemical experiments are usually performed under constant pressure, often the atmospheric pressure. Therefore, it is of importance to be able to implement such conditions in MD simulations as well.

Similar to temperature, it is possible to calculate the pressure in the simulation. This is usually done by using the quantity called *the virial of force*:

$$\Xi = -\frac{1}{2}\sum_{i<j} \vec{r}_{ij} \cdot \vec{F}_{ij} \tag{IV.21}$$

where $\vec{r}_{ij}$ is the vector connecting atoms i and j, and $\vec{F}_{ij}$ is the force acting between these atoms. The pressure then follows as[17]

$$P = \frac{2}{3V} \cdot (E_{\text{kin}} - \Xi) = \frac{2}{3V} \cdot \left(\frac{1}{2}\sum_{i} m_i \cdot |\vec{v}_i|^2 + \frac{1}{2}\sum_{i<j} \vec{r}_{ij} \cdot \vec{F}_{ij} \right) \tag{IV.22}$$

A surprising feature of pressure calculated in this way is that it fluctuates immensely along a simulation and can even assume negative values!

Once a means to *calculate* the pressure is available, it is possible to develop an algorithm to *maintain* it at a constant value. These *barostats* are equivalents of the Berendsen or Nosé–Hoover algorithms to maintain constant temperature. Instead of velocities, it is the volume of the simulation box that is varied in order to adjust pressure; this is done either directly (Berendsen) or again via an additional degree of freedom (Parrinello–Rahman).

[17] Note the difference between the kinetic theory of gases and this definition — the idea of the particles colliding with the wall of the container is not present here.

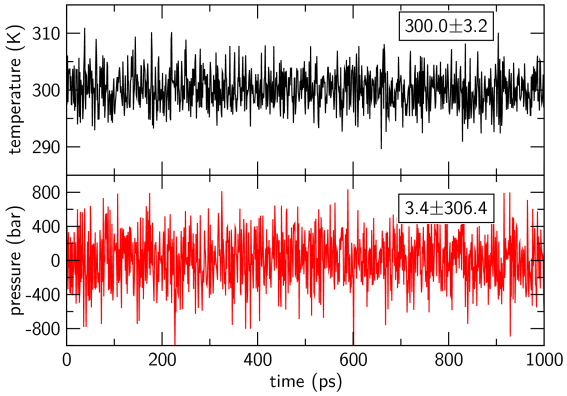

FIG. 24: Temperature and pressure in an NPT simulation of DNA oligomer in water ($T_{\mathrm{ref}} = 300$ K, $P_{\mathrm{ref}} = 1.0$ bar).

D. Exercise

Prove the equipartition theorem (Eq. IV.6) using the Maxwell–Boltzmann distribution (Eq. IV.5) as the phase-space density to evaluate the ensemble average $\left\langle v_{x,j}^2 \right\rangle_{\mathrm{ens}}$ (Eq. III.9). To do this, you have to solve integrals of the forms

$$\int_0^\infty x^2 \exp[-ax^2]\,\mathrm{d}x$$

and

$$\int_0^\infty \exp[-ax^2]\,\mathrm{d}x$$

which may be found at `http://en.wikipedia.org/wiki/Lists_of_integrals`.

V. NON-BONDED INTERACTIONS

There are several reasons to take particular care of the non-bonded interactions:

- They are a key to understand the structure, function and in particular the efficiency of action of many proteins. It is the electrostatic and/or van der Waals interaction of the protein with the ligand that is responsible for the efficiency of a reaction, color of the chromophore etc. The solvent surrounding is co-responsible for the particular structure of nucleic acids, polypeptides and proteins (hydrophobic-hydrophilic residues).

- The non-bonded interactions are treated in MM by two-body potentials, and the computational effort of $\mathcal{O}(N^2)$ dominates the overall requirements for large molecular systems. Therefore, the non-bonded (above all, the long-range electrostatic) interactions represent a good target for optimizations.

- Solvation plays a crucial role in determining the structure and function of biomolecules. However, the necessary amount of water is often extremely large, becoming the main source of computational cost.[18] Therefore, there is a need to efficiently describe the solvation effects, which are of a predominantly electrostatic character (due to the large dipole moment of the water molecule).

A. Introduction to electrostatic interaction

The electrostatic interaction energy of two point charges q and Q separated by a distance r is given by Coulomb's law

$$E^{\mathrm{el}} = \frac{1}{4\pi\varepsilon_0} \cdot \frac{q \cdot Q}{r} \tag{V.1}$$

Of importance is the concept of *electrostatic potential* (ESP), induced at the point $\vec{r}$ by a point charge Q located at $\vec{r}_1$:

$$\Phi(\vec{r}) = \frac{1}{4\pi\varepsilon_0} \cdot \frac{Q}{|\vec{r} - \vec{r}_1|} \tag{V.2}$$

[18] Typically, the simulated molecular system consists from more than 90 % of water, so that more than 80 % of the computational time is spent by calculating the forces among the (uninteresting) water molecules around the (interesting) solute.

If we know the electrostatic potential at a point $\vec{r}$ in space, then we can obtain the total electrostatic energy of a charge q at this point:

$$E^{\mathrm{el}}(\vec{r}) = \Phi(\vec{r}) \cdot q \tag{V.3}$$

In this way, we can have an 'electrostatic potential energy surface' in analogy to mechanics. There, if we know the topography of the Alps, then we immediately know the potential energy of a person with a weight of 70 kg, at any point. In a similar way, if we know the electrostatic potential induced by the atoms of a protein, then we can readily obtain for instance the binding energy of a point charge (like a metal cation) at any place. The electrostatic potential induced by a number of point charges Q_i follows simply as a sum

$$\Phi(\vec{r}) = \frac{1}{4\pi\varepsilon_0} \sum_i \frac{Q_i}{|\vec{r} - \vec{r}_i|} \tag{V.4}$$

with the energy of a point charge q at $\vec{r}$ given by Eq. V.3.

In case of a continuous charge distribution, we have to consider the charge density $\rho = Q/V$, with $\rho(\vec{r})$ being the charge density at the point $\vec{r}$. Then, $Q_i = \rho(\vec{r}_i) \cdot V_i = \rho(\vec{r}_i) \cdot \Delta V$ is the charge in the i-th volume element V_i. Summing over all elements, one obtains

$$\Phi(\vec{r}) = \frac{1}{4\pi\varepsilon_0} \sum_i \frac{\rho(\vec{r}_i) \cdot \Delta V}{|\vec{r} - \vec{r}_i|} \tag{V.5}$$

If we make the volume elements infinitesimally small, this changes to (with $\mathrm{d}^3\vec{r} = \mathrm{d}V$)

$$\Phi(\vec{r}) = \frac{1}{4\pi\varepsilon_0} \int \frac{\rho(\vec{r}_1)}{|\vec{r} - \vec{r}_1|} \, \mathrm{d}^3\vec{r}_1 \tag{V.6}$$

Finally, the electrostatic energy of a charge distribution $\rho(\vec{r})$ follows as

$$E = \frac{1}{2} \int \Phi(\vec{r}) \cdot \rho(\vec{r}) \, \mathrm{d}V = \frac{1}{8\pi\varepsilon_0} \iint \frac{\rho(\vec{r}_1) \cdot \rho(\vec{r})}{|\vec{r} - \vec{r}_1|} \, \mathrm{d}^3\vec{r} \, \mathrm{d}^3\vec{r}_1 \tag{V.7}$$

The main task is to get the electrostatic potential from a charge distribution. For that, one has to solve **Poisson's equation**

$$\nabla^2 \Phi(\vec{r}) = -\frac{\rho(\vec{r})}{\varepsilon} \tag{V.8}$$

(differential equation for Φ as a function of $\vec{r}$), or, if the permittivity ε is not constant,

$$\nabla \left(\varepsilon \nabla \Phi(\vec{r}) \right) = -\rho(\vec{r}) \tag{V.9}$$

As an example let us have a look at the ESP of a gaussian charge distribution. This distribution centered around the origin of coordinate system with a width σ is given as

$$\rho(r) = Q \cdot \frac{1}{\sigma^3 \sqrt{2\pi}^3} \cdot \exp\left[\frac{r^2}{2\sigma^2}\right] \tag{V.10}$$

The corresponding solution of the Poisson equation is

$$\Phi(r) = \frac{1}{4\pi\varepsilon} \cdot \frac{Q}{r} \cdot \mathrm{erf}\left[\frac{r}{\sqrt{2}\sigma}\right] \tag{V.11}$$

with erf being the error function. Here, if we move far enough from the center of the charge distribution (r is large), the error function converges to unity and the ESP is very near to that of a point charge placed in the origin (Eq. V.2). This is in accord with experience – a point charge and a well-localized charge distribution interact with distant charges in the same way. Actually, we need not go so far in order to see that – the error function assumes a value of 0.999 already at the distance of 2.4σ.

B. Periodic boundary conditions

The most frequent objective of MD simulations is to describe a molecular system in aqueous solution. The problem that we readily encounter is that we have to make the system as small as possible, in order to reduce the computational cost. The most straightforward way to do so is to consider only a single molecule of the solute (e.g. a protein or DNA species) with a smallest possible number of solvent (water) molecules. A typical size of such a system with several thousand water molecules is in the range of units of nanometer. Here, a serious issue occurs: while we are trying to describe the behavior of a molecule in *bulk solvent*, every point in such a small system is actually very close to the *surface*. The surface layer of a system has always properties very different from those of the bulk phase, and with such a setup, we would simulate something else that what we aim at.

An elegant way to avoid this problem is to implement the **periodic boundary conditions** (PBC). Here, the molecular system is placed in a box with a regular geometrical shape (the possibilities are listed below). This polyhedron is virtually replicated in all spatial directions, with *identical* positions (and velocities) of all particles, as shown in Fig. 25. This way, the system is made *infinite* – there is no surface in the system at all. The atoms in the vicinity of the wall of the *simulation cell* (like the black circle in Fig. 25) interact with the atoms in the neighboring replica.

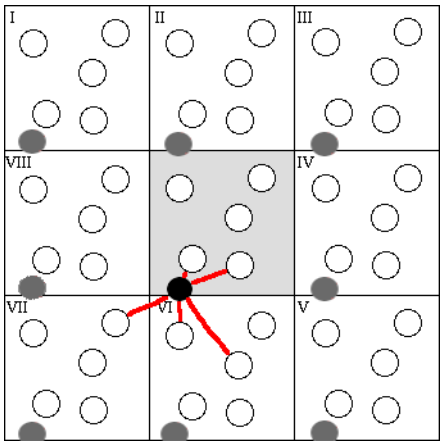

FIG. 25: Replication of the unit cell (grey) using periodic boundary conditions. Interactions of an atom (black) with the nearest images of all other atoms (red).

This method is not quite perfect as it introduces artificial periodicity in the system – all the replicas of the simulation cell look the same, making the thermodynamics of the system incorrect in principle.[19] However, this treatment is much better than simulating a too small system with artificial boundary with vacuum.

Practically, the implementation has the following features:

- Only the coordinates of the unit cell are recorded.
- If a particle leaves the box, then it enters the box from the other side.
- Carefull accounting of the interaction of the particles is necessary. The simplest approach is to make an atom interact only with the $N-1$ particles within the closest periodic image, i.e. with the nearest copy of every other particle (**minimum image convention**). This is to avoid the interaction of an atom with two different images of another atom, or even with another image of itself. If the box is cubic with boxsize L, then each atom can interact only with all atoms closer than $L/2$. Evidently, PBC have to be synchronized with the applied cut-offs, see below.

The unit cell may have a simple shape – cubic or orthorhombic, parallelepiped (specially, rhomboeder), or hexagonal prism; but also a more complicated like truncated octahedral

[19] For instance, the *entropy* of the entire system is obviously too small, because of its (wrong) translational symmetry. As a general rule, this is rarely a problem.

or rhombic dodecahedral. In the latter two cases, the corresponding PBC equations are quite complicated; the advantage of such shapes for the simulation of spherical objects (like globular proteins in solvent) is that there are no voluminous distant corners which increase the amount of solvent and thus the computational complexity (like in the case of cubic /orthorhombic box). Two-dimensional objects like phase interfaces are usually treated in a *slab* geometry.

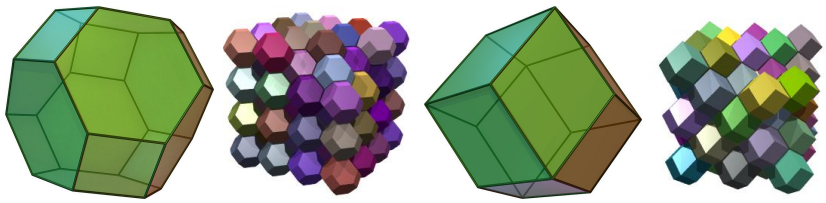

FIG. 26: Truncated octahedron (left) and rhombic dodecahedron (right).

C. Accelerating the calculation of non-bonded interactions: cut-off

As mentioned above, the evaluation of non-bonded terms becomes a bottleneck for large molecular systems, and in order to make simulations of extended systems possible, it is necessary to limit their computational cost.

The simplest and crudest approach is to neglect the interaction of atoms that are further apart than a certain distance r_c. This so-called *cut-off* is commonly used with the rapidly decaying ($1/r^6$) Lennard-Jones interaction, which indeed nearly vanish already for moderate distances r_c, commonly around 10 Å. However, with the slowly decaying electrostatic interaction ($1/r$), this would lead to a sudden jump (discontinuity) in the potential energy; even worse, this would be a disaster for the forces, which would become infinite at that point.

A better idea would be to *shift* the whole function by $V(r_c)$, so that there is no jump at r_c anymore. We would have

$$V^{\mathrm{sh}}(r) = \begin{cases} V(r) - V(r_c), & \text{for} \quad r \leq r_c, \\ 0, & \text{otherwise.} \end{cases} \tag{V.12}$$

However, the gradients (forces) are at r_c still not continuous! To eliminate this force jump,

it is possible to apply a *shift-force* potential ($V' \equiv \mathrm{d}V/\mathrm{d}r$):

$$V^{\mathrm{sf}}(r) = \begin{cases} V(r) - V(r_c) - V'(r_c) \cdot (r - r_c), & \text{for} \quad r \leq r_c, \\ 0, & \text{otherwise.} \end{cases} \tag{V.13}$$

The obvious drawback of this method is that the Coulomb energy is changed!

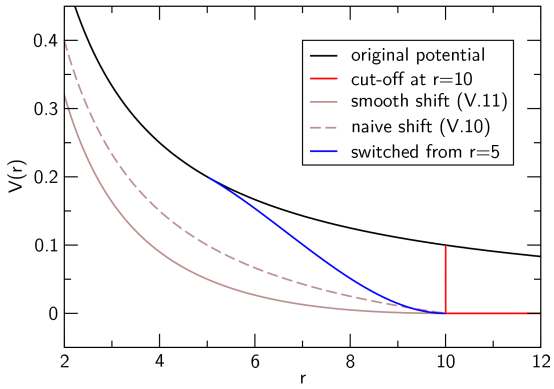

FIG. 27: Electrostatic interaction energy of two unit positive charges, evaluated using Coulomb's law and the various modifications.

A further alternative is the *switch potential*. Here, an additional potential is applied starting from a certain distance r_1, which brings the Coulomb interaction gradually to zero, as shown in Fig. 27. The drawback of this method is that the forces are altered in the cut-off region.

Both methods can be applied to either the energy or the forces: when applied to the energy, the forces follow through differentiation, and vice versa, when applied to forces, the energy follows through integration.

Generally, the cut-off schemes can be based either only on atomic distances, or on functional groups. Usually, the latter is employed to assure charge conservation in the Coulomb interaction.

D. Accelerating the calculation of electrostatic interactions: Ewald summation

In many cases, above all if highly charged molecular systems (like DNA or some proteins) are simulated, the use of cut-offs is a bad approximation. For instance, the artificial forces if using a switching function may lead to the accumulation of ions in the regions of solution in the cut-off distance (measured from DNA). Therefore, it is desirable to abandon the minimum image convention and the cut-offs, and rather sum up the long-range Coulomb interaction between *all* the replicas of the simulation cell

Let us introduce a vector $\vec{n}$, which runs over all the replicas of the cell, denoting them uniquely:

- For $|\vec{n}| = 0$, we have $\vec{n} = (0, 0, 0)$ – the central unit cell.
- For $|\vec{n}| = L$, we have $\vec{n} = (0, 0, \pm L)$, $\vec{n} = (0, \pm L, 0)$, $\vec{n} = (\pm L, 0, 0)$ – the six neighboring unit cells.
- Further, we continue with $|\vec{n}| = \sqrt{2} \cdot L$ and the 12 cells neighboring over an edge, etc.

With this vector, we can write the sum of Coulomb interactions over all replicas as

$$E^{\text{Coul}} = \frac{1}{2} \sum_{i,j} \sum_{\text{images}\,\vec{n}} \frac{q_i \cdot q_j}{|\vec{r_{ij}} + \vec{n}|} \tag{V.14}$$

for indices i and j running over all atoms in the unit cell (r_{ij} is then their distance). This expression is an infinite sum which has special convergence problems. Such a sum decays like $1/|\vec{n}|$ and is a *conditionally convergent* series, meaning that it converges ($\sum_{i=1}^{\infty} a_i < \infty$) but does not converge absolutely ($\sum_{i=1}^{\infty} |a_i|$ cannot be summed up). The problem is that the convergence of such a sum is slow and, even worse, dependent on the order of summation. So, a conditionally convergent series may add up to *any* (!) value, as shown in this example:

$$\begin{aligned}
\text{I}: \quad S &= 1 - \frac{1}{2} + \frac{1}{3} - \frac{1}{4} + \frac{1}{5} - \frac{1}{6} + \frac{1}{7} - \frac{1}{8} + \dots \\
\text{II}: \frac{1}{2}S &= \frac{1}{2} - \frac{1}{4} + \frac{1}{6} - \frac{1}{8} + \dots \\
\text{I} + \text{II}: \frac{3}{2}S &= 1 + \frac{1}{3} - \frac{1}{2} + \frac{1}{5} + \frac{1}{7} - \frac{1}{4} + \frac{1}{9} + \frac{1}{11} - \frac{1}{6} + \dots \\
&= 1 - \frac{1}{2} + \frac{1}{3} - \frac{1}{4} + \frac{1}{5} - \frac{1}{6} + \dots = S \quad \text{(sic!)}
\end{aligned} \tag{V.15}$$

Therefore, we need a clever way to evaluate the potential resulting from the interaction of all images of all charges

$$\Phi(\vec{r_i}) = \sum_j \sum_{\text{images}\,|\vec{n}|} \frac{q_j}{|\vec{r_{ij}} + \vec{n}|} \tag{V.16}$$

in order to evaluate the Coulomb energy of the charges q_i in the unit cell.

$$E^{\text{Coul}} = \frac{1}{2} \sum_i q_i \cdot \Phi(\vec{r_i}) \tag{V.17}$$

The idea of the Ewald methods is to convert the difficult, slowly convergent series to the sum of two series, which both converge much more rapidly, like

$$\sum \frac{1}{r} = \sum \frac{f(r)}{r} + \sum \frac{1 - f(r)}{r} \tag{V.18}$$

where $\sum 1/r$ represents the difficult series that we have to deal with. Whereas the terms on the right-hand side look more complicated, they actually exhibit a much more rapid convergence than $\sum 1/r$ in our case, and such an awkwardly looking 'decomposition' is the preferred way to go.

Since the summing over point charges leads to convergence problems with conditionally convergent sums, the Ewald method uses rather *normal distributions* of charge of the same magnitude:

$$q_j \;\rightarrow\; q_j \cdot \left(\frac{\alpha}{\sqrt{\pi}}\right)^3 \exp\left[-\alpha^2 \cdot |\vec{r_j}|^2\right] \tag{V.19}$$

To get the electrostatic potential induced by this smeared charge distribution, Poisson's equation (Eq. V.8) has to be solved. This leads to the potential being represented by the so-called *error function*:[20]

$$\Phi(\vec{r}) = q_j \cdot \frac{\text{erf}\left[\alpha \cdot r\right]}{r} \tag{V.20}$$

[20] The error function is defined as the definite integral of the normal distribution

$$\text{erf}[x] = \frac{2}{\sqrt{\pi}} \int_0^x \exp[-t^2]\,\mathrm{d}t$$

and the complementary error function as

$$\text{erfc}[x] = 1 - \text{erf}[x]$$

and, in the special case of $\vec{r} = \vec{o}$:

$$\Phi(\vec{o}) = q_j \cdot \frac{2\alpha}{\sqrt{\pi}} \tag{V.21}$$

If we sum up the potentials given by Eq. V.20 for all charges, we obtain

$$\Phi(\vec{r_i}) = \sum_j \sum_{\text{images}\,|\vec{n}|} q_j \cdot \frac{\text{erf}\,[\alpha \cdot |\vec{r_{ij}} + \vec{n}|]}{|\vec{r_{ij}} + \vec{n}|} \tag{V.22}$$

This has to be compared with the potential induced by the point charges (Eq. V.16). The difference between Eq. V.16 and Eq. V.22 is given by the complementary error function. The genuine potential induced by the point charges can then be expressed as

$$\Phi(\vec{r_i}) = \sum_j \sum_{\text{images}\,|\vec{n}|} q_j \cdot \frac{\text{erfc}\,[\alpha \cdot |\vec{r_{ij}} + \vec{n}|]}{|\vec{r_{ij}} + \vec{n}|} \tag{V.23}$$

$$+ \sum_j \sum_{\text{images}\,|\vec{n}|} q_j \cdot \frac{\text{erf}\,[\alpha \cdot |\vec{r_{ij}} + \vec{n}|]}{|\vec{r_{ij}} + \vec{n}|} \tag{V.24}$$

The first term V.23 called the *real-space contribution* is shown graphically in Fig. 28 (top). From a certain (quite small) distance, the point charges and the gaussian charge distributions (with opposite signs) cancel each other. This distance depends on the gaussian width α – a small gaussian width would lead to a rapid convergence.

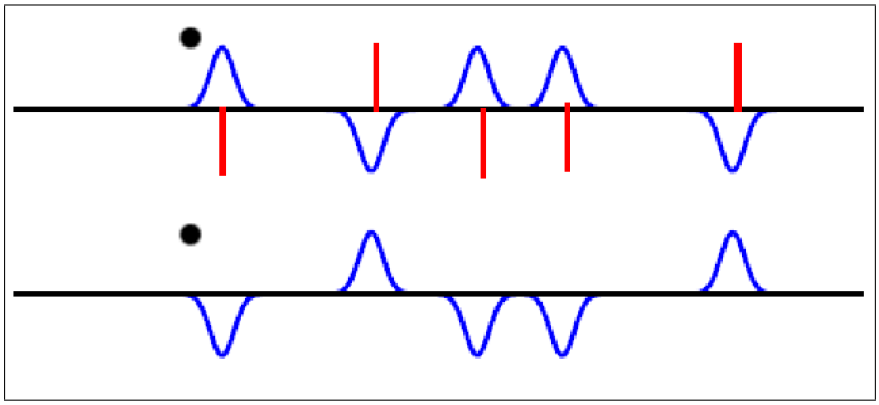

FIG. 28: Top: Real-space contribution to the Ewald sum consists of the original point charges (red) and gaussian charge distributions (blue) of the same magnitude but opposite sign. Bottom: Reciprocal-space contribution.

On the other hand, the second term V.24 called the *reciprocal-space contribution* is best evaluated in the form ($\vec{k}$ – the reciprocal lattice vector of periodic images)

$$E^{\text{rec}} = \frac{1}{2V\varepsilon_0} \cdot \sum_{\vec{k} \neq \vec{o}} \frac{1}{\vec{k}^2} \cdot \exp\left[-\frac{|\vec{k}|^2}{4\alpha^2}\right] \cdot \left|\sum_j q_j \cdot \exp[-\text{i} \cdot \vec{k} \cdot \vec{r_j}]\right|^2 \tag{V.25}$$

The usually applied *Fourier transform* techniques[21] need a large gaussian width α for fast convergence, therefore the value of α is a necessary compromise between the requirements for the real- and reciprocal-space calculations. All in all, both mentioned contributions exhibit quite favorable convergence behavior, making the evaluation of the electrostatic potential due to all periodic images feasible.

After calculating these two terms (Fig. 28), yet another one has to be taken into account: Since we have broadened charge distributions, they do interact with themselves, as shown in Fig. 29. This interaction has been brought about by the substitution of point charges by gaussian charge distributions, and thus it must be subtracted from the final result.

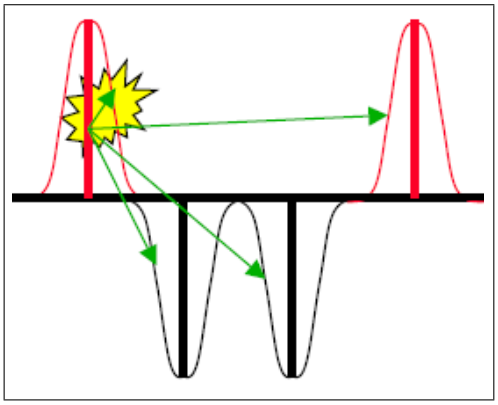

FIG. 29: Interaction of the charge with the gaussian distribution

The potential of a broadened gaussian is given by Eq. V.21, which leads to Coulomb energy of

$$E^{\text{self}} = \sum_j q_j \cdot \Phi(\vec{o}) = \sum_j q_j \cdot q_j \cdot \frac{2\alpha}{\sqrt{\pi}} \tag{V.26}$$

At the end, we have three energy contributions: one from the 'real-space' evaluation of Φ^{real} in Eq. V.23, which gives

$$E^{\text{real}} = \frac{1}{2} \sum_j q_j \cdot \Phi^{\text{real}}(\vec{r_j}) \tag{V.27}$$

one from the 'reciprocal-space' evaluation of Φ^{rec} in Eq. V.25 and the 'self-energy' in Eq. V.26, so that

$$E^{\text{Ewald}} = E^{\text{real}} + E^{\text{rec}} - E^{\text{self}} \tag{V.28}$$

[21] A popular implementation is the FFTW (Fastest Fourier Transform in the West), with a favorable computational cost scaling as $\mathcal{O}(N \cdot \ln N)$.

E. Accelerating even more: smooth particle–mesh Ewald

The Ewald summation method makes it possible to evaluate the electrostatic interaction energy though, but this comes at a quite high computational cost: The computational time scales with the number of particles as $\mathcal{O}(N^2)$, which may be improved down to $\mathcal{O}(N^{\frac{3}{2}})$. Sadly, this is still not quite efficient to make applications for huge (bio)molecular systems possible.[22] To improve the efficiency of the long-range sum, a method has been proposed in 1990s under the name particle–mesh Ewald (PME). PME combines ideas from crystallography (Ewald method) and plasma physics (particle–mesh method), and makes use of 3D fast Fourier transform techniques.

A calculation of long-range Ewald contribution with smooth PME calculation proceeds as follows:

1. The point charges are converted to Gaussian charge densities and spread on the grid in the form of 3D cardinal B-spline polynomials. These functions turned out to be a better choice than the originally used Lagrange polynomials, and the PME procedure is therefore called 'smooth'. Practically, it is just important to have the charge density evaluated on a set of discrete points (the grid). If an atom is close to the edge of the box, a corresponding part of its charge density must be taken into account at the opposite side of the box, because of PBC.

2. The complete charge density is processed with a discrete 3D fast Fourier transform technique. Then, the Poisson equation is solved in the *reciprocal space*, yielding the energy contribution E^{rec}:

$$E^{\mathrm{rec}} = \frac{1}{2} \sum_{k_1=0}^{K_1-1} \sum_{k_2=0}^{K_2-1} \sum_{k_3=0}^{K_3-1} Q(k_1, k_2, k_3) \cdot (\Theta^{\mathrm{rec}} \star Q)(k_1, k_2, k_3) \tag{V.29}$$

   Here, 3D-FFT is used to calculate the convolution $\Theta^{\mathrm{rec}} \star Q$,[23] which actually corresponds to the electric potential in reciprocal space. Θ^{rec} is something that depends on the geometry of the box and the character of the used splines, but in no way on the charge density.

[22] Compared to computational complexities of quantum-chemical methods, which are often $\mathcal{O}(N^3)$ or even much higher, this looks like heaven. However, we really need something better for MD simulations.

[23] Convolution ('Faltung') is an operation on two functions that yields another function, which may be seen as a smeared version of the former function, where the degree of smearing is controlled by the latter.

3. To evaluate the long-range contribution to forces, the electric potential in reciprocal space is inverse Fourier transformed to the real space. Since it is expressed in terms of splines (much the same way that the charge density is), its derivative can be obtained analytically – note the the splines are just 3D polynomials, and derivatives of polynomials are simple. With that, the reciprocal-space contribution is done.

4. Further, the remaining two Ewald components are needed: E^{real} and E^{self}. Both are calculated directly from the above presented expressions. An efficient implementation of the error function may be desired for E^{real}. Further, it has to be noted that the reciprocal-space energy and forces include also contributions from atom pairs that are connected with covalent bonds. These contributions are *excluded* from non-bonded energies because bonded energy terms cover these interactions, and so they have to be subtracted from the reciprocal Ewald component:

$$E^{\text{rec}}_{\text{excl}} = -\sum_{i,j}^{\text{list}} \frac{1}{4\pi\varepsilon_0} \frac{q_i \cdot q_j}{r_{ij}} \operatorname{erf}\left[\alpha \cdot r_{ij}\right] \tag{V.30}$$

Typical spacing of the grid to discretize charge densities is 1 Å; typical value of the Ewald parameter α is 2.5 Å, which makes it possible to cut off the short-ranged Ewald component at 10 Å or even at shorter distances. Another important contribution to the computational efficiency comes from the application of *neighbor lists*. Once in a while, typically every ten steps in a simulation, the distances of every pair of atoms are measured. If the distance is smaller than a pre-defined value (which is probably slightly larger than short-ranged non-bonded cutoff), the atom pair is put onto a list. Then, in the following ten steps, the short-ranged interactions (Lennard-Jones and real-space Ewald, typically) are only evaluated for the interaction pairs on this neighbor list.[24] As the number of such interactions is proportional to the number of atoms in the system, the computational complexity of the short-ranged non-bonded calculations is reduced to linear scaling ($\mathcal{O}(N)$).

The complexity of the long-range Ewald component scales as $\mathcal{O}(N \cdot \log N)$ with smooth PME: as a consequence of the extraordinary efficiency of fast Fourier transform techniques, the calculation of the long-range component does not take significantly longer than the short-ranged one, even though the method appears much more complex, at the first sight.

[24] Such neighbor lists were applied already in the landmarking work by Verlet published in 1967.

F. Explicit solvent models – water

The most simulations of biomolecules are performed with water as the solvent, to mimic the physiological or *in vitro* experimental conditions. If a not too concentrated solution is to be simulated, then the necessary amount of the solvent is quite large, often many thousand molecules.

For instance, in a typical simulation of a DNA oligomer with ten base pairs (see Fig. 30), the dimensions of the PBC box are $3.9 \times 4.1 \times 5.6$ nm, and there are 630 atoms in the DNA molecules, 8346 atoms of water and 18 sodium counterions. The macroscopic concentration of DNA in this 'sample' reaches an astonishingly large value of 18 mmol/L![25] At the same time, 86 % of all *pair interactions* are those where each of the partner atoms belongs to a water molecule,[26] and the most remaining interactions involve one atom of water. This is a huge portion, and the smallest possible at the same time, as we have the minimal number of water molecules.

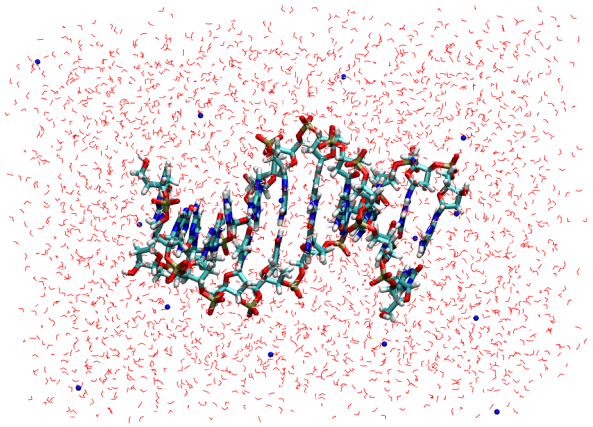

FIG. 30: Typical setup of the simulation of a DNA oligomer.

We can see that the most interactions involve water, and that is why it is necessary to turn our attention to the description of water in the simulations. The model of water must be made simple enough in order to reduce the computational complexity, but at the same time it is necessary not to compromise the accuracy of the description.

[25] Due to the commonly accepted criteria, such a box is the smallest possible. Thus, the amount of water is also the smallest possible, and the concentration the highest possible.

[26] There are 8346 water atoms, that is roughly 8346^2 interactions water–water, and 8994 atoms altogether, corresponding to 8994^2 pair interactions. The ratio of these figures is 0.86.

Many simple water models have been developed so far. They are usually *rigid*, so that the bond lengths as well as angles remain constant during the simulation. A molecule is composed of at least three sites (corresponding to atoms in this case), but possibly also as many as six sites – three atoms and optional dummy particles corresponding to a 'center' of electron density, or to the lone electron pairs on the oxygen atom.

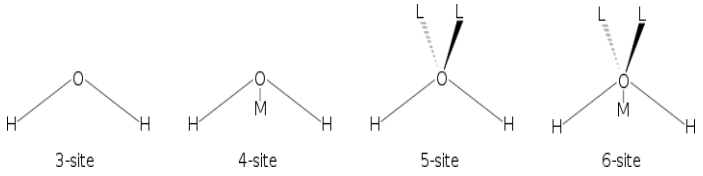

The most frequently used atomic model of water is the TIP3P (very similar is the SPC). A TIP3P molecule consists of three atoms connected by three rigid bonds. A charge is placed on every atom (-0.834 on the O and $+0.417$ on the Hs), while *only* the oxygen atom possesses non-zero Lennard-Jones parameters.[27]

If the negative charge is placed on a dummy atom M rather than on the oxygen, then the electric field around the molecule is described better. This idea is implemented e.g. in the TIP4P model.

A further improvement may be achieved if two dummy particles L bearing negative charge are placed near the oxygen atom, to mimic the lone electron pairs. Consequently, such a five-site model (like TIP5P) describes the directionality of hydrogen bonding and derived effects (radial distribution function, temperature of highest density) better than less sophisticated models.

[27] This makes it possible to additionally optimize the algorithm for the calculation of energy and forces.

VI. PRINCIPLES OF STATISTICAL MECHANICS

In the last chapters, we often used the notion that a particular ensemble generated by a simulation does not represent a canonical ensemble. This means that the phase space is sampled differently in the simulation than what would correspond to the canonical ensemble. The question is what the correct **canonical probability distribution function** looks like. First, however, we turn our attention to the microcanonical ensemble.

Interestingly, the statistics is simpler for quantum mechanics (QM) than for classical mechanics (CM). The reason is that while everything is continuous in CM, QM system may be considered to assume discrete states, which may be easier to describe. In QM, we can use the discrete energy states of molecules or quantum oscillators as simple examples, and this is what we will do in the following. The derivations will be valid for all kinds of systems though, and we will generalize for continuous energy spectra (relevant for CM) at the end, passing to phase space densities and infinitesimal elements of volume in phase space.

A. Microcanonical ensemble – microstates with constant energy

If the energy of the system is the same for every *microstate*, then we assume that every microstate of the system occurs with the same probability. With microstate we understand the particular distribution of energy among the particles in the system. Another important concept is that of the *configuration* or *macrostate*, which is defined by the occupations of energy levels by the individual *indistiguishable particles* – see Fig. 31. Importantly, since all microstates have *equal* probabilities, the probability of a configuration is given by the *number of microstates* that correspond to the configuration. Thus, to obtain the probability of a configuration, we have to count the microstates that compose the configuration.

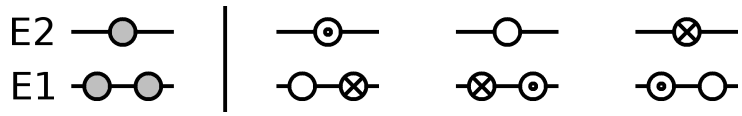

FIG. 31: A system of three particles with two available energy levels. In one of the possible *configurations* (left), two indistinguishable particles (grey) occupy the level E1 while the remaining one sits on the level E2. This configuration is composed of three *microstates* (right) which differ in the exact distribution of particles (with various symbols) among the energy levels.

1. Example – counting the microstates

Consider a system of three particles that possess three identical energy quanta altogether. We will discuss the ways to distribute these three energy quanta, see Fig. 32.

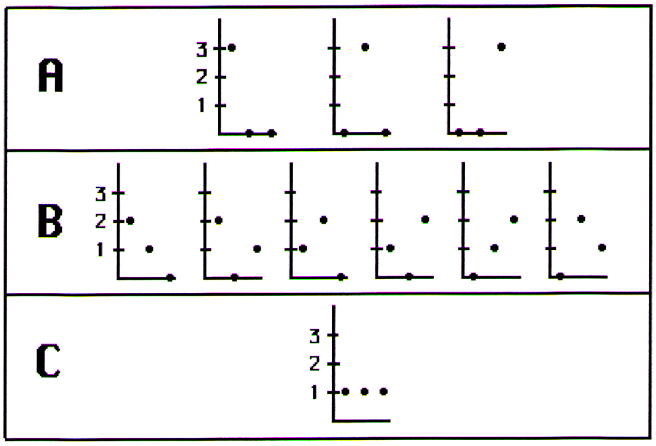

FIG. 32: Possible microstates with three equal energy quanta in the system.

Let us proceed systematically: One particle obtains l quanta, the next m, and the last one n quanta of energy, so that $l+m+n=3$. There are three possibilities to divide three energy quanta between three particles: (3,0,0), (2,1,0) and (1,1,1) – these are the configurations (macrostates) A, B and C, respectively. Now, for every configuration, we have to assign the quanta specifically to the individual particles. This goes as follows:

- We start by picking a first particle and giving it the largest number of energy quanta in the configuration. We have *3 choices*.
- Then, we assign the second-largest number of quanta to another particle. There are *2 choices*.
- There is only one particle left to accomodate the smallest number of quanta – *1 choice*.
- This makes $3 \cdot 2 \cdot 1 = 3! = 6$ choices in total, for the given configuration.

This way, we would obtain six macrostates for every configuration. However, there are energy *degeneracies* in some cases, meaning that multiple particles possess the same number of energy quanta. Then, we obtain less than six different microstates for the touched configuration. Let us analyze each configuration separately:

Cfg. A: Let us give particle α three quanta. Then, it does not matter if we choose particle β first to obtain zero quanta and particle γ next, or particle γ obtains zero quanta first and article β follows. The result is the same, as we can see in Fig. 32. There are two particles that obtain the same number of quanta, and these two assignments are thus indistinguishable, leading to an identical result. However, we have counted both ways, and to obtain the right number of microstates we have to divide by $2 \cdot 1$ (two times one redundant assignment). The number of microstates is thus

$$\frac{3!}{2!} = 3$$

Cfg. B: All three particles are given a different number of quanta, so that no degeneracy occurs actually. The number of possibilities to distribute the quanta is truly

$$3! = 6$$

Cfg. C: Trivially, there is only one microstate for this configuration. In detail, we have to assign three identical numbers of energy quanta to the particles, and so we obtain the number of microstates by dividing by 3!:

$$\frac{3!}{3!} = 1$$

Thus, there are $3 + 6 + 1 = 10$ microstates for our system; these are shown in Fig. 32.

2. Number of microstates for a configuration; the dominating configuration

Generally, if there are N particles, then there are N ways to pick the first, $N-1$ ways to pick the second etc. Thus, we have $N!$ ways to build the system. But then, if n_a particles have to accomodate the same number of energy quanta, then we have to divide by $n_a!$ to get the real number of different microstates. Consequently, we find the number of microstates W for a system of N particles in a certain configuration as

$$W = \frac{N!}{n_a! \cdot n_b! \cdot \ldots} \tag{VI.1}$$

where n_i are the numbers of particles carrying the same number of energy quanta, which we shall also call *occupation numbers* of the energy levels.

For a large number of particles N, W follows as an extensively large number, and thus it is practical to consider its logarithm:

$$\ln W = \ln \frac{N!}{n_a! \cdot n_b! \cdot \ldots} = \ln[N!] - \ln[n_a!] - \ln[n_b!] - \ldots = \ln[N!] - \sum_i \ln[n_i!] \quad \text{(VI.2)}$$

and using Stirling's approximation $\ln a! = a \cdot \ln a - a$ we find[28]

$$\ln W = N \cdot \ln N - \sum_i n_i \cdot \ln n_i \quad \text{(VI.3)}$$

We introduce the *fraction* of particles in state i, or the *probability* of a particle to be found in state i, as

$$p_i = \frac{n_i}{N} \quad \text{(VI.4)}$$

and it follows that

$$\ln W = \sum_i n_i \cdot \ln N - \sum_i n_i \cdot \ln n_i = -\sum_i n_i \cdot \ln \frac{n_i}{N} = -N \cdot \sum_i p_i \cdot \ln p_i \quad \text{(VI.5)}$$

Now, we can calculate the number of microstates corresponding to a given configuration. The crucial point is to find out which configuration has the largest *weight*, in other words, is the most likely. This will be the configuration with the largest number of correspoding microstates – the task is thus to find the maximum of W as the function of occupation numbers n_i.

Method of Lagrange multipliers

We want to find the maximum of a function $f(\vec{x})$ under the condition that certain constraints $y_k(\vec{x}) = 0$ are fulfilled. To do this, we search for the maximum of function $f - \sum_k \lambda_k y_k$ in the following way:

$$\begin{aligned} \frac{\partial}{\partial x_i}\left(f(\vec{x}) - \sum_k \lambda_k \cdot y_k(\vec{x})\right) &= 0 \\ \frac{\partial}{\partial \lambda_i}\left(f(\vec{x}) - \sum_k \lambda_k \cdot y_k(\vec{x})\right) &= 0 \end{aligned} \quad \text{(VI.6)}$$

with x_i running over the components of $\vec{x}$. So, we add the constraints to the function and set all the derivatives to zero, as usually.

[28] This approximation is sufficient. A more accurate one would be $\ln a! = a \cdot \ln a - a + \frac{1}{2}\ln[2\pi a]$.

This may be applied to the microcanonical ensemble: We are looking for the configuration with maximum weight of a system of N particles distributed among energy levels ε_i, with the total energy E. Subject to maximization is then the weight

$$\ln W = N \cdot \ln N - \sum_i n_i \cdot \ln n_i \tag{VI.7}$$

under the conditions of constant number of particles and constant energy

$$\sum_i n_i - N \;=\; 0 \tag{VI.8}$$

$$\sum_i n_i \cdot \varepsilon_i - E \;=\; 0 \tag{VI.9}$$

The application of Lagrange's method leads to the equations

$$\frac{\partial}{\partial n_i}\left[\ln W + \alpha \cdot \left(\sum_j n_j - N\right) - \beta \cdot \left(\sum_j n_j \cdot \varepsilon_j - E\right)\right] \;=\; 0 \tag{VI.10}$$

$$\frac{\partial \ln W}{\partial n_i} + \alpha - \beta \cdot \varepsilon_i \;=\; 0 \tag{VI.11}$$

once we used $-\alpha$ and β for the Lagrange multipliers. We note for the derivative of $\ln W$ with respect to n_i:

$$\frac{\partial}{\partial n_i}\left(\sum_i n_i \cdot \ln \sum_i n_i - \sum_i n_i \ln n_i\right) = \ln N + N \cdot \frac{1}{N} - \left(\ln n_i + n_i \cdot \frac{1}{n_i}\right) = -\ln \frac{n_i}{N} \tag{VI.12}$$

This leads to the solution

$$\frac{n_i}{N} = \exp\left[\alpha - \beta \cdot \varepsilon_i\right] \tag{VI.13}$$

where the parameter α may be obtained from the condition VI.8 as

$$\exp \alpha = \frac{1}{\sum_j \exp[-\beta \cdot \varepsilon_j]} \tag{VI.14}$$

so that

$$\frac{n_i}{N} = \frac{\exp[-\beta \cdot \varepsilon_i]}{\sum_j \exp[-\beta \cdot \varepsilon_j]} \tag{VI.15}$$

In the microcanonical ensemble, the parameter β might be estimated from the condition VI.9 in the form

$$\frac{E}{N} = \frac{\sum_j \varepsilon_j \cdot \exp[-\beta \cdot \varepsilon_j]}{\sum_j \exp[-\beta \cdot \varepsilon_j]} \tag{VI.16}$$

An important observation is that if the number of particles N is huge, there is always one configuration with a much larger weight than that of all other configurations. This *dominating configuration* is determined by the occupation numbers n_i obtained above, and it actually determines the properties of the system.

B. Microscopic definition of entropy

The configurations $p_i = \frac{1}{n}, \frac{1}{n}, \frac{1}{n}, \ldots$ and $p_i = 1, 0, 0, \ldots$ are the extreme cases. In the former case, $\ln W$ is maximal (for large number of states n)

$$\ln W = N \cdot \ln n$$

whereas it is minimal (zero) in the latter case

$$W = 1 \rightarrow \ln W = 0$$

(note that the formula by Stirling is not valid here).

We define the **microscopic entropy** as

$$S = k_\mathrm{B} \cdot \ln W \tag{VI.17}$$

where k_B is the universal *Boltzmann constant*. This property tells us something about the travel of the system through the configuration (phase) space. When entropy is small, few states are occupied; when it is large, many states are occupied. We may see the requirement of the maximal number of microstates corresponding to the optimal configuration in the microcanonical ensemble as the effort to reach *maximal entropy*.

Entropy can be related to the **order** in the system. When entropy is small, only a small part of the configuration space is accessible, and we consider the system to be ordered. On the other hand, when entropy is large, an extended part of the configuration space is covered. Think of the books on your desk. When they are all stapled on one place on your desk, you consider this state to be ordered, while when they are freely distributed over the entire room, you would probably call this state disordered.[29]

There is also another route to the entropy, via the so-called **information entropy**. If entropy is minimal, we have perfect knowledge about a system – it is in the state i because $p_i = 1$. If entropy reaches its maximum, we have no information at all, as every possibility is equally likely. Think again of the books in your room: if $S = 0$ then $p_1 = 1$ and you know that a particular book is on your desk. If $S = k_\mathrm{B} \cdot \ln N$, you know that the book is in one of the N possible places in your room. In this case, you have no idea where to look first!

[29] Jan Černý (Charles University in Prague, Department of Cellular Biology) once coined the term *anthropy* for "entropy of human origin" as is the case of the books on your desk.

Second law of thermodynamics

The second law claims that entropy increases in every irreversible process:

$$\frac{\partial}{\partial t} S \geq 0.$$

For a closed system, the microscopic entropy does not have this property. This can be most easily seen in a quantum mechanical example: Consider particles in a box with a wavefunction Ψ, for which we solve the Schrödinger equation

$$-\mathrm{i}\hbar\dot{\Psi} = \hat{H}\Psi$$

We can expand this in the set of eigenfunctions of the box ϕ_i

$$\Psi = \sum_i c_i \phi_i$$

to get

$$-\mathrm{i}\hbar\dot{\Psi} = \hat{H}\Psi$$

$$-\mathrm{i}\hbar \cdot c_i \dot{\phi_i} = \sum_j c_j H_{ij} \phi_j$$

We see that the probability to find the particle in state ϕ_i ($p_i = |c_i|^2$) does not change during the dynamics: $\dot{p_i} = 0$. This leads to the entropy change of

$$\frac{\partial}{\partial t} S = k_\mathrm{B} \cdot \frac{\partial}{\partial t} \left(-k_\mathrm{B} \sum_i p_i \cdot \ln p_i \right) = 0$$

The microscopic equations do not lead to any change in entropy, in contradiction with the second law. Yet, we can understand that this has to be so: We know the initial conditions of a system p_i. Then, since our equations of motion are perfectly deterministic, we know how every trajectory evolves – we know p_i at every instant! This way, the change of information entropy is zero!

In the example of your books on the desk. Initially, they are all on the desk. Since you know all the equations of motion of every book, you know exactly where every book is at any later time T. So, you have perfect knowledge of your system and the entropy change is zero!

C. Canonical ensemble – system in equilibrium with the environment

For the microcanonical ensemble, we maximized W. This way, we sought for such a combination of probabilities p_i that gave the largest number of states. Then, the entropy was maximal. In our example, W was the number of microstates for a certain configuration of particles over the energy states ε_i in the system $(\varepsilon_1, \varepsilon_2, \ldots)$. We saw that we got the largest number of states for the set of occupation numbers (2,1,0) in the configuration B. This was the dominating configuration, meaning that the most microstates belonged to it.

Now, we shall consider the system to be in thermal contact with the environment. Under such circumstances, it is the temperature rather than energy that remains constant. The **Boltzmann distribution** of p_i applies

$$p_i = \frac{\exp[-\beta \cdot \varepsilon_i]}{\sum_j \exp[-\beta \cdot \varepsilon_j]} \qquad \ln p_i = -\beta\varepsilon_i - \ln Q \tag{VI.18}$$

$$Q = \sum_j \exp[-\beta \cdot \varepsilon_j] \tag{VI.19}$$

with Q being designated as the *canonical partition function* (Zustandssumme).

To derive the meaning of β, we have to consider some basic thermodynamics. The energy as the basic thermodynamic potential depends on the extensive variables:

$$E = E(S, V, N) = TS - pV - \mu N \tag{VI.20}$$

Therefore, the *thermodynamic temperature* comes into play by means of

$$\frac{\partial E}{\partial S} = T \qquad \text{or} \qquad \frac{\partial S}{\partial E} = \frac{1}{T} \tag{VI.21}$$

Now, we can use the microscopic definition of S to calculate

$$\begin{aligned} \frac{1}{T} &= \frac{\partial S}{\partial E} = \frac{\frac{\partial S}{\partial \beta}}{\frac{\partial E}{\partial \beta}} = \frac{-k_\mathrm{B} N \frac{\partial}{\partial \beta} \sum_i p_i \ln p_i}{N \frac{\partial}{\partial \beta} \sum_i p_i \varepsilon_i} = \frac{-k_\mathrm{B} N \sum_i \frac{\partial p_i}{\partial \beta} \ln p_i}{N \sum_i \frac{\partial p_i}{\partial \beta} \varepsilon_i} = \\ &= -k_\mathrm{B} \cdot \frac{\sum_i \frac{\partial p_i}{\partial \beta} \cdot \beta\varepsilon_i + \sum_i \frac{\partial p_i}{\partial \beta} \cdot \ln Q}{\sum_i \frac{\partial p_i}{\partial \beta} \cdot \varepsilon_i} = k_\mathrm{B} \cdot \beta \end{aligned} \tag{VI.22}$$

using

$$\begin{aligned} \sum_i \frac{\partial p_i}{\partial \beta} &= \frac{\partial}{\partial \beta} \sum_i p_i = \frac{\partial}{\partial \beta} 1 = 0 \\ \frac{\partial}{\partial \beta} \sum_i p_i \ln p_i &= \sum_i \frac{\partial p_i}{\partial \beta} \ln p_i + \sum_i \frac{\partial p_i}{\partial \beta} = \sum_i \frac{\partial p_i}{\partial \beta} \ln p_i \end{aligned}$$

Finally, we have estimated the factor β as

$$\beta = \frac{1}{k_\mathrm{B}T} \tag{VI.23}$$

For continuous systems, the spacing between the energy levels becomes infinitesimally small and we can introduce the occupation density of energy states ρ

$$\rho(\vec{r},\vec{p}) = \frac{1}{Q} \cdot \exp\left[-\frac{E(\vec{r},\vec{p})}{k_\mathrm{B}T}\right] \tag{VI.24}$$

– this is the phase space density that we wish to obtain from an ergodic MD simulation! The canonical partition function in such a case is

$$Q = \int \exp\left[-\frac{E(\vec{r},\vec{p})}{k_\mathrm{B}T}\right] \mathrm{d}\vec{r}\,\mathrm{d}\vec{p} \tag{VI.25}$$

D. Canonical partition function – the way to the thermodynamic quantities

The partition function Q seems to be a purely abstract quantity at the first sight, but the very opposite is true actually! In order to characterize the thermodynamics of a system, we need just to evaluate Q and the desired thermodynamics observables follow as functions of Q, in principle. This illustrates the purpose for which the statistical thermodynamics has been developed: it makes us able to derive the (macroscopic) thermodynamic properties of a system from the knowledge of (microscopic) properties of the molecules that compose the system, with the partition function connecting the microscopic and the macroscopic.

As an example, we may calculate the mean total energy of a system from the dependence of canonical partition function Q on the parameter β or the temperature T:

$$\langle E\rangle = -\frac{\partial \ln Q}{\partial \beta} = k_\mathrm{B}T^2 \cdot \frac{\partial \ln Q}{\partial T} \tag{VI.26}$$

E. Exercises

1. You have 20 (identical) cookies and six boxes (for six of your friends, which makes the boxes distinguishable). How many possibilities do you have to distribute them as follows: {1,0,3,5,10,1} (this is the distribution of cookies in the 6 boxes). Use Eq. VI.1.
2. Prove Eq. VI.22.
3. Calculate the average energy of the classical harmonic oscillator using the Boltzmann distribution.

VII. THERMODYNAMIC PROPERTIES OF MOLECULAR SYSTEMS

We got to know the principles of statistical mechanics and its significance as the way from the properties of particles to the thermodynamic properties of ensembles. The role of the mediator of information is played by the *partition function*.

In this chapter, we will see

- how the thermodynamic equilibrium is characterized, which quantities are of interest and how these may be derived from the partition function
- how the partition function is connected to the phase-space density
- how to derive the ensemble partition function from the partition function of a single molecule
- that MD simulation provides an alternative way to thermodynamic quantities
- that it is difficult to obtain free energies from normal simulations

A. Driving forces of thermal processes. Equilibrium

Classical thermodynamics introduces the concepts of *thermodynamic equilibrium* and *spontaneous process*, and identifies the quantites that are maximized/minimized in the equilibrium and show a definite change in the course of a spontaneous process. So if the system does not exchange energy with the surroundings, as is the case in the microcanonical ensemble, the equilibrium is reached if *entropy* S is maximized. Consequently, a process proceeds spontaneously whenever it is accompanied by an increase of entropy ($\Delta S > 0$).

The case of microcanonical ensemble is simple as there is no exchange of energy with the surroundings, but the situation is more complex when we pass to the canonical ensemble. Here, we have to consider a *super-system* composed of the system of interest *together* with the surroundings, once we wish to identify the equilibrium and the spontaneity of processes. Of course, it is impossible to estimate the entropy of such a super-system, as we cannot handle the whole universe in a calculation. Therefore, we have to search for an alternative criterion of equilibrium and spontaneity.

A way to concentrate on our molecular system and to leave out the surroundings, is to introduce a new thermodynamic function. The key function is the *Helmholtz free energy* F in a canonical ensemble, and the *Gibbs free energy/enthalpy* G in an NPT ensemble.

$$F = U - TS \qquad\qquad G = H - TS = U + pV - TS \tag{VII.1}$$

The equilibrium state exhibits a minimum of Helmholtz (or Gibbs) energy, and F (or G) *decreases* in the course of a spontaneous process. Free energy/enthalpy is the fundamental property that we are interested in because (we discuss only F here; the same apply to G)

- $F = F(T, V)$: F depends on the variables T and V, which are experimentally controllable, while $U = U(S, V)$ depends on S and V. We have no means to control entropy in experiments. In particular, F is the energetic property which is measured when T and V are constant, a situation we often model in our simulations.

- $\Delta F = F_f - F_i = W^{\max}$ is the *maximum amount of work* that the system can perform between an initial (i) and final (f) state. In the first law $\mathrm{d}U = \delta Q + \delta W$, we can cast in a formulation of the second law $T\mathrm{d}S \geq \delta Q$ to obtain[30]

  $$\mathrm{d}U \leq T\mathrm{d}S + \delta W \tag{VII.2}$$

  and for the amount of work

  $$\delta W \geq W^{\max} = \mathrm{d}U - T\mathrm{d}S = \mathrm{d}F \tag{VII.3}$$

  Therefore, the work is always greater or equal the change of free energy.[31] In other words, a certain amount of internal energy $\mathrm{d}U$ can *never* be converted to work, because a part of it is always lost as an increase of entropy.

- In principle, it does not make sense to search for the minimum of internal energy U (as often done in quantum-chemical studies). The energy is conserved though, but within the entire universe (the universe thus samples a microcanonical ensemble). Once we have defined a quantity like *free energy*, the idea of a minimization procedure is restored: Systems will evolve in order to minimize the free energy; however, this is nothing else than the maximization of entropy of the super-system (universe).

[30] This inequality becomes an equality for a *reversible* process.

[31] Note that if the system *performs* work, then the value of δW is *negative*. So, the value of $W^{\max}$ is the *most negative possible*, and its magnitude represents truly the maximum possible work.

B. Thermodynamic functions from statistical mechanics

Now, we want to apply the formalism to calculate enthalpies and free energies of molecules. The main trick we learned is that we only have to calculate the **partition function** Q, since we get all thermodynamic functions from there:[32]

$$U = \langle E \rangle = k_\mathrm{B} T^2 \frac{\partial \ln Q}{\partial T} \tag{VII.4}$$

$$S = k_\mathrm{B} T \cdot \frac{\partial \ln Q}{\partial T} + k_\mathrm{B} \cdot \ln Q \tag{VII.5}$$

$$F = -k_\mathrm{B} T \cdot \ln Q \tag{VII.6}$$

$$P = k_\mathrm{B} T \cdot \left(\frac{\partial \ln Q}{\partial V} \right)_T \qquad \text{(equation of state)} \tag{VII.7}$$

$$H = U + pV \tag{VII.8}$$

$$G = F + pV = H - TS \tag{VII.9}$$

Therefore, the computational problem reduces to the need to determine Q.

The problem of evaluation of the partition function may be greatly simplified for two special cases. If the system is composed of n *identical distinguishable particles*, as is the ideal crystal, then the ensemble partition function Q is obtained from the *molecular partition function* q as

$$Q = q^n \tag{VII.10}$$

In the other case, if the n particles composing the system are *identical and indistinguishable*, as in the gas phase, then another relation is valid:

$$Q = \frac{q^n}{n!} \tag{VII.11}$$

Note the immensely reduced need of effort that we have to make in these cases: It is only necessary to evaluate the *molecular partition function* q for *one* molecule of the substance in the studied system, and we obtain directly the thermodynamic quantities of interest, via the ensemble partition function Q.

[32] Michal Otyepka (Palacký University Olomouc, Department of Physical Chemistry): "You just need to hold the partition function at the tail, and then you have everything!"

C. Discrete and continuous systems

1. Discrete systems

So far, we often (typically, but not necessarily) considered a quantum-mechanical system, i.e. a system with *discrete energy levels* E_i. For that, we found a partition function

$$Q = \sum_i \exp[-\beta E_i] \tag{VII.12}$$

and a (discrete) Boltzmann distribution function

$$p_i = \frac{1}{Q} \exp[-\beta E_i] \tag{VII.13}$$

which is the probability to find the system in state i with energy E_i.

A prominent example is the harmonic oscillator with energy levels

$$E_i = \left(i + \frac{1}{2}\right) \cdot \hbar\omega \tag{VII.14}$$

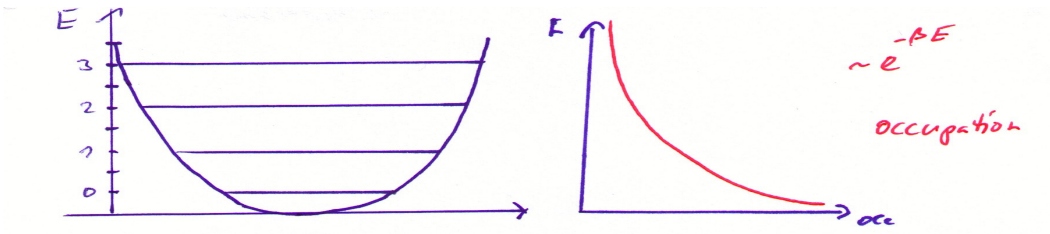

FIG. 33: States of a quantum-mechanical harmonic oscillator. Thermal distribution of energy over the vibrational states leads to the number of microstates and a value of entropy/free energy.

2. Continuous systems

On the other hand, we discussed the dynamics of molecules, where temperature allows to sample a certain part of the conformational space of a protein. This means, that at a certain temperature only certain values of the coordinates (r_i) and also only certain values of momenta (p_i, cf. the Maxwell distribution) are reached, and thus only a **part of the phase space is sampled**. The phase space density $\rho(\vec{r}, \vec{p})$ gives the probability to find a system at positions $\vec{r}$ and momenta $\vec{p}$. Now, since we force the dynamics to generate a canonical ensemble, we know the following:

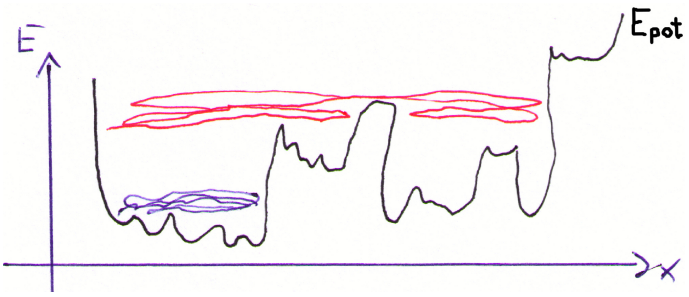

FIG. 34: Complex energy landscape $E(x, p)$. Note that the p-axis is not shown; for $p = 0$, the system 'lies' on the potential energy curve (black line); for $p > 0$, various trajectories (sampling various phase-space volumes) are accessible indicated by the blue and red curves.

- Every point in the phase space has potential energy depending on the coordinates $\vec{x}$ ($V = V(\vec{x})$), coming from the force field, and kinetic energy related to $\vec{p}$. This way, every point $(\vec{r}, \vec{p})$ in the phase space is assigned a certain energy value.

- From the canonical distribution we know that the probability to find the system in a state with energy E is

$$p(\vec{r}, \vec{p}) = \rho(\vec{r}, \vec{p}) = \frac{1}{Q} \cdot \exp\left[-\frac{E(\vec{r}, \vec{p})}{k_\mathrm{B}T}\right] \tag{VII.15}$$

- To obtain the partition function Q, we now have to substitute the summation (in the discrete case) by an integral over the entire phase space:

$$Q = \int \exp\left[-\frac{E(\vec{r}, \vec{p})}{k_\mathrm{B}T}\right] \mathrm{d}\vec{x}\,\mathrm{d}\vec{p} \tag{VII.16}$$

The canonical distribution function gives the probability of finding the system at a point $(\vec{r}, \vec{p})$ in the phase space. Typically, the system will be only sampling a part of the phase space, with non-zero probabilities, as shown schematically in Fig. 35.

At the start of an MD simulation, we only know the form of the potential (force field) and kinetic energy. **The fundamental aim of MD simulations is to render the correct phase-space density.** Then, we obtain the thermodynamic potentials U, H etc. as time averages, provided the simulation is ergodic. However, this holds only if the phase-space density is truly that of the canonical ensemble (if the simulation sampled the canonical ensemble correctly); otherwise, the derivations in the last chapter would not be valid!

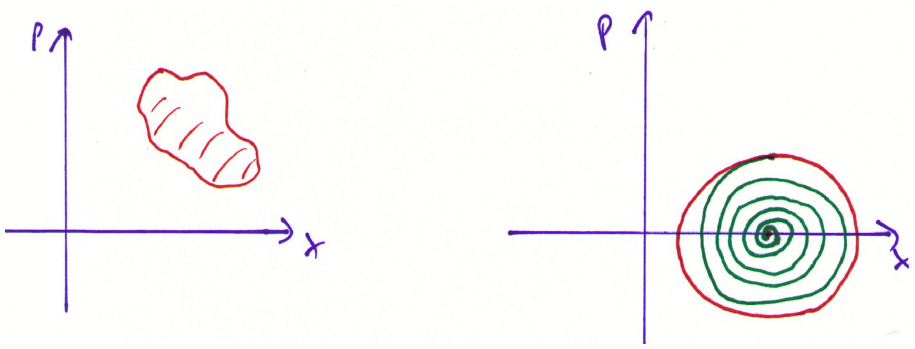

FIG. 35: Part of the phase space sampled in MD. Example – classical harmonic oscillator.

Thus, we have the following to do:

- Perform an MD simulation to get a trajectory in phase space. We have to set up the simulation in order to sample the canonical ensemble; for instance, we have to choose the right thermostat! Only then will the distribution of points of the trajectory in the phase space be the same as that given by the canonical distribution.

- Now we can use the ergodic theorem: The time series we get can be used to evaluate time averages of thermodynamic quantities, which will be equal to the ensemble averages of those.

In quantum chemistry, we commonly use both the discrete and the continuous situation, to compute thermal corrections to the total energy E in order to get H, S, F or G. Here, we consider the two situations as follows:

- If we have simple molecules (like benzene) with only one local minimum of energy, we can use the harmonic approximation. The energy is given by the ground state energy of the molecule plus the translational, rotational and vibrational contributions to the energy. Based on the vibrational Hamiltonian, we compute the Boltzmann distribution, then the partition function and in turn the thermodynamic potentials.

- For molecules where a multitude of local minima can be reached, a single minimum does not make sense any more. Here, we perform MD simulations to sample the phase space appropriately and evaluate the time averages of the thermodynamic quantities of interest.[33]

[33] These will be equal to the ensemble averages due to the ergodic theorem.

D. Vibrational contribution to the thermodynamic functions

Consider a simple molecule with one or only a small number of well characterized minima. For one of the minima, we can calculate the electronic energy (here: the force field energy), the translational, rotational and vibrational energy, i.e. we have:

$$E = E^{\mathrm{el}} + E^{\mathrm{trans}} + E^{\mathrm{rot}} + E^{\mathrm{vib}} \tag{VII.17}$$

The partition function follows as

$$\begin{aligned} Q &= \exp\left[-\beta\left(E^{\mathrm{el}} + E^{\mathrm{trans}} + E^{\mathrm{rot}} + E^{\mathrm{vib}}\right)\right] = \\ &= \exp[-\beta E^{\mathrm{el}}] \cdot \exp[-\beta E^{\mathrm{trans}}] \cdot \exp[-\beta E^{\mathrm{rot}}] \cdot \exp[-\beta E^{\mathrm{vib}}] = \\ &= Q^{\mathrm{el}} \cdot Q^{\mathrm{trans}} \cdot Q^{\mathrm{rot}} \cdot Q^{\mathrm{vib}} \end{aligned} \tag{VII.18}$$

Since we often need $\ln Q$, we have:

$$\ln Q = \ln Q^{\mathrm{el}} + \ln Q^{\mathrm{trans}} + \ln Q^{\mathrm{rot}} + \ln Q^{\mathrm{vib}} \tag{VII.19}$$

1. Electronic states

We usually consider the molecule to occupy the ground electronic state only, as the electronic excitation energy is quite high. Then, we set the ground state energy arbitrarily to zero ($E^{\mathrm{el}}(0) = 0$) and the electronic partition function is equal to unity:

$$Q^{\mathrm{el}} = \exp[-\beta E^{\mathrm{el}}(0)] + \exp[-\beta E^{\mathrm{el}}(1)] + \ldots \approx 1 + 0 + \ldots = 1 \tag{VII.20}$$

This unity may be neglected in the product in Eq. VII.19.

2. Translational and rotational contribution

These contributions will not discussed in detail. They are calculated for the quantum-mechanical particle in a box and for a quantum-mechanical rotator. One obtains

$$U^{\mathrm{trans}} = \frac{3}{2} k_{\mathrm{B}} T \tag{VII.21}$$

$$U^{\mathrm{rot}} = \frac{3}{2} k_{\mathrm{B}} T \tag{VII.22}$$

For both kinds of motion, also entropic contributions can be calculated. With those, we can estimate free energies.

3. *Vibrational contribution*

To get this contribution, we have to optimize the geometry of a molecule and calculate its vibrational frequencies ω_k. Each normal mode represents one harmonic oscillator k. For example, a water molecule has three modes, $k = 1, 2, 3$. Every harmonic oscillator has energy levels

$$E_k^m = (m + \frac{1}{2}) \cdot \hbar\omega_k \tag{VII.23}$$

where $E_k^0 = \frac{1}{2}\hbar\omega_k$ is called the *zero point vibrational energy.* Let us evaluate the partition function of one harmonic oscillator:[34]

$$\begin{aligned} Q_k &= \sum_{m=0}^{\infty} \exp\left[-\beta\left(m + \frac{1}{2}\right)\hbar\omega_k\right] = \exp\left[-\frac{1}{2}\beta\hbar\omega_k\right] \cdot \sum_{m=0}^{\infty} \exp\left[-\beta m\hbar\omega_k\right] = \\ &= \frac{\exp\left[-\frac{1}{2}\beta\hbar\omega_k\right]}{1 - \exp\left[-\beta\hbar\omega_k\right]} \end{aligned} \tag{VII.24}$$

Then, we can derive the internal energy U_k

$$\ln Q_k = -\frac{1}{2}\beta\hbar\omega_k - \ln\left[1 - \exp[-\beta\hbar\omega_k]\right] \tag{VII.25}$$

$$U_k = -\frac{\partial \ln Q_k}{\partial\beta} = \frac{1}{2}\hbar\omega_k - \left(\frac{\hbar\omega_k \exp[-\beta\hbar\omega_k]}{1 - \exp[-\beta\hbar\omega_k]}\right) = \hbar\omega_k\left(\frac{1}{2} + \frac{1}{\exp[\beta\hbar\omega_k] - 1}\right) \tag{VII.26}$$

We have to do this for the $N - 6$ vibrational degrees of freedom of the molecule – each molecule thus consists of $N - 6$ harmonic oscillators. Then, we get for the internal energy

$$U = \sum_{k=1}^{N-6} U_k = \sum_{k=1}^{N-6} \hbar\omega_k\left(\frac{1}{2} + \frac{1}{\exp[\beta\hbar\omega_k] - 1}\right) \tag{VII.27}$$

The zero-point vibrational energy contributions are not temperature dependent, and they are usually added to the electronic part of the energy (see above), so that the vibrational part of the internal energy is defined merely as

$$U^{\text{vib}} = \sum_{k=1}^{N-6}\left(\frac{\hbar\omega_k}{\exp[\beta\hbar\omega_k] - 1}\right) \tag{VII.28}$$

and for the corresponding entropy contribution and the Helmholtz free energy we find

$$S^{\text{vib}} = k_{\text{B}} \ln Q^{\text{vib}} + \frac{U^{\text{vib}}}{T} = k_{\text{B}} \sum_{k=1}^{N-6}\left(\frac{\beta\hbar\omega_k}{\exp[\beta\hbar\omega_k] - 1} - \ln\left[1 - \exp[-\beta\hbar\omega_k]\right]\right) \tag{VII.29}$$

$$F^{\text{vib}} = -k_{\text{B}}T \ln Q^{\text{vib}} = \sum_{k=1}^{N-6} k_{\text{B}}T \ln\left[1 - \exp[-\beta\hbar\omega_k]\right] \tag{VII.30}$$

[34] In the last step, we use the formula for the sum of geometric series ($\sum_{k=0}^{\infty} x^k = \frac{1}{1-x}$).

4. The pV term

To obtain the *enthalpy* H, we have to add the contribution of pV to the internal energy. This term would be difficult to estimate unless we did not adopt the ideal gas approximation:

$$PV = Nk_{\mathrm{B}}T \tag{VII.31}$$

Then, we obtain the enthalpy and the Gibbs free energy:

$$H = U + pV = U + Nk_{\mathrm{B}}T \tag{VII.32}$$

$$G = F + pV = F + Nk_{\mathrm{B}}T \tag{VII.33}$$

Many quantum chemical as well as molecular mechanics programs (like Gaussian, respectively CHARMM) perform a calculation of the thermal contributions by default, whenever vibrational analysis is requested. This is because the calculation of vibrational frequencies is the most time consuming step and the evaluation of thermodynamic functions is done virtually 'for free'.

E. Aiming at free energies

For a molecule with many conformations, we have to approach the phase-space density with MD simulations ($\vec{r} = \{r_1, \ldots, r_{3N}\}$, $\vec{p} = \{p_1, \ldots, p_{3N}\}$):

$$\rho(\vec{r}, \vec{p}) = \frac{\exp[-\beta E(\vec{r}, \vec{p})]}{Q} \tag{VII.34}$$

which is the (canonical) probability of finding the system at the point $(\vec{r}, \vec{p})$.

The central point now is, how long an MD simulation we can perform. If we integrate the equations of motion for 1 ps, we will have 1,000 points in the trajectory; if we extend it to 1 ns, we already have a million points etc. Here, a nanosecond is close to the limit of what can be done!

Imagine we have simulated for 1 ps: Then, we will barely have sampled the points $(\vec{r}, \vec{p})$ for which $\rho(\vec{r}, \vec{p}) \leq \frac{1}{1000}$, meaning that any points with high energy will hardly be reached, while the low-energy region may already have been sampled very well.

We get a problem when we are willing to calculate the averages of thermodynamic potentials like the free energies. It is necessary to think about the phase-space density $\rho(\vec{x}, \vec{p})$,

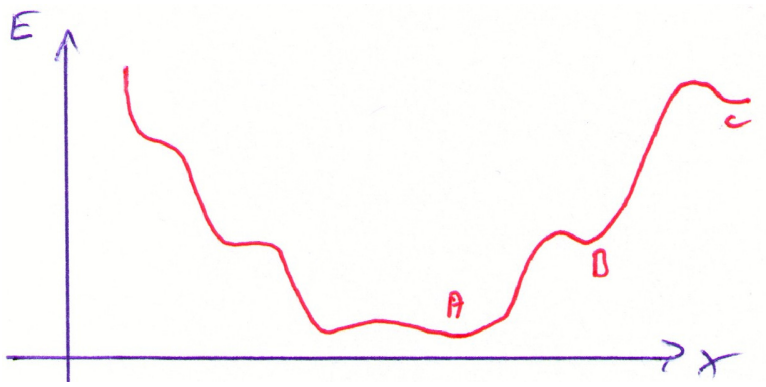

FIG. 36: High-energy points B and C may not be sampled sufficiently in an MD simulation.

which tells us how often the MD trajectory passes through the particular point $\{\vec{x}, \vec{p}\}$. If we do not sample long enough, we will not have visited the points with low ρ (due to high energies $E(\vec{r}, \vec{p})$), and we will miss the corresponding large energies in the averaging.

One could think that since we miss large values, the average of any quantity will be systematically wrong. Interestingly, this is not very serious for the internal energy, because the canonical probability distribution

$$\rho(\vec{r}, \vec{p}) = \frac{\exp[-\beta E(\vec{r}, \vec{p})]}{Q} \tag{VII.35}$$

is very small if the energy is high due to the exponential dependence, and the neglect of such points causes no large error.

For free energies, however, the situation is much worse, as we can write

$$\begin{aligned} F &= -k_\mathrm{B}T \ln Q = k_\mathrm{B}T \ln \frac{1}{Q} = k_\mathrm{B}T \ln \left[\frac{c^{-1} \cdot \iint \exp[\beta E(\vec{r}, \vec{p})] \cdot \exp[-\beta E(\vec{r}, \vec{p})] \, \mathrm{d}\vec{r} \, \mathrm{d}\vec{p}}{Q} \right] = \\ &= k_\mathrm{B}T \ln \iint \exp[\beta E(\vec{r}, \vec{p})] \cdot \rho(\vec{r}, \vec{p}) \, \mathrm{d}\vec{r} \, \mathrm{d}\vec{p} - \ln c = k_\mathrm{B}T \ln \left\langle \exp \left[\frac{E}{k_\mathrm{B}T} \right] \right\rangle - \ln c \end{aligned} \tag{VII.36}$$

(where the complicated integral in the numerator on the first line is just a resolution of the integral of unity, which corresponds to $c^{-1} = (8\pi^2 V)^N$; the canonical probability distribution ρ was cast). Now, we have a real problem: The large energy values enter an exponential term in the calculation of free energy, and so the high-energy regions may contribute significantly. So, if we have too few points in these high-energy regions, we may find large errors in the calculated averages. Therefore, a really good idea is needed here to improve the sampling.

VIII. ANALYSIS OF THE SIMULATION

A. Thermodynamic properties

As explained in detail earlier, we are able to obtain *time averages* of thermodynamic quantites from MD simulation. As long as the simulation is ergodic, these correspond to the *ensemble averages*, which are the values observed (in an experiment).

Some quantities may be evaluated directly, like the total (internal) energy:

$$U = \langle E \rangle_t \tag{VIII.1}$$

An interesting point is that the magnitude of *fluctuations* of certain quantities determines other thermodynamic properties of interest. So, it can be derived (from the 2nd derivative of partition function) that the isochoric *heat capacity* is given by the variance of total energy:

$$C_V = \left(\frac{\partial U}{\partial T}\right)_V = \frac{\sigma_E^2}{k_\mathrm{B} T^2} = \frac{\langle E^2 \rangle - \langle E \rangle^2}{k_\mathrm{B} T^2} \tag{VIII.2}$$

Using this expression, we can obtain the heat capacity of the system in a very elegant way from a single NVT simulation at a given temperature.

B. Structural data

1. Single molecule immersed in solvent

In the area of biomolecular simulation, we usually deal with a single solute molecule (protein, DNA) immersed in solvent. The solute molecule is then the central object while our interest in the solvent is merely secondary. In such a case, we obviously wish to characterize the structure of the solute.

A common way to do so is to calculate the *average structure* of the molecule. The coordinates of every atom $\vec{r}_i$ are obtained as the arithmetic mean from the snapshots n saved along the MD trajectory:

$$\vec{r}_i = \frac{1}{N} \sum_{n=0}^{N} \vec{r}_i^{(n)} \tag{VIII.3}$$

This is a very clear and simple concept, which often yields a reasonable result. However, it may be problematic in some situations.

Imagine there are freely rotatable single bonds in the molecule, e.g. methyl groups in thymine (DNA) or in alifatic side chains (proteins). Then, be averaging of the coordinates, all three hydrogens of the methyl groups collapse to a single point, due to the free rotation of the group. This is just a minor issue; hydrogen atoms are usually excluded from the structure analysis, which is the restricted to the *heavy atoms* (C, N, O etc.).

A more serious issue would come up if the entire molecule rotated in the box from the initial orientation to another, in the course of the simulation. Then, the average structure of the molecule would be complete nonsense. To remedy this, the calculation of average structure usually involves the *fitting* of every snapshot to a reference structure[35] – the molecule (regarded as a rigid body) is translated and rotated so that its *RMS deviation* from the reference structure is minimized. Then, the coordinates are taken to the sum in Eq. VIII.3.

The most unfavorable situation comes up if the molecule does not oscillate around a single structure. This may happen if the free energy surface (FES) features several available minima, which correspond to different structures. Then, the molecule will assume all these structures for certain periods of time, and the averaging of coordinates will most likely lead to an absurd structure, not corresponding to any of the minima on the FES. In such a case, it may be desirable to perform the averaging of structure on separate intervals of the trajectory, where the individual minima are being sampled.

The average structure of the molecule provides valuable information, however of an inherently static character. The development of the structure in time may be followed very simply by evaluating the *root mean square deviation* (RMSD) of the structure in time t with respect to a suitable reference structure $\vec{r}^{\,\mathrm{ref}}$:

$$\mathrm{RMSD}(t) = \sqrt{\frac{1}{N}\sum_{i=1}^{N}\left|\vec{r}_i(t) - \vec{r}_i^{\,\mathrm{ref}}\right|^2} \qquad \text{(VIII.4)}$$

The reference structure may be for instance the starting one or the average structure obtained as in Eq. VIII.3, see Fig. 37 left. Another possibility is to measure RMSD from another geometry of interest, to see if the structure of the molecular system approaches this geometry during the simulation. In case of a DNA oligonucleotide, we may look how the structure oscillates between A-like and B-like (Fig. 37 right).[36]

[35] The starting structure may be taken as the reference.
[36] Similarly, the structure of a peptide may be compared with the idealized geometries of α-helix and β-sheet.

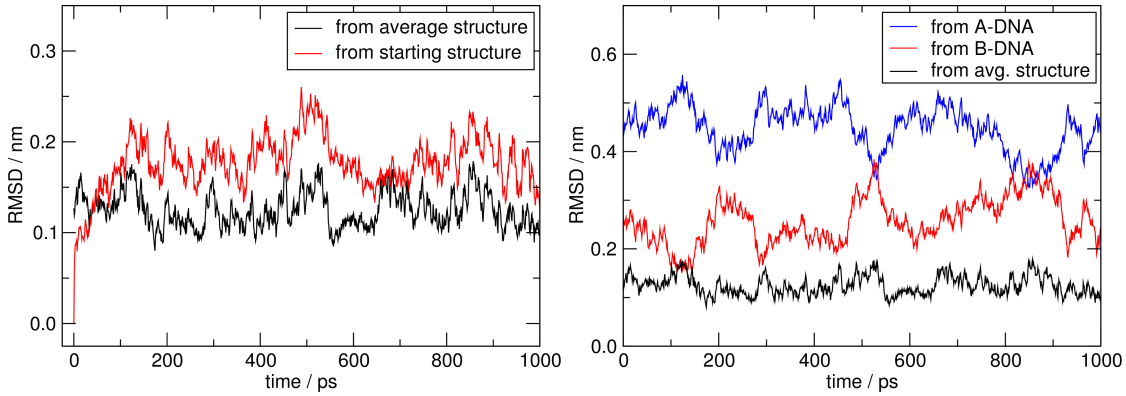

FIG. 37: RMSD of non-hydrogen atoms of a DNA oligonucleotide from given geometries.

Another quantity describing the dynamics and flexibility is the *root mean square fluctuation* (RMSF) of atomic positions, or in other words the square root of mean *variance* of the position of atom i:

$$\mathrm{RMSF}_i = \sqrt{\left\langle |\vec{r}_i - \langle \vec{r}_i \rangle|^2 \right\rangle} \tag{VIII.5}$$

This value tells us how vigorously the position of every individual atom fluctuates.

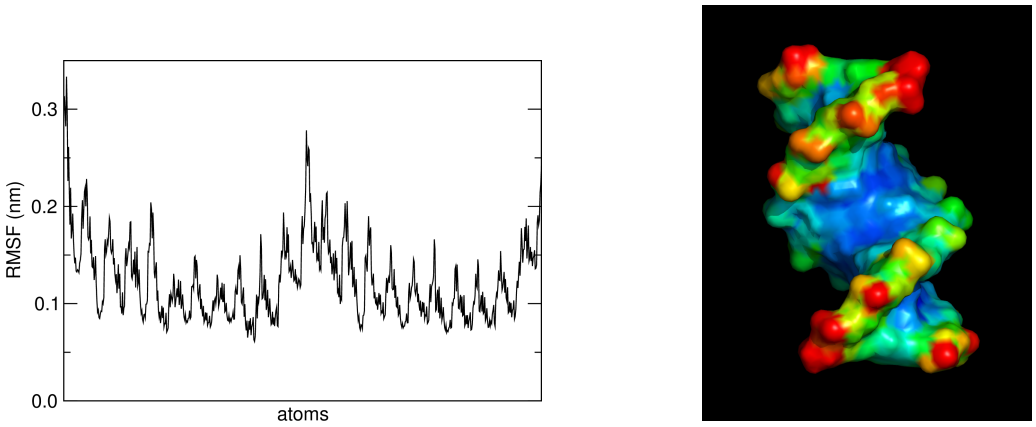

FIG. 38: RMSF of atomic positions in DNA oligonucleotide (blue < green < yellow < red).

RMSF may be converted to the *B-factor*, which is an observable quantity in diffraction experiments (X-ray etc.):

$$B_i = \frac{8}{3}\pi^2 \cdot \mathrm{RMSF}_i^2 \tag{VIII.6}$$

Typically, the structure files deposited in the PDB contain these B-factors for all atoms. However, the comparison of B-factors obtained from a simulation with those from diffrac-

tion experiments may not be quite straightforward, as the simulation parameters and the experimental conditions may differ largely.

It is worth mentioning several further means of structure analysis which are used above all in the studies of proteins. It is possible to measure simply the distances of the individual amino-acid residues, represented for instance by their centers of mass or by the C^{α} atoms. This way, a *distance matrix* is constructed, which may be either time-dependent or averaged over the simulation. Distance matrices found their use in bioinformatics, and various tool have been developed for their analysis.

A classical means of analysis of peptide/protein structure is the *Ramachandran plot* – a two-dimensional histogram of dihedral angles ϕ and ψ along the protein backbone. In a structural analysis of a protein, any amino acids lying outside of the common regions in the Ramachandran plot (as in Fig. 39) would be paid special attention. Simulation programs usually contain tools to generate Ramachandran plots automatically.

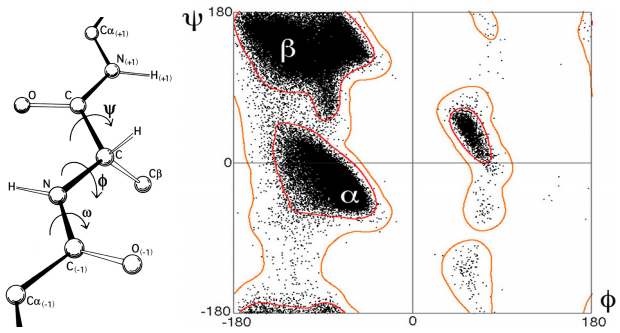

FIG. 39: Dihedral angles ϕ and ψ; Ramachandran plot from analysis of a protein databank.

2. *Fluids*

The situation in a neat fluid (liquid or gas), for example pure argon or water, is different. Rather than one prominent molecule, we have many molecules in the system which are all equally important. A useful way to describe the structure of such a system are the *radial distribution functions*. These describe how the molecular (or atomic) density varies as a function of the distance from one particular molecule (or atom). Consider a spherical shell of thickness δr at a distance r from a chosen atom, with volume of $\delta V \approx 4\pi r^2 \cdot \delta r$. We count the number of molecules (atoms) present in this shell n, and divide this by δV to obtain a

kind of 'local density' at the distance r. The dimensionless *pair distribution function* $g(r)$ is then obtained by dividing by the ideal-gas distribution, which is the macroscopic density. It determines how likely it is to find a molecule (atom) in the distance of r from the reference particle, compared to the homogeneous distribution in the ideal gas:

$$g(r) = \frac{n/\delta V}{\rho} = \frac{n}{4\pi r^2 \cdot \delta r} \cdot \frac{1}{\rho} \tag{VIII.7}$$

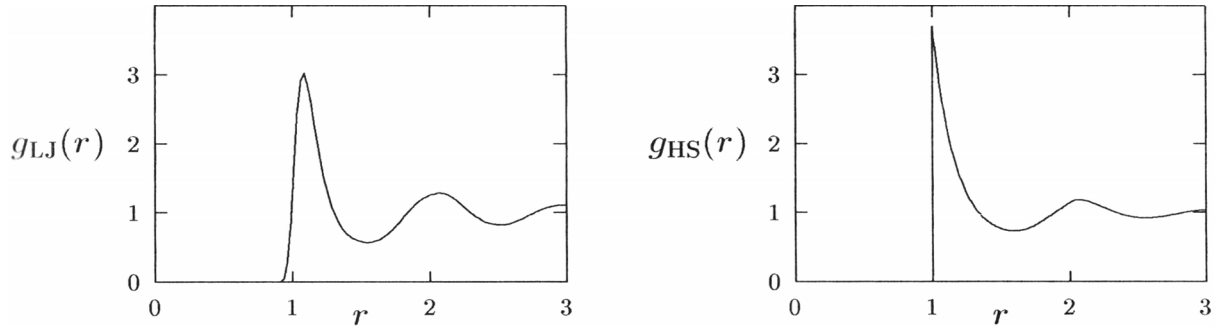

FIG. 40: Radial distribution function for a Lennard-Jones fluid near the triple point (left) and for a hard-sphere fluid (right). Reprinted from Nezbeda, Kolafa and Kotrla 1998.

A typical example of $g(r)$ for liquid water as well as hard spheres is shown in Fig. 40. The function vanishes on short distances, as the molecules cannot intersect. A high peak follows on roughly the van der Walls radius, where the interaction of molecules is favorable.[37] In other words, it is much more likely to find two molecules on this distance in a real liquid than in the ideal gas. On longer distances, several shallow minima and maxima are found, and $g(r)$ converges to unity at large distances – there, the probability of finding a particle is uniform, the same as in the ideal gas.

The importance of radial distribution functions consists not only in the information about the structure. If the pairwise additivity of forces is assumed, then thermodynamic properties can be calculated using $g(r)$ and the potential energy $u(r)$ and force $f(r)$ of a pair of particles. For example, the corrections to the ideal-gas values of total energy and pressure follow as

$$E - \frac{3}{2} N k_{\mathrm{B}} T \;=\; 2\pi N \rho \int_0^\infty r^2\, u(r)\, g(r)\, \mathrm{d}r \tag{VIII.8}$$

$$P - \rho\, k_{\mathrm{B}} T \;=\; -\frac{2\pi}{3} \rho^2 \int_0^\infty r^3 f(r)\, g(r)\, \mathrm{d}r \tag{VIII.9}$$

[37] However, such a peak would be present in the case of hard spheres (which do not feature any attractive interaction) as well.

The Fourier transform of the pair distribution function is the *structure factor*, which may be measured in diffraction experiments (X-ray of neutron diffraction).

C. Monitoring the equilibration

Every simulation aimed at producing structural and/or thermodynamic data has to be performed in the *termodynamic equilibrium*. Therefore, the production simulation shall always by preceded by an *equilibration* run, in order to provide the system a possibility to achieve the equilibrium. The equilibration should proceed until the values of certain monitored properties become stable, i.e. until these does not exhibit a drift any more.

It is convenient to monitor the thermodynamic properties that are being evaluated and written out by the simulation program. These are usually the potential energy and the temperature; in case of NPT simulations, the pressure or the density should also be taken into account.

Apart from the thermodynamics, the structure of the system must be taken care of. Many simulations of the liquid state are being started from a configuration that exhibits some artifical regularity, like that of the crystal lattice.[38] This makes also the thermodynamics wrong, because the artifical regularity causes the entropy to be too small. Anyway, the equilibration must continue until such structural regularities are washed out. To guarantee this, we need appropriate quantities to characterize the regularity of the structure.

A measure of translational order/disorder was proposed by Verlet in the form of an *order parameter* λ

$$\lambda = \frac{\lambda_x + \lambda_y + \lambda_z}{3}, \qquad \lambda_x = \frac{1}{N}\sum_{i=1}^{N} \cos\left[\frac{4\pi x_i}{a}\right] \quad \text{etc.} \tag{VIII.10}$$

where a is the length of the edge of the unit cell. In the ideal crystal, λ assumes the value of one, while it drops to zero for a completely disordered structure. Thus, in an equilibration, one should see λ to decrease to zero and then fluctuate around zero.

Another useful quantity may be the *mean squared displacement* (MSD) given by

$$\mathrm{MSD} = \frac{1}{N}\sum_{i=1}^{N} \left|\vec{r}_i(t) - \vec{r}_i(0)\right|^2 \tag{VIII.11}$$

[38] Note that we usually fill the simulation box with water in the form of small and *identical* 'bricks'.

which should increase gradually with time in a fluid with no specific molecular structure, whereas it would oscillate about a mean value for a solid.

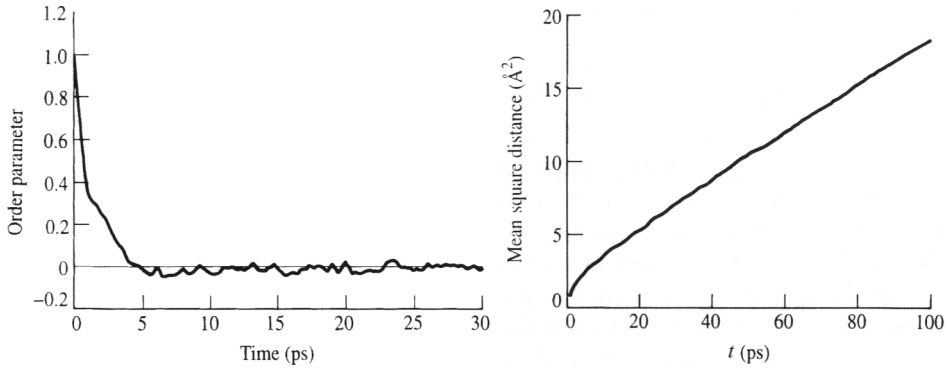

FIG. 41: The course of equilibration of liquid argon being followed by the Verlet order parameter (left) and the mean squared displacement (right). Reprinted from Leach: Molecular Modelling.

D. Time-dependent properties

1. Correlation functions

Suppose there are two physical quantities x and y, which may exhibit some *correlation*. This term indicates a relation of the quantities, opposed to *independence*. To quantify correlation, several kinds of *correlation functions* or *correlation coefficients* have been developed. Most common are the Pearson correlation coefficients, which describe the potential *linear* relationship between the quantities. Typically, we consider two quantities fluctuating around their mean values $\langle x\rangle$ and $\langle y\rangle$. Then, it is of advantage to consider only the fluctuating part and introduce a correlation coefficient ρ_{xy}

$$\rho_{xy} = \frac{\langle (x - \langle x\rangle) \cdot (y - \langle y\rangle)\rangle}{\sqrt{\langle (x - \langle x\rangle)^2\rangle \cdot \langle (y - \langle y\rangle)^2\rangle}} = \frac{\mathrm{cov}(x, y)}{\sigma_x \cdot \sigma_y} \tag{VIII.12}$$

where $\mathrm{cov}(x, y)$ stands for the *covariance* of x and y, which is the generalization of variance.

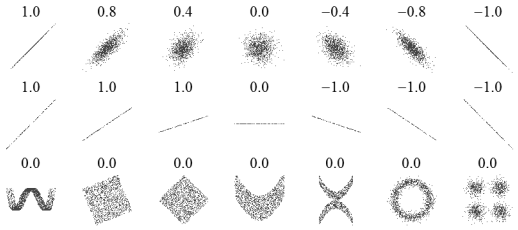

FIG. 42: Correlation of two quantities (on the x and y axes) and the coresponding correlation coefficients. Downloaded from WIKIPEDIA.

In an MD simulation, we obtain the values of various properties at specific times. It can happen at some point in time, that the value of a property x is correlated with the value of the same property at an earlier time point. This behavior may be described by the *autocorrelation function* (ACF) of this property

$$c_x(t) = \frac{\langle x(t) \cdot x(0) \rangle}{\langle x(0) \cdot x(0) \rangle} = \frac{\int x(t')\, x(t'+t)\, \mathrm{d}t'}{\int x^2(t')\, \mathrm{d}t'} \tag{VIII.13}$$

which denotes the correlation of the same property x at two time points separated by t, and the denominator $\langle x(0) \cdot x(0) \rangle$ normalizes c_x so that it takes values between -1 and 1.

2. *Autocorrelation of velocity*

The autocorrelation function indicates, to which extent the system retains a 'memory' of its previous values, or conversely, how quickly it takes for the system to 'forget' its previous state. A useful example is the *velocity autocorrelation function*, which tells us how closely the velocities of atoms at a time point t resemble those at a time 0. It is a good idea to average the ACF of velocity over all atoms i in the simulation:

$$c_v(t) = \frac{1}{N} \sum_{i=1}^{N} \frac{\langle \vec{v}_i(t) \cdot \vec{v}_i(0) \rangle}{\langle \vec{v}_i(0) \cdot \vec{v}_i(0) \rangle} \tag{VIII.14}$$

Typical ACF starts at the value of one in $t = 0$ and decreases afterwards. The time needed for the system to lose the autocorrelation of the quantity (velocity) whatsoever is often called *correlation time* or *relaxation time* τ_v:

$$\tau_v = \int_0^\infty c_v(t)\, \mathrm{d}t \tag{VIII.15}$$

There is a statistical issue related to the evaluation of properties of interest. In order to obtain correct average values of properties related to velocity (i.e. dynamical properties),

it is necessary to calculate the average of *uncorrelated* values. And now, the longer the relaxation time is, the fewer values can we take from the simulation of a certain length, to obtain correct averages. On the other hand, if the quantity (velocity) has short relaxation time, then it is possible to take many values for averaging.

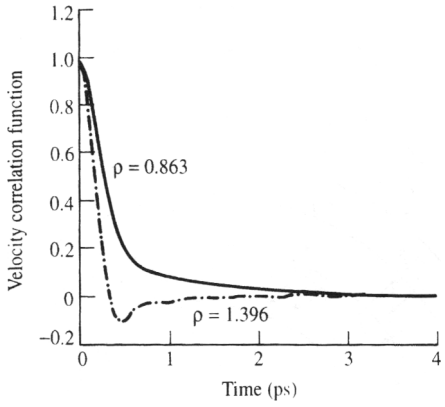

FIG. 43: Velocity autocorrelation functions for liquid argon (densities in g·cm^{-3}). Reprinted from Leach: Molecular Modelling.

Fig. 43 shows the velocity ACF from the simulations of a liquid at two different densities. At lower density, the ACF decreases gradually to zero. Unlike that, at higher density, the ACF comes faster to zero and even assumes negative values for a period of time. This means that the velocities point in the direction opposite to that at $t = 0$, which can be interpreted by the concept of a 'cage' structure of the liquid. The initial decay of ACF is slower than predicted by the kinetic theory, and this result together with its (slightly complex) explanation represents one of the most interesting achievements of early simulations.

There is a quite straightforward connection between the velocity ACF and the *transport properties* of the system. One of the Green–Kubo relations expresses the *self-diffusion coefficient* D by using the integral of the velocity ACF:[39]

$$D = \frac{1}{3}\int_0^\infty \langle \vec{v}_i(t) \cdot \vec{v}_i(0) \rangle_i \, \mathrm{d}t \tag{VIII.16}$$

Diffusion coefficients are very interesting observable quantities, and it is an important point that we are able to obtain them from MD simulations. Interestingly, D may be obtained from another property easily accesible in the simulation – the mean squared displacement (see Eq. VIII.11). The respective Einstein relation reads

$$D = \frac{1}{6}\lim_{t\to\infty} \frac{\left\langle |\vec{r}_i(t) - \vec{r}_i(0)|^2 \right\rangle_i}{t} \tag{VIII.17}$$

[39] Recall Fick's laws of diffusion for flux J and concentration ϕ: $J = -D\frac{\partial \phi}{\partial x}$, $\frac{\partial \phi}{\partial t} = D\frac{\partial^2 \phi}{\partial x^2}$

3. Autocorrelation of dipole moment

Velocity is an example of a property of a single atom. Contrary to that, there are quantities that need to be evaluated for the entire molecular system. Such a property of the system is the *total dipole moment*, which is the sum of the dipole moments of all individual molecules i in the system:

$$\vec{\mu}_{\mathrm{tot}}(t) = \sum_{i=1}^{N} \vec{\mu}_i(t) \tag{VIII.18}$$

The ACF of total dipole moment is given as

$$c_\mu(t) = \frac{\langle \vec{\mu}_{\mathrm{tot}}(t) \cdot \vec{\mu}_{\mathrm{tot}}(0) \rangle}{\langle \vec{\mu}_{\mathrm{tot}}(0) \cdot \vec{\mu}_{\mathrm{tot}}(0) \rangle} \tag{VIII.19}$$

This quantity is very significant because it is related to the vibrational spectrum of the sample. Indeed, it is possible to obtain the infrared spectrum as the Fourier transform of the dipolar ACF. An example is presented in Fig. 44. Rather than sharp peaks at well-defined frequencies (as is the case of molecules in the gas phase), we see continuous bands, as the liquid absorbs at many frequencies in a broad interval. The frequencies correspond to the rate at which the total dipole moment is changing.

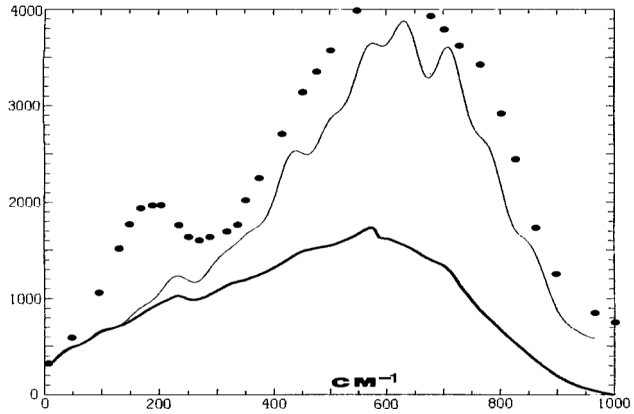

FIG. 44: Infrared spectra for liquid water. Black dots – experiment; thick curve – result from classical MD; thin curve – result with quantum corrections. B. Guillot, J. Phys. Chem. 1991.

4. Principal component analysis

It is possible to perform covariance analysis on the atomic coordinates in MD snapshots. This *principal component analysis* (PCA), also called *essential dynamics* uses the symmetric $3N$-dimensional covariance matrix C of the atomic coordinates $r_i \in \{x_i, y_i, z_i\}$:

$$C_{ij} = \langle (r_i - \langle r_i \rangle) \cdot (r_j - \langle r_j \rangle) \rangle_t \qquad \text{or} \tag{VIII.20}$$

$$C_{ij} = \left\langle \sqrt{m_i}(r_i - \langle r_i \rangle) \cdot \sqrt{m_j}(r_j - \langle r_j \rangle) \right\rangle_t \tag{VIII.21}$$

The latter definition is mass-weighted, with m_i being the masses of the respective atoms.

Standard diagonalization techniques can be used to obtain the eigenvalues and eigenvectors of this matrix. The eigenvectors the correspond to the principal or essential modes of motion of the system, an analogy of the normal modes; the respective eigenvalues may be expressed in terms of quasi-harmonic frequencies of these modes.

The first few eigenvectors with the largest eigenvalues (and thus the lowest frequencies of as little as 1 cm^{-1}) usually correspond to global, collective motions in which many atoms are involved. In the example of double-stranded DNA, the three weakest modes (see Fig. 45) are the same as would be expected for a simple rod made of a flexible material – two bending modes around axes perpendicular to the principal axis of the DNA, and a twisting mode.

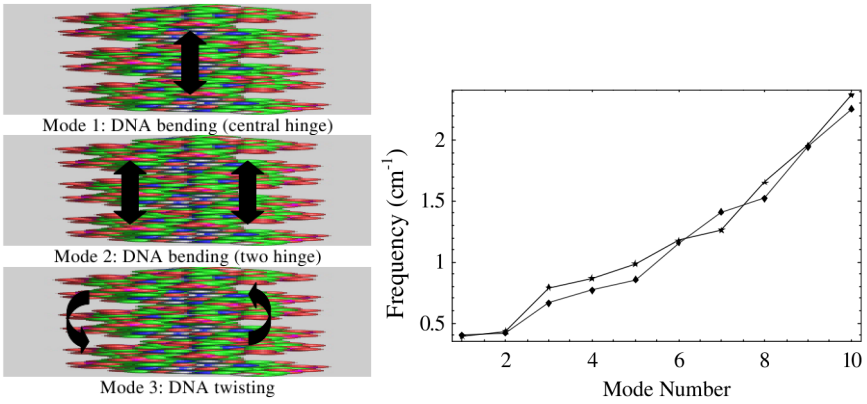

FIG. 45: First three principal modes of motion of double-stranded DNA (left) and their frequencies for two different sequences (right). Reprinted from S. A. Harris, J. Phys. Condens. Matter 2007.

Not only does this analysis give us an idea of what the modes of motion look like, it can also be used in thermodynamic calculations. The obtained vibrational frequencies may be used to evaluate *configurational entropy* of the molecule, which is otherwise hardly accessible.

E. Appendix – Fourier transform

The Fourier transform (FT) is an operation that transforms one function of a real variable into another. In such applications as signal processing, the domain of the original function is typically time and is accordingly called the time domain. That of the new function is frequency, and so the FT is often called the 'frequency domain representation of the original function.' It describes *which frequencies* are present in the original function. In effect, the Fourier transform decomposes a function into oscillatory functions.[40]

FT of a function $f(x)$ in the domain of frequency ω is given by the expression

$$F(\omega) = \int_{-\infty}^{\infty} f(x) \cdot \exp\left[-\mathrm{i}\,\omega x\right]\,\mathrm{d}x \tag{VIII.22}$$

where the connection to oscillatory functions is evident by noting that

$$\exp\left[-\mathrm{i}\,\omega x\right] = \cos\left[\omega x\right] - \mathrm{i}\sin\left[\omega x\right] \tag{VIII.23}$$

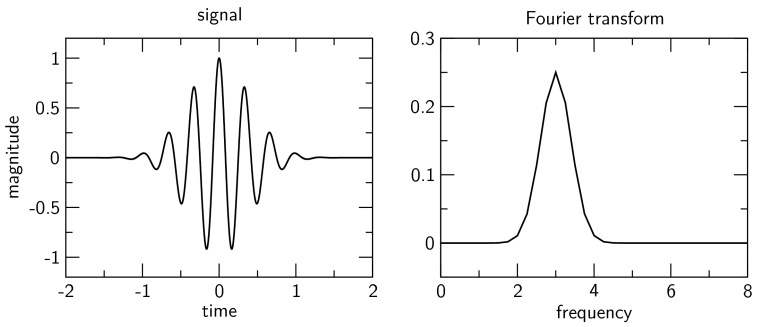

FIG. 46: Example of the Fourier transform (right) of a signal periodic on a time interval (left).

F. Exercises

- What does the radial distribution function of the ideal gas look like?
- What does the radial distribution function of an ideal crystal look like?

[40] The term Fourier transform refers both to the frequency domain representation of a function and to the process or formula that "transforms" one function into the other.

IX. FREE ENERGY SIMULATIONS

When searching for a physical quantity that is of most interest in chemistry, we could hardly find anything more appropriate than free energies – Helmholtz F or Gibbs G. Truly, these represent the holy grail of computational chemistry, both for their importance and because they are difficult to calculate.

These difficulties were hinted at in one of previous chapters. Recall that we can write

$$F = k_\mathrm{B}T \ln \iint \exp[\beta E(\vec{r},\vec{p})] \cdot \rho(\vec{r},\vec{p})\,\mathrm{d}\vec{r}\,\mathrm{d}\vec{p} + c \tag{IX.1}$$

The problem is that the large energy values (far from the minimum of energy) enter an exponential term, so that these high-energy regions may contribute significantly to the free energy F. So, in a simulation, if we have too few points in these high-energy regions of the phase space (*undersampling*), we may introduce sizeable errors in the calculated averages.

There are two fundamental approaches to overcome this difficulty: *free energy perturbation* and *thermodynamic integration*. Also, several computational tricks may be used for particular types of reactions, like *alchemical simulations* or *umbrella sampling*. An important observation is that it is not necessary to find the absolute value of the free energy. When considering a chemical reaction,[41] it is important to know merely the *free energy difference* (ΔF, ΔG) between the involved states (reactant A and product B).

A. Free energy perturbation (FEP)

For these states with energies $E_A(\vec{r},\vec{p})$ and $E_B(\vec{r},\vec{p})$, and partition functions Q_A and Q_B, free energy difference may be derived as

$$\begin{aligned}
\Delta F &= F_B - F_A = -k_\mathrm{B}T \ln \frac{Q_B}{Q_A} = -k_\mathrm{B}T \ln \frac{\iint \exp[-\beta E_B]\,\mathrm{d}\vec{r}\,\mathrm{d}\vec{p}}{\iint \exp[-\beta E_A]\,\mathrm{d}\vec{r}\,\mathrm{d}\vec{p}} \\
&= -k_\mathrm{B}T \ln \frac{\iint \exp[-\beta E_B]\ \exp[\beta E_A]\,\exp[-\beta E_A]\,\mathrm{d}\vec{r}\,\mathrm{d}\vec{p}}{\iint \exp[-\beta E_A]\,\mathrm{d}\vec{r}\,\mathrm{d}\vec{p}} \\
&= -k_\mathrm{B}T \ln \iint \exp[-\beta E_B]\exp[\beta E_A] \cdot \rho_A(\vec{r},\vec{p})\,\mathrm{d}\vec{r}\,\mathrm{d}\vec{p} \\
&= -k_\mathrm{B}T \ln \iint \exp[-\beta (E_B - E_A)] \cdot \rho_A(\vec{r},\vec{p})\,\mathrm{d}\vec{r}\,\mathrm{d}\vec{p}
\end{aligned} \tag{IX.2}$$

[41] in a very general sense of a reaction that need not involve chemical bonds being created or broken – ligand binding a protein, passage of a molecule through membrane, or protein folding are reactions as well

The integral has the form of an average of a property S taken with the phase space density of state A

$$\langle S \rangle_A = \iint S(\vec{r}, \vec{p}) \cdot \rho_A(\vec{r}, \vec{p}) \, \mathrm{d}\vec{r} \, \mathrm{d}\vec{p} \tag{IX.3}$$

and so we can write equivalently

$$\begin{aligned} \Delta F(A \to B) &= -k_\mathrm{B} T \ln \langle \exp[-\beta(E_B - E_A)] \rangle_A \\ \Delta F(B \to A) &= -k_\mathrm{B} T \ln \langle \exp[-\beta(E_A - E_B)] \rangle_B \end{aligned} \tag{IX.4}$$

which is the free energy formula by Zwanzig (1954) and the essence of the FEP method. Thus, in principle, it is possible to perform a simulation of state A and obtain the free energy by averaging the exponential of the difference of energies of states B and A, or vice versa. Practically, we start an MD in state A to get the phase space density ρ_A, and then calculate the difference between the energies of states B and A along the trajectory.

- Free energy of deprotonation of an amino acid side chain in a protein. We would run the dynamics for the protonated species, and then evaluate the energy difference between protonated and unprotonated species to get the average of $\exp[-\beta(E_B - E_A)]$. This would only work if the conformations of the protein, and above all the configuration of water molecules, sampled along the MD were very similar with both forms. Usually, this is not the case.

- The ionization of a molecule. Again, we would perform a simulation of the neutral species and evaluate the energy differences. Alas, the configuration of water would be quite different here, too, leading to a very small overlap of phase space densities.

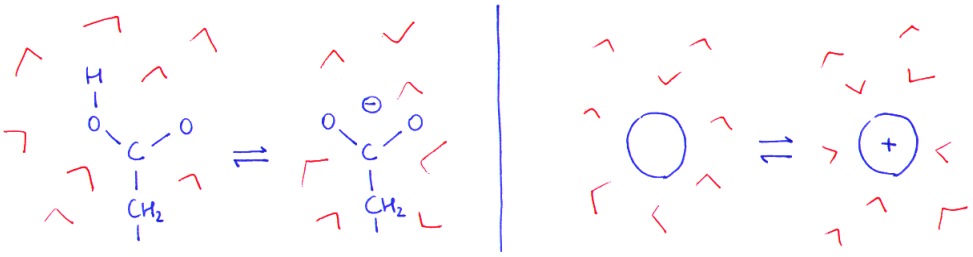

FIG. 47: Deprotonation of an amino acid (left) and ionization of a molecule (right), both in water.

Once again, let us emphasize the advantage of FEP over the direct evaluation of free energies. In the latter case, two simulations would be performed, one for each state A and

B, and the free energy difference would follow (using Eq. IX.1) as

$$\Delta F(A \to B) = k_\mathrm{B}T \ln \langle \exp[\beta E_B] \rangle_B - k_\mathrm{B}T \ln \langle \exp[\beta E_A] \rangle_A \qquad \text{(IX.5)}$$

Here, note that the free energy difference is very small, of a few kcal/mol, while the total energies are very large, of hundreds or thousands kcal/mol, if the solvent or the like is included. So, we have to subtract two large numbers in order to get a small one. However, a small relative uncertainty (error) of the large values would be huge in comparison with the possibly small resulting free energy difference. Therefore, it is necessary to obtain these large values extremely accurate, which would mean the necessity to perform exceedingly long MD simulations – so long that we will never be able to afford it!

That is why we avoid performing individual simulations for the end states and rather evaluate the free energy difference directly in one simulation. Then, it is no longer necessary to sample the regions of the molecular system which do not change and are not in contact with the regions that are changing, as these do not contribute to the energy difference $E_B - E_A$. The region of phase space that has to be sampled thoroughly is much smaller, and the necessary simulation length may become feasible.

For the following, the concept of *overlap in phase space* or *overlap of phase space densities* is crucial. In a straightforward way, the more similar the states A and B are, the more similar are also the corresponding phase space densities, and they may exhibit an overlap, see Fig. 48. If the phase space densities for states A and B are similar (overlapping, Fig. 48

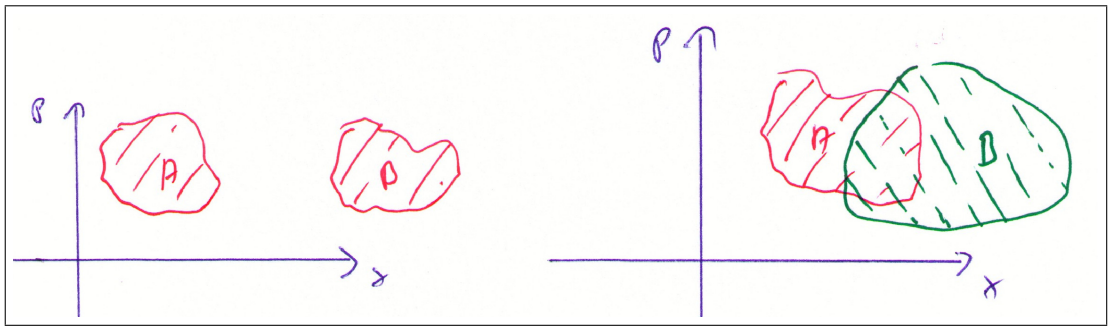

FIG. 48: Large (right) and no (left) overlap of phase space densities corresponding to two states.

right), then the low-energy regions of state B may be sampled well even in the simulation of state A, and the free energy difference $\Delta F(A \to B)$ in Eq. IX.4 may converge. If this is not the case (like in Fig. 48 left), then the simulation of state A hardly comes to the region of phase space where the state B has low energy; this region is undersampled, the averaging

of the energy E_B is wrong, and the calculation will not converge. As a rule of thumb, this is the case if

$$|E_B - E_A| > k_\mathrm{B}T \tag{IX.6}$$

A way to overcome this problem is to insert an intermediate state (designated '1') which overlaps with both A and B, as in Fig. 49. The underlying idea is to make use of the fact

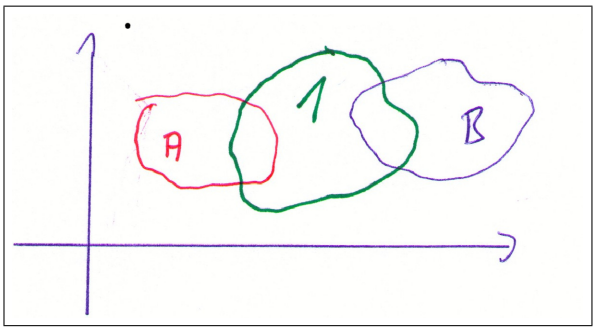

FIG. 49: Intermediate state '1' overlapping with state A and B

that free energy is a *state function*, and so

$$\Delta F(A \to B) = \Delta F(A \to 1) + \Delta F(1 \to B) \tag{IX.7}$$

Therefore, we can perform *two* MD simulations, one for each of the states A and 1, and evaluate free energies for the two subprocesses. These may be expected to converge better, and their sum gives the free energy of $A \to B$:

$$\begin{aligned} \Delta F &= -k_\mathrm{B}T \ln \left[\frac{Q_1}{Q_A} \cdot \frac{Q_B}{Q_1} \right] = \\ &= -k_\mathrm{B}T \ln \langle \exp[-\beta(E_1 - E_A)] \rangle_A - k_\mathrm{B}T \ln \langle \exp[-\beta(E_B - E_1)] \rangle_1 \end{aligned} \tag{IX.8}$$

Obviously, it is possible to insert more than one intermediate state between A and B, if these differ exceedingly. For N intermediate states $1, 2, \ldots, N$, we obtain

$$\begin{aligned} \Delta F = &- k_\mathrm{B}T \ln \left[\frac{Q_1}{Q_A} \cdot \frac{Q_2}{Q_1} \cdot \ldots \cdot \frac{Q_B}{Q_N} \right] = \\ = &- k_\mathrm{B}T \ln \langle \exp[-\beta(E_1 - E_A)] \rangle_A - k_\mathrm{B}T \ln \langle \exp[-\beta(E_2 - E_1)] \rangle_1 - \\ &- \ldots - k_\mathrm{B}T \ln \langle \exp[-\beta(E_B - E_N)] \rangle_N \end{aligned} \tag{IX.9}$$

and we have to perform $N + 1$ simulations, e.g. of states $A, 1, 2, \ldots, N$.

The description of this procedure may sound complicated, but it is implemented in the common simulation packages in a convenient way. Since we can change the chemical identities of the atoms or functional groups, this practice is often called *computational alchemy*. Typically, one introduces a parameter λ which 'converts' the force-field parameters (i.e. the Hamiltonian) from these of state A to those of state B:

$$E_\lambda = (1-\lambda)\cdot E_A + \lambda \cdot E_B \tag{IX.10}$$

- The (solvation) free energy difference of argon and xenon in aqueous solution. The two atoms differ only in the vdW parameters – the well depth ε and the radius σ. To transmutate the energy function from that of one species to the other, we interpolate:

$$\varepsilon_\lambda = (1-\lambda)\cdot \varepsilon_A + \lambda \cdot \varepsilon_B \tag{IX.11}$$

$$\sigma_\lambda = (1-\lambda)\cdot \sigma_A + \lambda \cdot \sigma_B \tag{IX.12}$$

  In the simulation, we start from $\lambda = 0$, i.e. an argon atom, and change it in subsequent steps to 1. For each step (called *window*), we perform an MD with the corresponding values of the vdW parameters, and calculate the relative free energies.

- A true chemical reaction like HCN $\rightarrow$ CNH. The situation is more complicated as we need the topologies of both molecules. Thus, a *dual-topology* simulation is performed: we have both molecules simultaneously in the simulation. These two molecules do *not* interact with each other, and we gradually switch off the interaction of one species with the solvent during the simulation while we switch on the other at the same time.

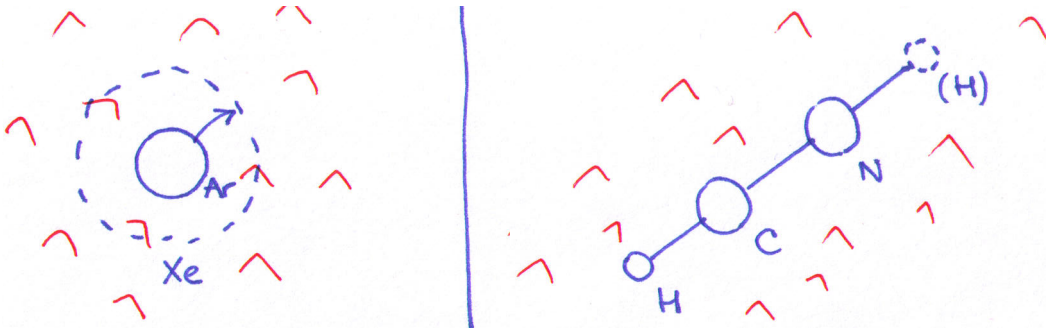

FIG. 50: Examples of 'alchemical' simulations.

B. Thermodynamic integration (TI)

In the last chapter, we have written the energy E as a function of the parameter λ. This means, that the free energy also becomes dependent on λ:

$$F = F(\lambda) \tag{IX.13}$$

with $F(0) = F(A)$ and $F(1) = F(B)$. Thus, we can write

$$\Delta F = F(B) - F(A) = \int_0^1 \frac{\partial F(\lambda)}{\partial \lambda} \mathrm{d}\lambda \tag{IX.14}$$

with

$$F(\lambda) = -k_\mathrm{B} T \ln Q(\lambda) \tag{IX.15}$$

The derivative of F rearranges to

$$\begin{aligned}
\frac{\partial F}{\partial \lambda}(\lambda) &= -k_\mathrm{B} T \frac{\partial \ln Q}{\partial \lambda}(\lambda) = -k_\mathrm{B} T \frac{1}{Q(\lambda)} \cdot \frac{\partial Q}{\partial \lambda}(\lambda) = -k_\mathrm{B} T \frac{1}{Q(\lambda)} \cdot \frac{\partial}{\partial \lambda} \iint \exp[-\beta E_\lambda] \, \mathrm{d}\vec{r} \, \mathrm{d}\vec{p} = \\
&= -k_\mathrm{B} T \frac{1}{Q(\lambda)} \cdot \iint (-\beta) \frac{\partial E_\lambda}{\partial \lambda} \exp[-\beta E_\lambda] \, \mathrm{d}\vec{r} \, \mathrm{d}\vec{p} = \\
&= -k_\mathrm{B} T \cdot (-\beta) \cdot \iint \frac{\partial E_\lambda}{\partial \lambda} \frac{\exp[-\beta E_\lambda]}{Q(\lambda)} \, \mathrm{d}\vec{r} \, \mathrm{d}\vec{p} \\
&= 1 \cdot \iint \frac{\partial E_\lambda}{\partial \lambda} \rho_\lambda(\vec{r}, \vec{p}) \, \mathrm{d}\vec{r} \, \mathrm{d}\vec{p} = \left\langle \frac{\partial E_\lambda}{\partial \lambda} \right\rangle_\lambda
\end{aligned} \tag{IX.16}$$

This is the essence of TI – the derivative of free energy F with respect to the coupling parameter λ is calculated as the average of derivative of total MM energy E, which can be directly evaluated in the simulation. Then, the free energy difference follows simply as

$$\Delta F = \int_0^1 \left\langle \frac{\partial E_\lambda}{\partial \lambda} \right\rangle_\lambda \mathrm{d}\lambda \tag{IX.17}$$

Practically, we perform a MD simulation for each chosen value of λ; it is usual to take equidistant values in the interval (0,1) like 0, 0.05,..., 0.95 and 1. Each of these simulations produces a value of $\left\langle \frac{\partial E}{\partial \lambda} \right\rangle_\lambda$, so that we obtain the derivative of free energy in discrete points for $\lambda \in (0, 1)$. This function is then integrated numerically, and the result is the desired free energy difference ΔF.

An example of the TI simulation is shown in Fig. 51. An atom of rare gas (neon) is dissolved in water; in course of the NPT simulation, the van der Walls parameters of the

neon atom are being gradually switched off by means of the λ parameter, so that the atom is effectively disappearing. The derivative of total energy with respect to λ is evaluated for several (21) values of λ ranging from 0 to 1. Eq. IX.17 is then used to obtain the (Gibbs) free energy difference of the two states: (i) a neon atom in water, and (ii) no neon atom in water, i.e. outside of the solution in vacuo. Thus, the calculated free energy difference corresponds directly to the solvation free energy, a quantity which is of considerable value in chemistry.

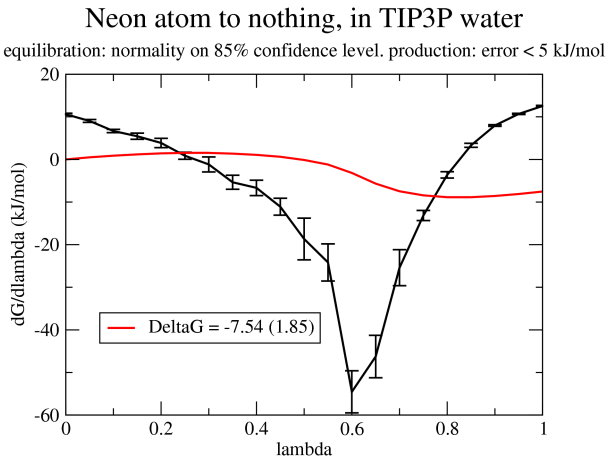

FIG. 51: TI simulation of a neon atom in water being disappeared. See text for explanation.

Finally, let us summarize the features of FEP and TI. Irrespective of the nature of the studied reaction, both FEP and TI require the introduction of a coupling parameter λ, which plays the role of the reaction coordinate with $\lambda = 0$ corresponding to the reactant and $\lambda = 1$ to the product. The fact that free energy is a state function guarantees the independence of the result on the chosen path between the reactant and the product, and so it does not matter if the reaction coordinate corresponds to an unphysical process like a change of chemical identity of one or more atoms (as is the case in the alchemical simulations).

The remaining open question regards the necessary number of windows in the simulation. We would like to have as few windows as possible, without compromising numerical precision of the calculation. In FEP, the assumption is that while simulating the state A, the low-energy regions of state B are sampled well. The closer the windows are, the better is this condition fulfilled. On the other hand, the free energy derivative is always evaluated for *one* λ-value with TI, and the problem present in FEP does not occur here. It is the numerical integration of the free energy derivative that brings on the numerical inaccuracy of TI.

C. Free energy from non-equilibrium simulations

A major disadvantage of the described methodology – TI using equilibrium simulations for discrete values of λ – is the very slow convergence of $\partial G/\partial\lambda$ once the alchemical change becomes large. So, it is often possible to describe the mutation of a single amino acid side chain in a protein provided the structure of the protein remains the same, but this should be considered a practical limit of the method.

To avoid this problem, the current development of free-energy methods makes use of *non-equilibrium simulations*. Here, the usual process of "equilibration" of the system for every of the selected values of λ followed by a "production phase" is not used; a non-equilibrium simulation consists of n MD steps, where the parameter λ starts at 0 and increases by $1/n$ in every MD step. This way, the simulation does not describe the system in equilibrium in any moment, as the external parameter λ is changing all the time. Whereas a single simulation of this kind is probably worthless, the remarkable equality by Jarzynski provides a link between an *ensemble* of such simulations and the desired free energy:

$$\exp[-\beta\Delta F] = \langle\exp[-\beta W]\rangle \tag{IX.18}$$

The true value of free energy ΔF is obtained as a special kind of ensemble average, for the ensemble of non-equilibrium TI simulations yielding "free energies" W. These values $W = \int_0^1 \partial E/\partial\lambda\,\mathrm{d}\lambda$ are no free energies whatsoever; instead, they may be called *(irreversible) work*. Since no convergence of any quantity is required within a single non-equilibrium simulation, these simulations may be very short – and this is the actual practice. However, the sampling problem persists because the largest statistical weight is carried by rarely occuring simulations (due to the unfavorable averaging in Eq. IX.18).

This sampling issue may be circumvented by *exponential work averaging* with gaussian approximation. An ensemble of simulations is performed for the 'forward' process $0 \to 1$ as well as for the 'reverse' process $1 \to 0$, and the obtained distributions of forward and backward irreversible work are approximated by gaussians with mean and standard deviation W_f, σ_f and W_r, σ_r, respectively. The free energy is calculated as an average of values

$$\begin{aligned} \Delta F_f &= W_f - \frac{1}{2}\beta\sigma_f^2 \\ \Delta F_r &= -W_r + \frac{1}{2}\beta\sigma_r^2 \end{aligned} \tag{IX.19}$$

A more general expression (than the Jarzynski equality) is the *Crooks fluctuation theorem* (CFS), according to which the distributions of forward and reverse work are related like

$$\frac{P_f(W)}{P_r(-W)} = \exp[\beta(W - \Delta F)] \tag{IX.20}$$

Then, once we have obtained well-converged distributions P_f and P_r, it is possible to apply *Bennett's acceptance ratio* for an equal number of forward and reverse simulation; the free energy follows from

$$\left\langle \frac{1}{1 + \exp[\beta(W - \Delta F)]} \right\rangle_f = \left\langle \frac{1}{1 + \exp[-\beta(W - \Delta F)]} \right\rangle_r \tag{IX.21}$$

It is possible to apply CFS more directly. A closer look at Eq. IX.20 reveals that the free energy corresponds to the value of work W for which the probabilities P_f and P_r are equal – to the intersection point of the distributions. To determine this point readily from the distributions may be difficult and a source of large errors if the overlap of the distributions is very small. Again, this issue can be solved by the assumption of normal distribution of the forward and reverse work, which was proven for a system with a large number of degrees of freedom. The procedure thus requires to perform a number of forward and reverse simulations sufficient to perform a good-quality gaussian fit to the resulting distributions of irreversible work. The free energy is calculated directly as the intersection points of these gaussian curves.

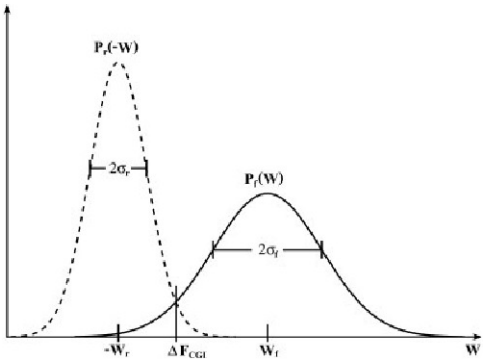

FIG. 52: The Crooks gaussian intersection (from Goette and Grubmüller 2009).

D. Thermodynamic cycles

Quite often, we are interested not in the absolute free energies and not even in the reaction free energies, but rather in the difference (Δ) of reaction free energies (ΔF) corresponding to two similar reactions. These may the be denoted as $\Delta\Delta F$ or $\Delta\Delta G$.

Consider as an example the binding of an inhibitor molecule I to an enzyme E, as shown in Fig. 53 left. Usually, we are interested in differences of binding free energies, for instance of an inhibitor I to two very similar enzymes E and E′:

$$\begin{aligned} \mathrm{E} + \mathrm{I} &\rightleftharpoons \mathrm{EI} \qquad \Delta G_1 \\ \mathrm{E}' + \mathrm{I} &\rightleftharpoons \mathrm{E}'\mathrm{I} \qquad \Delta G_2 \end{aligned} \tag{IX.22}$$

The binding of the inhibitor can induce large structural changes in the enzyme, and it would be very difficult (if not impossible) to describe this reaction in a simulation both correctly and efficiently at the same time. So, significant errors would seem to be inevitable. A way to solve this would be to simulate not the reaction of binding but rather the alchemical transmutation of enzyme E to E′. As we consider the enzymes to be very similar,[42] it is plausible to assume the structure of complexes EI and E′I to be similar as well. Then, the alchemical simulation may well be successful. As free energy is a state function, the sum of

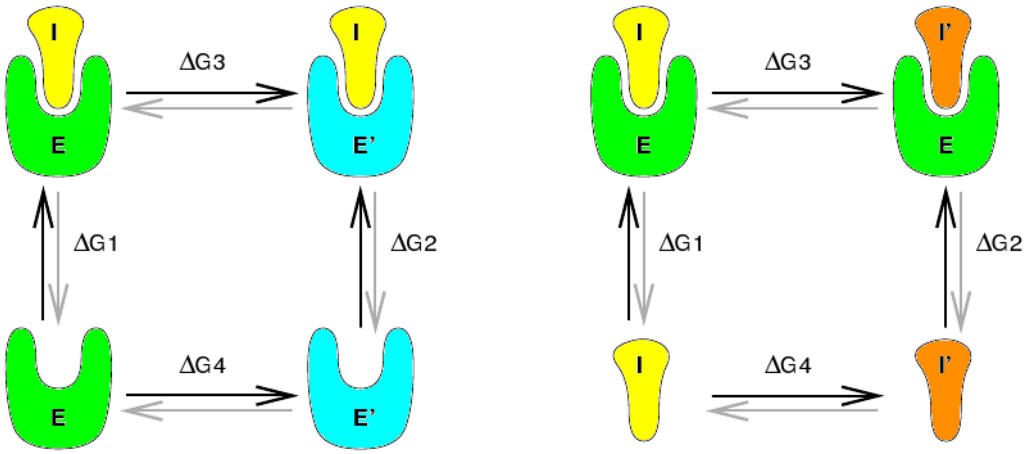

FIG. 53: Examples of the thermodynamic cycle.

free energies around a *thermodynamic cycle* vanishes (e.g. clockwise in Fig. 53 left):

$$\Delta F_1 + \Delta F_3 - \Delta F_2 - \Delta F_4 = 0 \tag{IX.23}$$

[42] Imagine E′ to be derived from E by a mutation of a single amino acid, e.g. leucine to valine.

The difference of binding free energies then follows to be equal the difference of free energies calculated in alchemical simulations:

$$\Delta\Delta F = \Delta F_1 - \Delta F_2 = \Delta F_3 - \Delta F_4 \tag{IX.24}$$

Similarly, it is possible to calculate the free energy difference of binding of two similar ligands to the same enzyme (Fig. 53 right), or the difference of solvation energy of two similar molecules. In the latter case, two alchemical simulations would be performed: one in vacuo and the other in solvent.

E. Potentials of mean force (PMF) and umbrella sampling

Sometimes, we wish to know not only the free energy difference of two states (the reactant and the product), but rather the free energy along the *reaction coordinate* q within a certain interval; the free energy is then a function of q while it is integrated over all other degrees of freedom. Such a free energy function $F(q)$ is called the *potential of mean force*. Examples of such a reaction coordinate q may be the distance between two particles if the dissociation of a complex is studied, the position of a proton for a reaction of proton transfer, or the dihedral angle when dealing with some conformational changes.

To separate the degree of freedom spanned by the reaction coordinate, we perform a coordinate transformation from $\vec{r} = (r_1, r_2, \ldots, r_{3N})$ to a set $(u_1, u_2, \ldots, u_{3N-1}, q)$, where the $(3N-1)$-dimensional vector $\vec{u}$ represents all remaining degrees of freedom, and we can write

$$\mathrm{d}\vec{r} = \mathrm{d}\vec{u} \cdot \mathrm{d}q \tag{IX.25}$$

Looking for the free energy at a certain value of q, all remaining degrees of freedom are averaged over (or 'integrated out'). One could think of performing an MD simulation and sampling *all* degrees of freedom except for q.

An example would be the free energy of formation of an ion pair in solution, as shown in Fig. 54. An MD simulation would be performed to calculate the free energy for every value of the reaction coordinate q.

The free energy is given by:

$$F = -k_\mathrm{B}T \ln \iint \exp[-\beta E(\vec{r}, \vec{p})]\, \mathrm{d}\vec{r}\, \mathrm{d}\vec{p} \tag{IX.26}$$

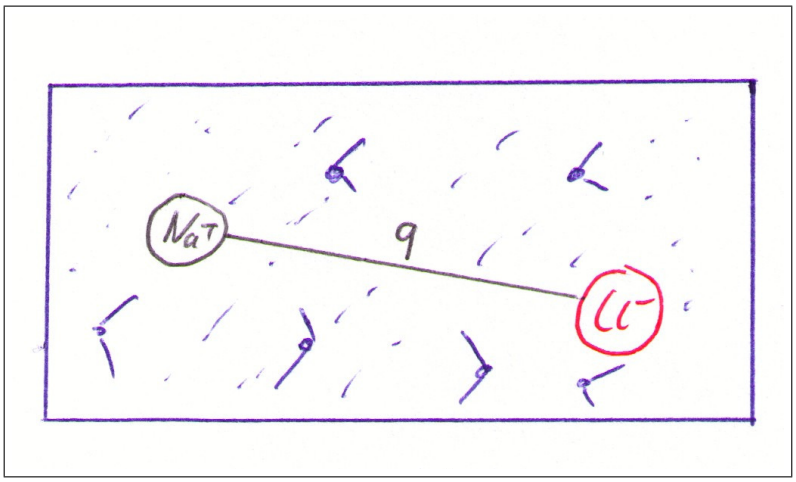

FIG. 54: Na^+ and Cl^- in water solution. The distance between the ions is the reaction coordinate q, and all other degrees of freedom (water) are represented by $\vec{u}$ and are free to vary.

If we wish to evaluate an expression for a coordinate q taking a certain value q_0, it is convenient to use the *Dirac delta function*,[43] $\delta(q - q_0)$. With that, we can write the free energy for the fixed reaction coordinate q_0 as

$$\begin{aligned} F(q_0) &= -k_\mathrm{B}T \ln \iint \delta(q - q_0) \exp[-\beta E(\vec{r}, \vec{p})] \, \mathrm{d}\vec{p} \, \mathrm{d}\vec{u} \, \mathrm{d}q \\ &= -k_\mathrm{B}T \ln \left[Q \cdot \iint \delta(q - q_0) \frac{\exp[-\beta E(\vec{r}, \vec{p})]}{Q} \, \mathrm{d}\vec{p} \, \mathrm{d}\vec{u} \, \mathrm{d}q \right] \\ &= -k_\mathrm{B}T \ln \left[Q \cdot \iint \delta(q - q_0) \cdot \rho(\vec{r}, \vec{p}) \, \mathrm{d}\vec{p} \, \mathrm{d}\vec{u} \, \mathrm{d}q \right] \\ &= -k_\mathrm{B}T \ln \left[Q \cdot \langle \delta(q - q_0) \rangle \right] \\ &= -k_\mathrm{B}T \ln Q - k_\mathrm{B}T \ln \langle \delta(q - q_0) \rangle \end{aligned} \tag{IX.27}$$

How to interpret this? $\rho(\vec{r}, \vec{p})$ is the probability, that the system is at the point $(\vec{r}, \vec{p})$. Then,

$$P(q_0) = \iint \delta(q - q_0) \cdot \rho(\vec{r}, \vec{p}) \, \mathrm{d}\vec{r} \, \mathrm{d}\vec{p} = \langle \delta(q - q_0) \rangle \tag{IX.28}$$

is the *probability* that the reaction coordinate q in the system takes the value of q_0 , because the integral proceeds over the whole phase space and the delta function 'cancels out' all points, where the reaction coordinate is *not equal* q_0! So, the integration collects all points in phase space, where the reaction coordinate has this specific value.

[43] This is a generalized function representing an infinitely sharp peak bounding unit area; $\delta(x)$ has the value of zero everywhere, except at $x = 0$ where its value is infinitely large in such a way that its integral is 1.

What would it work like in the example of the ion pair? We perform an MD simulation for the system, and then *count* how many times the reaction coordinate takes the specified value, in other words we calculate the probability $P(q_0)$ of finding the system at q_0.

Then, the free energy difference of two states A and B is:

$$\begin{aligned} F_B - F_A &= -k_\mathrm{B}T \ln Q - k_\mathrm{B}T \ln \langle \delta(q - q_B) \rangle - (-k_\mathrm{B}T \ln Q + k_\mathrm{B}T \ln \langle \delta(q - q_A) \rangle) \\ &= -k_\mathrm{B}T \ln \frac{\langle \delta(q - q_B) \rangle}{\langle \delta(q - q_A) \rangle} \\ &= -k_\mathrm{B}T \ln \frac{P(q_B)}{P(q_A)} \end{aligned} \tag{IX.29}$$

which is actually the known definition of the *equilibrium constant* $P(B)/P(A)$.

So, the task is clear: perform a MD, specify a coordinate, and then just count, how often the system is at special values of the reaction coordinate. The ratio of these numbers gives the free energy difference!

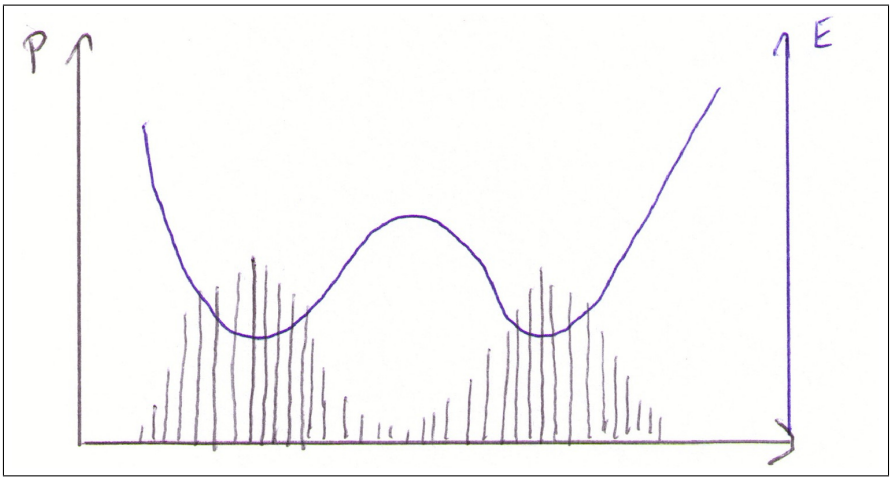

FIG. 55: Energy profile and probability distribution along the reaction coordinate. Note the undersampled region of the barrier.

This is very good, in principle. But, we also know the problem: If we there is a high barrier to be crossed along the reaction coordinate to come from A to B, a pure (*unbiased*) MD simulation will hardly make it,[44] and even if it does, the high-energy region (barrier) will be sampled quite poorly.

Then, a straightforward idea is to apply an *additional potential*, also called *biasing potential* in order to make the system spend a larger amount of time in that (those) region(s)

[44] In other words, the ergodicity of the simulation is hindered.

of phase space that would otherwise remain undersampled. This is the underlying principle of the *umbrella sampling*.[45] The additional potential shall depend only on the reaction coordinate: $V = V(q)$.[46] Then, what will the free energy look like in such a biased case? Let us start with the previously obtained expression:

$$\begin{aligned}
F(q_0) &= -k_\mathrm{B}T \ln \left[\frac{\iint \delta(q-q_0)\, \exp[-\beta E]\, \mathrm{d}\vec{r}\,\mathrm{d}\vec{p}}{\iint \exp[-\beta E]\, \mathrm{d}\vec{r}\,\mathrm{d}\vec{p}} \right] \\
&= -k_\mathrm{B}T \ln \left[\frac{\iint \delta(q-q_0) \exp[\beta V]\, \exp[-\beta(E+V)]\, \mathrm{d}\vec{r}\,\mathrm{d}\vec{p}}{\iint \exp[-\beta(E+V)]\, \mathrm{d}\vec{r}\,\mathrm{d}\vec{p}} \cdot \frac{\iint \exp[-\beta(E+V)]\, \mathrm{d}\vec{r}\,\mathrm{d}\vec{p}}{\iint \exp[-\beta E]\, \mathrm{d}\vec{r}\,\mathrm{d}\vec{p}} \right] \\
&= -k_\mathrm{B}T \ln \left[\langle \delta(q-q_0) \exp[\beta V] \rangle_{E+V} \frac{\iint \exp[-\beta(E+V)]\, \mathrm{d}\vec{r}\,\mathrm{d}\vec{p}}{\iint \exp[\beta V] \exp[-\beta(E+V)]\, \mathrm{d}\vec{r}\,\mathrm{d}\vec{p}} \right] \\
&= -k_\mathrm{B}T \ln \left[\langle \delta(q-q_0) \exp[\beta V] \rangle_{E+V} \frac{1}{\langle \exp[\beta V] \rangle_{E+V}} \right] \\
&= -k_\mathrm{B}T \ln \left[\exp[\beta V(q_0)]\, \langle \delta(q-q_0) \rangle_{E+V} \frac{1}{\langle \exp[\beta V] \rangle_{E+V}} \right] \\
&= -k_\mathrm{B}T \ln \langle \delta(q-q_0) \rangle_{E+V} - V(q_0) + k_\mathrm{B}T \ln \langle \exp[\beta V \rangle_{E+V} \\
&= -k_\mathrm{B}T \ln P^*(q_0) - V(q_0) + k_\mathrm{B}T \ln \langle \exp[\beta V] \rangle_{E+V}
\end{aligned} \tag{IX.30}$$

giving the free energy as function of reaction coordinate, or PMF in the form

$$F(q) = -k_\mathrm{B}T \ln P^*(q) - V(q) + K \tag{IX.31}$$

This result is very interesting: We have added an arbitrary potential $V(q)$ to our system. Now, we have to calculate the ensemble averages with the biased potential $E+V$ as indicated by $\langle\rangle_{E+V}$. We obtain the *biased probability* $P^*(q)$ of finding the system at the value of the reaction coordinate for the ensemble $E+V$, which can obviously be very different from that of the unbiased ensemble $P(q)$. Yet, we still get the right (unbiased) free energy $F(q)$, once we take the biased probability $P^*(q)$, subtract the biasing potential $V(q)$ at the value of the reaction coordinate and add the term K.

We can use this scheme efficiently, by way of moving the biasing (harmonic) potential along the reaction coordinate as shown in Fig. 56. In this case, we perform k simulations with the potentials V_k and get:

$$F(q) = -k_\mathrm{B}T \ln P^*(q) - V_k(q) + K_k \tag{IX.32}$$

[45] This should evoke the image of an interval of the reaction coordinate being covered by an umbrella.
[46] In such a case, $\langle \delta(q-q_0) \cdot \exp[\beta V] \rangle = \langle \delta(q-q_0) \cdot \exp[\beta V(q_0)] \rangle = \exp[\beta V(q_0)] \cdot \langle \delta(q-q_0) \rangle$ in the following.

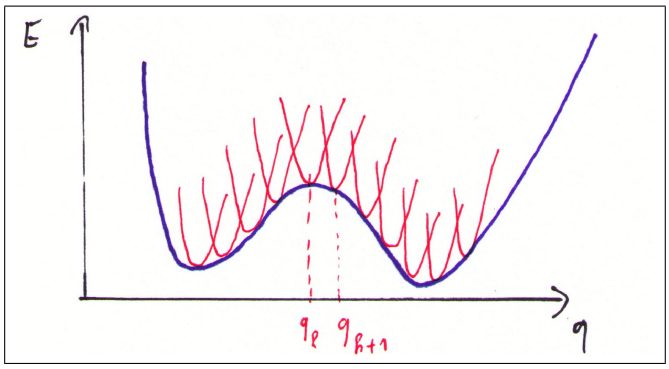

FIG. 56: Harmonic biasing potentials keep the system in the desired regions of reaction coordinate.

For each of these k simulations, we extract the probability $P^*(q)$ for every value of q and easily calculate $V^k(q)$. The curves of $-k_\mathrm{B}T \ln P^*(q) - V^k(q)$ for the simulations k and $k+1$ differ by a constant shift, which corresponds to the difference of K values, as shown in Fig. 57. The main task is to match the pieces together. One way is to fit the K_k in order

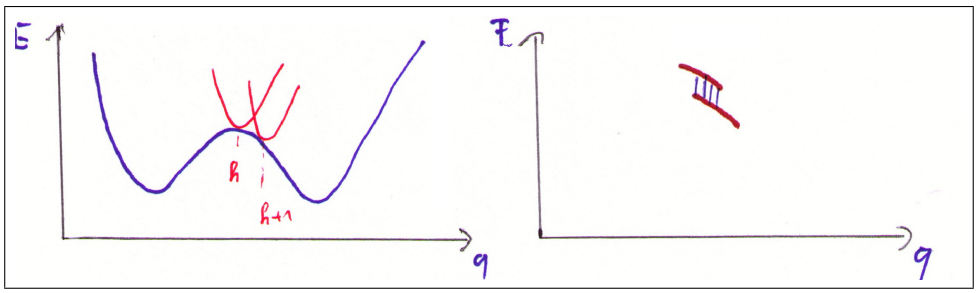

FIG. 57: The offset of free energy curves between two simulations k and $k+1$ is given by $K_k - K_{k+1}$

to get a smooth total $F(q)$ curve. This is possible if the pieces k and $k+1$ have sufficient 'overlap'.

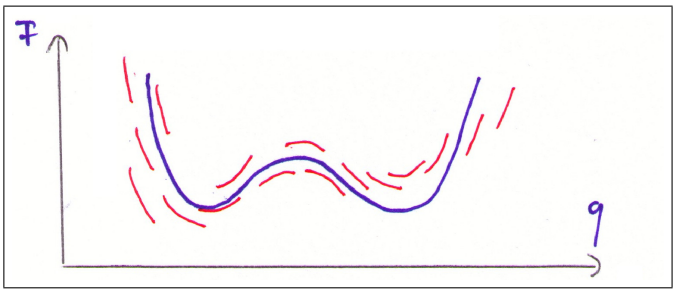

FIG. 58: Matching of histograms from different simulations

Another, quite involved method is the weighted histogram analysis method (WHAM). The starting point is the requirement of a perfect match, minimizing the total error. The

unbiased probabilities $P(x_j)$ of coordinate x falling into the bin j of the histogram and the shifts K_i are obtained by a self-consistent solution of a set of equations

$$\begin{aligned} P(x_j) &= \frac{\sum_{i=1}^{N} n_i(x_j)\ \exp[-\beta V_i(x_j)]}{\sum_{i=1}^{N} N_i\ \exp[-\beta(V_i(x_j) - K_i)]} \\ K_i &= -k\mathrm{T}\ \log \sum_{j}^{\text{bins}} P(x_j)\ \exp[-\beta V_i(x_j)] \end{aligned} \tag{IX.33}$$

(for a total of N simulations, i-th simulation contains N_i frames, $n_i(x_j)$ is the number of hits in bin j in simulation i). The WHAM procedure is included in a range of modern packages for MD simulations.

X. QM/MM

The standard force fields are designed to evaluate the energy of the system as fast as possible, and this requirement makes several quite crude approximations necessary. One of them is that the topology of the molecule remains the same in course of the simulation, meaning that the covalent bonds may be neither created nor broken in the simulation. Then, it is impossible to use such a force field to study the processes that would usually be designated as *chemical reactions*.

A. Empirical approaches to chemical reactions

In spite of the mentioned problems, it is not quite impossible to describe a chemical reaction with a force field. However, this may be done always for a single reaction, or a restricted class of reactions only, using approximations that are appropriate in the specific case; still, a generic force field applicable for *any* reaction is a mere illusion.

A possible way to describe a reaction would be as follows: An existing force field is used for all of the system, except the bonds that are being broken or created. The bonds involved in the reaction will then be re-parameterized, using probably a variant of Morse's potential or the like. Evidently, such an approach requires an *ad hoc* model of the molecule, and considerable effort is likely to be spent by the parameterization.

Also obvious are certain limitations of such an approach. The restrictions on the use of force field methods are more general than just that of the invariant connectivity of the molecules. Rather, it is the *electron density* that does not change at all. It is thus further impossible (or impracticable at the very least) to use a force field to describe a process involving *charge transfer*, in other words, the change of atomic charges. This fact poses another strong restraint on the classes of reactions that might be treated with molecular mechanics force fields. Other phenomena of interest that cannot be described with molecular mechanics, include *photochemical processes*, which involve electronic excitation of molecules.

B. The principle of hybrid QM/MM methods

Without loss of generality, we may assume that the changing electronic structure is localized in a small part of the studied molecular system. An example may be a reaction

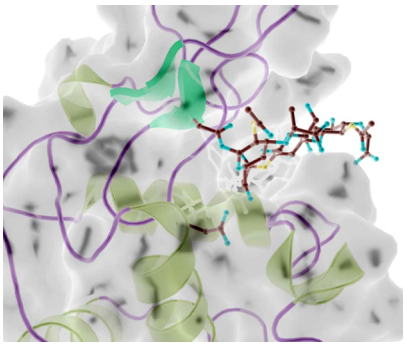

FIG. 59: Enzymatic reaction. The substrate in the binding pocket and the amino acids in contact shown as atoms; the rest of the enzyme shown as ribbons. Mulholland et al. (2008).

on a substrate which is catalyzed by an enzyme, see Fig. 59. Of the huge system, only the substrate and several atoms of the protein are involved in the reaction, while the rest of the protein and all the surrounding water and ions stay outside of the process. However, these seemingly inactive parts do interact with the substrate be means of non-bonded forces, and maintain the structure of the entire system.

So, the studied process is of quantum nature (a chemical reaction, but it may be some photochemistry as well) and thus, it must be described by a quantum chemical method. The overwhelming majority of the system (most of the enzyme and all of the water) is not directly involved in the process, but affects the reaction by way of non-bonded interactions; here, a description with an MM force field would be sufficient. It turns out to be a good idea to combine both approaches: The (small) region where the chemical reaction occurs will be described with a quantum-chemical method, while an MM force field will be used to deal with the (large) remaining part of the system, see Fig. 60. Obviously, the interaction

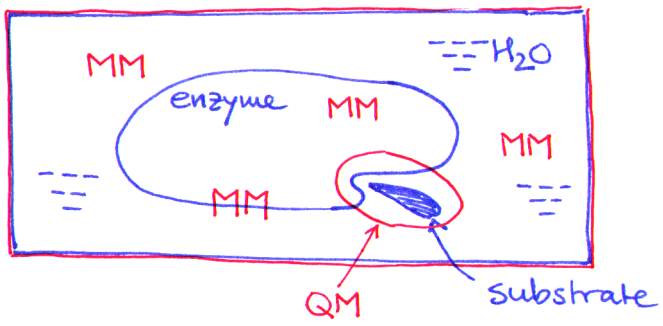

FIG. 60: QM/MM treatment of an enzymatic reaction.

of both subsystems must be taken into account correctly, as well, so that the total energy may by expressed in a simple fashion as

$$E_{\text{total}} = E_{\text{QM}} + E_{\text{MM}} + E_{\text{QM/MM}} \tag{X.1}$$

Quite a few hybrid schemes like that have been proposed so far, and they are usually called *quantum mechanics-molecular mechanics* (QM/MM) or *embedding*. These date back to a first study by Warshel and Levitt in 1976.

Both QM and MM calculations (yielding E_{QM} and E_{MM}) do not differ much from those performed on 'normal' systems not taking part in any QM/MM scheme. However, the key issue is how to treat the coupling of both parts of the system, to obtain $E_{\text{QM/MM}}$. This is the art of QM/MM calculations, and the rest of this section will deal with that topic.

C. Embedding schemes

The methods to couple the QM and MM systems differ in the excess of this coupling, or in that how large a part of this coupling is neglected. We will have a look at these methods in the order of increasing complexity (corresponding to the increasing completeness).

1. Unpolarized interactions (Mechanical embedding)

The simplest idea to account for the interactions between the QM and MM regions is to use a force field. In order to do that, atom types must be assigned to the QM atoms, because these determine the vdW parameters; further, their atomic charges must be evaluated – for instance, Mulliken charges may be used. It is then possible to calculate the QM/MM energy with the Coulomb law and the Lennard-Jones potential as

$$E_{\text{QM/MM}} = \sum_{i}^{\text{QM atoms}} \sum_{m}^{\text{MM atoms}} \left(\frac{q_i^{\text{Mull}} \cdot q_m}{r_{im}} + 4\varepsilon_{im} \left(\frac{\sigma_{im}^{12}}{r_{im}^{12}} - \frac{\sigma_{im}^{6}}{r_{im}^{6}} \right) \right) \tag{X.2}$$

where the Coulomb interaction may prove necessary to be scaled up for neutral QM zones, to account for the missing polarization of the wave function by the MM zone.

Certain specific combinations of force fields and quantum-chemical methods lead to very good results for specific classes of molecules and reactions; generally, care must be taken...

2. Polarized QM / unpolarized MM (Electronic embedding)

The clear deficiency of the mentioned model is that the QM system, or its wave function, is not affected by the MM system whatsoever. Actually, the wave function should be *polarized* by the environment (MM system), which is represented by point charges.

A step to improve the description is to include the electrostatic interaction with the MM charges in the QM Hamiltonian, whatever the QM method is – semiempirical, HF, DFT or a correlated method. The interaction of QM electrons with MM point charges moves from the $E_{\mathrm{QM/MM}}$ term (where it was described with a force field) to the quantum energy E_{QM}, and is described as an interaction of a charge density with point charges; then, it has the same form as the interaction with QM nuclei and brings on *little* increase of the computational cost. The interaction of QM nuclei with MM point charges may remain in $E_{\mathrm{QM/MM}}$.

Thus, the QM Hamiltonian changes to (schematically, may be method-dependent)

$$\hat{H}'_{\mathrm{QM}} = \hat{H}_{\mathrm{QM}} - \sum_{j}^{\text{QM electrons}} \sum_{m}^{\text{MM atoms}} \frac{q_m}{r_{jm}} \tag{X.3}$$

and the $E_{\mathrm{QM/MM}}$ term is considered excluding the electrostatic interaction of QM electrons with MM atoms, so that only the nuclear charges Z_i remain:

$$E'_{\mathrm{QM/MM}} = \sum_{i}^{\text{QM atoms}} \sum_{m}^{\text{MM atoms}} \left(\frac{Z_i \cdot q_m}{r_{im}} + 4\varepsilon_{im} \left(\frac{\sigma_{im}^{12}}{r_{im}^{12}} - \frac{\sigma_{im}^{6}}{r_{im}^{6}} \right) \right) \tag{X.4}$$

A QM/MM study would then run as follows:

1. The choice of specific QM and MM methods. Since the quantum-chemical calculation is used to describe the most interesting part of the system, as well as it is by far the most resource- and time-consuming component of the calculation, particular care must be taken with the selection of the QM method – the requirements regard both accuracy and computational efficiency, at the same time.

2. Determination of the Lennard-Jones parameters for the QM part of the system (for the calculation of $E_{\mathrm{QM/MM}}$). One can use either 'normal' parameters from a force field, or attempt to develop a special set of LJ parameters for the used QM method.

3. The simulation itself. Every step of the simulation involves one QM calculation, one MM calculation and a calculation of $E_{\mathrm{QM/MM}}$. The properties of interest (possibly but not necessarily of quantum character) are then evaluated as ensemble averages.

3. Fully polarized (Polarized embedding)

The QM/MM variant just described is already a very good approach with good changes for acceptable accuracy. The point at which it may be considered somewhat unbalanced is that whereas the QM system is being polarized by the MM charges, the MM molecules themselves cannot be polarized.

Should this fact be problematic in a study of a particular chemical process, it is possible to include this phenomenon in the QM/MM framework as well. However, in such a case, it is necessary to use a force field that makes it possible to account for the polarization of MM atoms or molecules.

Most of the standard force fields do not include polarization terms, mainly because of the extra computational effort. Every MM atom or molecule is assigned a polarizability α,[47] and an *induced dipole* at each polarizable center is then obtained as

$$\vec{\mu}^{\text{ind}} = \alpha \cdot \vec{E} \tag{X.5}$$

where $\vec{E}$ is the intensity of electric field induced by all the surrounding atomic point charges *and* all the induced dipoles. Because of that, the induced dipoles must be evaluated iteratively, until convergence (self-consistence) is reached. There are two possible issues with this procedure: (i) its iterative character makes the calculation an order of magnitude more time-consuming than a non-polarizable MM calculation of the same system, and (ii) the convergence of dipoles may be potentially problematic.

Within a QM/MM scheme involving a polarized MM method, the induced dipoles $\vec{\mu}^{\text{ind}}$ interact with the QM nuclei (i.e. some extra point charges) and with the QM electron density. Thus, the *entire* QM/MM calculation has to be performed iteratively until self-consistency is reached, and both the QM calculation and the MM treatment of induced charges proceed in a loop. This makes the computational cost rise dramatically.

To date, no conclusive answer has been given to the question if the completely polarized methodology brings a significant improvement if compared with the previously mentioned approach (polarized QM / unpolarized MM). Above all, the improvement would have to be necessary to justify the quite extreme computational cost.

[47] In principle, polarizability is a symmetrical tensor of rank 2. If isotropic polarizability is considered then α becomes a single value (scalar).

D. Covalent bonds across the boundary

All of the QM/MM schemes discussed so far involved purely non-bonded interaction between the QM and the MM subsystems. However, it may well turn out desirable or even necessary to divide the whole system in such a way that the QM and MM regions are connected with one or several covalent bonds. In such a case, a special treatment of the QM/MM boundary is necessary in order to perform a QM/MM calculation. Several possibilities are presented in the following.

1. Linear combination of molecular fragments

Imagine one wishes to simulate a large molecule, of which actually only a small part has to be treated quantum-chemically. The situation is more favorable if the interaction of the intended QM region with the rest of the molecule may be regarded as exclusively *steric*, i.e. if the electronic structure of the QM region is virtually unaffected by the rest of the molecule. This would be the case if this rest is composed of non-polar, i.e. alifatic or aromatic (even though large) groups(s), see Fig. 61 for an example.

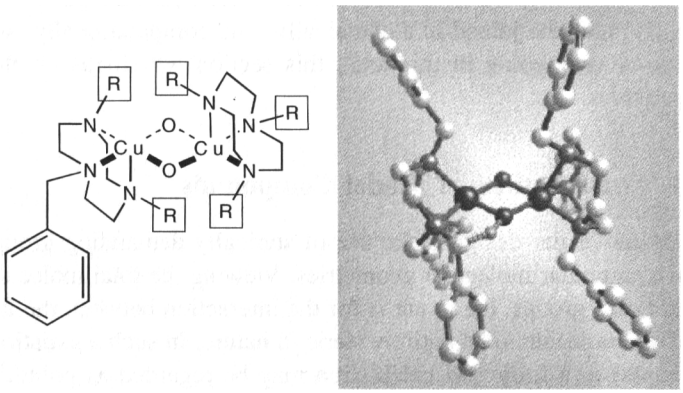

FIG. 61: A metallic complex with bulky non-polar functionalities. The five benzyl groups labeled with R are 'substituted' by H atoms in QM calculations. The remaining benzyl group is the donor in a hydrogen transfer reaction, and is thus included in the QM region. Reprinted from Cramer.

In such a case, the molecule may be regarded as a kind of a sum of the individual functional groups. The electronic structure of the QM system will be regarded as equal to the structure of a similar molecule where the bulky non-polar groups are replaced by *hydrogen atoms*. Then, the total energy may be expressed as the sum of energies of the

moleculare fragments (the QM-molecule 'capped' with hydrogens, and the bulky non-polar MM-molecules) like

$$\begin{aligned} E_{\text{total}} &= E_{\text{MM}}^{\text{large}} + \left(E_{\text{QM}}^{\text{small}} - E_{\text{MM}}^{\text{small}}\right) = \\ &= E_{\text{QM}}^{\text{small}} + \left(E_{\text{MM}}^{\text{large}} - E_{\text{MM}}^{\text{small}}\right) \end{aligned} \tag{X.6}$$

where the 'large' system is the entire molecule, and 'small' denotes the QM region. One can understand this approach so that the part of the MM energy corresponding to the 'small', interesting molecular fragment is substituted by corresponding QM energy (first line in Eq. X.6). The alternative way to think of Eq. X.6 (second line) is to concentrate on the 'small' fragment and its QM energy; the effect of the added non-polar groups is the added as a correction (in parentheses).

2. Link atoms

A more difficult situation arises if the intended MM region cannot be regarded as interacting only sterically, and there is for instance strong electrostatic interaction with the QM region. Typically, this is the case in proteins, where there are always polar and even charge amino-acid residues in the MM region, which polarize the electron density of the QM region (which is usually the binding site of a ligand or similar). What is missing in the approach presented in Section X C 2 is the description of covalent bonds crossing the QM/MM boundary.

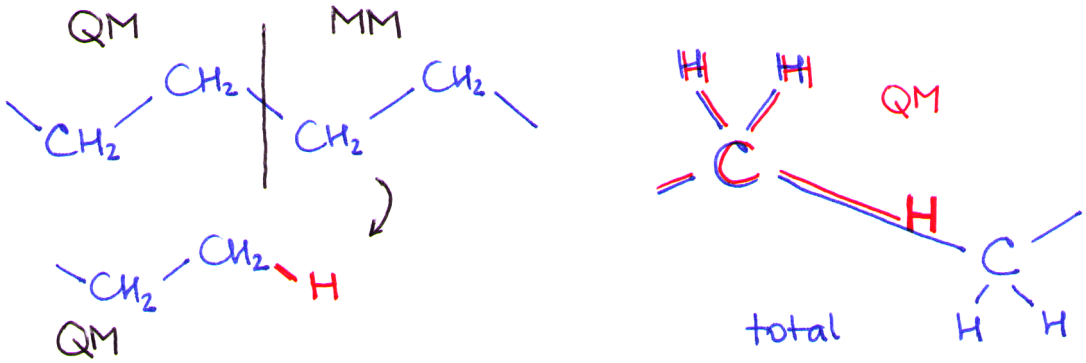

FIG. 62: Link atoms. Left: The QM/MM boundary cuts a bond between two sp^3-C atoms and a link hydrogen atom is used. Right: The link atom is placed on the C–C bond that has been cut; possible problem is that non-bonded interactions between the **H** and close MM atoms may diverge.

Link atoms are atoms that replace the covalently bonded MM system at the boundary, see Fig. 62. Usually, bonds between two sp^3-carbon atoms are chosen to be cut, and hydrogens are used as link atoms because of the similar electronegativity of carbon and hydrogen. It is thus desirable to define the QM region so that the bonds to be cut are as unpolar as possible, in order to minimize errors. The link hydrogen atom is then placed on the original C–C bond, in a typical C–H bonding distance from the QM carbon atom (Fig. 62 right).

The total energy may then be evaluated in the fashion called *additive coupling*. As the link atom is not really part of the QM region, the terms in expression for E_{QM} that involve the orbitals on the link atom are not evaluated. An obviously interesting point are the bonded interactions (bonds, angles and dihedral angles) involving the bond crossing the boundary. Their energy contributions are generally calculated with the force field. A possible exclusion are angles involving 2 QM atoms and 1 MM atom, and dihedrals with 3 QM atoms and 1 MM atom, which are omitted in some approaches.

Another important issue is that of MM atoms bearing point charges, that are situated very close to the QM system – typically, extremely close to a link atom. These would have unphysically large influence on the electronic structure of the QM system. Therefore, particular care must be taken of the charges of close MM atoms: These may be scaled down or even zeroed; alternatively, only their interaction with the QM atoms near the boundary may be scaled down or zeroed. A promising approach consists in the replacement of the close point charges by gaussian charge distributions – this maintains all charges while avoiding most of the trouble with too high interaction energies.

Alternatively, it is possible to apply the Eq. X.6 again, with the QM region ('small') now including the link atoms:

$$E_{\mathrm{total}} \;=\; E_{\mathrm{MM}}^{\mathrm{large}} + \left(E_{\mathrm{QM}}^{\mathrm{small+L}} - E_{\mathrm{MM}}^{\mathrm{small+L}}\right) \tag{X.7}$$

This is called the *subtractive coupling*.

The concept of link atoms is used very frequently in the studies of biomolecules, when quantum description is desired. The artifical separation of the molecular system in two brings on certain issues that need to be resolved in order to obtain correct results. Nevertheless, the development of QM/MM methodology has advanced considerably in the recent years, so that it is now considered to be a de facto standard tool in computational biophysics.

Deficiency of subtractive coupling – deprotonation of an alcohol

$$CH_3CH_2CH_2CH_2OH \rightarrow CH_3CH_2CH_2CH_2O^- + H^+$$

This reaction takes place in a small region of a large molecule. So, we can describe the 'interesting' region with QM – this will correspond to a *methanol* molecule. The rest of the molecule will be described as whole butanol with MM:

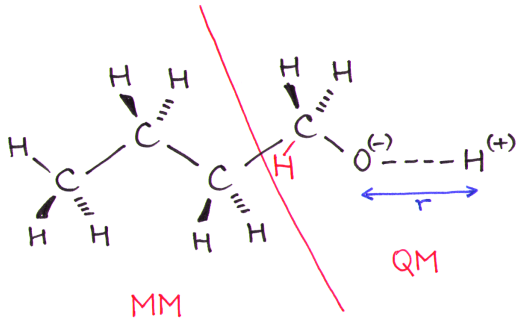

$$E^{\mathrm{QM/MM}}_{\mathrm{butanol}} = E^{\mathrm{QM}}_{\mathrm{methanol}} + \left(E^{\mathrm{MM}}_{\mathrm{butanol}} - E^{\mathrm{MM}}_{\mathrm{methanol}}\right)$$

We wish to evaluate the energy as a function of the O–H distance r. Let us assume the parameters for methanol and butanol to differ only in the force constant k^{OH} for the O–H bond. The remaining terms will give a constant independent of r:

$$\begin{aligned} E^{\mathrm{QM/MM}}_{\mathrm{butanol}}(r) &= E^{\mathrm{QM}}_{\mathrm{methanol}}(r) + \left(\frac{1}{2}k^{\mathrm{OH}}_{\mathrm{butanol}} \cdot (r - r_0)^2 - \frac{1}{2}k^{\mathrm{OH}}_{\mathrm{methanol}} \cdot (r - r_0)^2\right) + \text{const.} \\ &= E^{\mathrm{QM}}_{\mathrm{methanol}}(r) + \frac{1}{2}\left(k^{\mathrm{OH}}_{\mathrm{butanol}} - k^{\mathrm{OH}}_{\mathrm{methanol}}\right) \cdot (r - r_0)^2 + \text{const.} \end{aligned}$$

The MM energy remains in the form of a term proportional to r^2. For large r, the QM energy will be proportional to $-\frac{1}{r}$, due to Coulomb's law:

$$\lim_{r\to\infty} E^{\mathrm{QM}}_{\mathrm{butanol}}(r) = \lim -\frac{1}{r} = 0$$

The asymptotic behavior of total energy will look like

$$\lim_{r\to\infty} E^{\mathrm{QM/MM}}_{\mathrm{butanol}}(r) = \lim\left(-\frac{1}{r} + \frac{1}{2}k \cdot r^2\right) = \lim r^2 = \infty$$

The inequality of k^{OH} for methanol and butanol will make the total energy grow over all limits for large distance r. The entire effort will go in vain.

This will not happen in the *additive coupling*: Methanol will be calculated with QM, and propane with MM. The MM parameters for –OH group *are not required* at all.

Excursion – the linking scheme

The atom charge in most force fields are designed in such a way that certain groups of atoms maintain neutral or integral charge. See an example of the CHARMM force field:

```
RESI SER          0.00
GROUP
ATOM N    NH1    -0.47  !      |
ATOM HN   H       0.31  !   HN-N
ATOM CA   CT1     0.07  !      |   HB1
ATOM HA   HB      0.09  !      |   |
GROUP                   !   HA-CA--CB--OG
ATOM CB   CT2     0.05  !      |   |     \
ATOM HB1  HA      0.09  !      |   HB2    HG1
ATOM HB2  HA      0.09  !    O=C
ATOM OG   OH1    -0.66  !      |
ATOM HG1  H       0.43
GROUP
ATOM C    C       0.51
ATOM O    O      -0.51
```

Now, let us take the side chain as the QM system. Then, the atom CA is very close to the link atom placed in between CA and CB, and so the point charge on CA would disturb the QM region drastically. Also, it is impossible to remove the CA atom simply, because the entire backbone would not be charge-neutral any more. There are a couple of possibilities to deal with this problem:

- A drastic but still often used linking scheme ('exgroup' in CHARMM) is to remove *all* charges of the group close to the QM region. In our example, these are CA, HA, N and HN. Obviously, we would lose the strong N–HN dipole within this scheme, which could lead to very inaccurate result.

- A better way ('div' in CHARMM) is to *divide* the charge of the so-called host atom (here CA) among the remaining atoms of the whole host group (composed of HA, N and HN). The resulting charges in this example would be: CA=0, HA=0.11, N=−0.44, HN=0.33.

The latter approach is limited by the requirement to have the QM/MM boundary between two individual charge groups. 'Cutting' of a covalent bond within a single charge group (e.g. between CB and OG in this residue) is only possible with the former approach (the modified charges would be CB=0, HB1=0, HB2=0).

3. Frozen orbitals

As mentioned, the introduction of link atoms may cause problems with non-bonded interactions, because of the possibly extremely short distance between these artificially added QM atoms and nearby MM atoms. Also, the representation of charge densities by MM point charges may result in inaccuracy and/or computational instability. A promising attempt to avoid this issue may be to introduce no new *atoms*, but rather treat the orbitals on the QM/MM boundary in a special way. The shape of these orbitals can be held constant during the simulation, hence the term *frozen orbitals*.

With this approach, we will have not two but rather *three* regions in the simulation: the QM and MM regions as before, and an *auxiliary region* on the QM/MM boundary on top of that. The atoms in this auxiliary region possess their normal nuclei and electron densities expressed using the basis of atomic orbitals. Then, the auxiliary region actually possesses a quantum character, but still its interaction with itself as well as with the MM system can be calculated classically.[48] Another only slight complication is the energy of interaction of the QM system with the auxiliary – this adds another term to the Hamiltonian which corresponds to the interaction of the wave function with the frozen charge density in the auxiliary region, which is only slightly more complex than the interaction with point charges.

In the simple case of a single covalent bond being cut by the QM/MM boundary, the auxiliary region may be very small, as seen in Fig. 63.

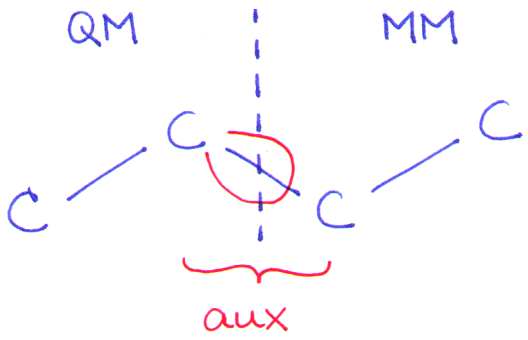

FIG. 63: Frozen orbital scheme. Red – the frozen sp^3 orbital for the bond crossing the boundary.

There are basically two approaches how to freeze the electron density. In the localized

[48] This may seem awkward but it is not so bad: interaction of (frozen) charge density with itself, and interaction of (frozen) charge denstity with a set of point charges; this is no issue in a calculation whatsoever.

SCF method (LSCF), every covalent bond crossing the QM/MM boundary is represented by a single frozen orbital – this is the (hybrid) atomic orbital localized on the QM atom before the boundary, which is calculated once at the beginning of the simulation and does not change shape afterwards any more. Some care must be taken of the occupation of the frozen orbitals in order to handle the density correctly, and this requires accurate accounting.

The generalized hybrid orbital approach (GHO) is different in that the QM/MM boundary does not cut any covalent bond, but rather the boundary passes through *an atom*. Here, the (hybrid) atomic orbitals on this particular atom which would belong to the MM region, are considered to be frozen. Their populations are calculated so that the resulting charge density corresponds to the point charge that this atom would have in an MM calculation. The remaining orbital on the atom, which points inwards the QM region, is frozen in shape but its occupation is free to vary in the QM calculation.

The approaches using frozen orbitals have received certain attention in the recent years and they are constantly being developed. However, the method of link atoms is clearly being applied more often, and has already been implemented in many popular simulation packages.

E. Advanced stuff and examples

1. QM/QM/MM

It is possible to improve the process of dividing the entire molecular system, so that there are *three* disjunctive regions: Then, one may be treated with an advanced, expensive QM method (correlated methods like CC, CAS...), another region surrounding the first one will be described with a faster QM method (like DFT or semiempirical), MM will be used for the rest of the system, probably including the solvent. This approach may be referred to as QM/QM/MM, and an example is the ONIOM scheme[49] implemented in GAUSSIAN.

2. Photochemistry–Retinal

Retinal is a polyene, covalently bound to a lysine side chain via a protonated Schiff base.

[49] a clear connotation with the layers of an onion

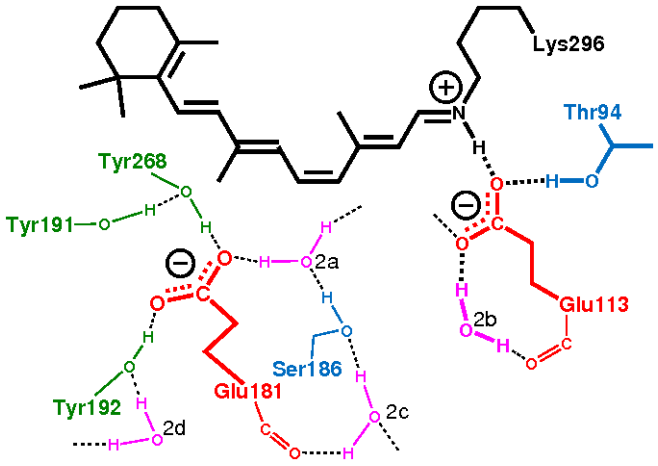

FIG. 64: Retinal (the chromophore) in rhodopsin, with the counterion Glu113 and charged Glu181.

It is not easy to choose a correct size of the QM region, and there are many possibilities:

	size	goodness, issue
	polyene (ring to NH)	**bad**, boundary cuts a polar bond
	retinal+CH_2	**bad**, link atom too close to the important region
QM1	retinal+sidechain to CB	**fair, but** no charge transfer to Glu113 possible
QM2	QM1+counterion	**better, but** no charge transfer to Wat
QM4	QM2+Wat2b+Thr94	**good, but** no polarization at Glu181
	QM4+Glu181	**very good, but**...

A highly correlated method (like CAS-PT2) is required to calculate the electronic spectrum of a chromophore in a protein (like the retinal within a rhodopsin). Also, it is crucial to describe the interaction of the electronic structure of retinal with the atoms of the protein. On the other hand, the vdW interaction with the protein is not so important, because the structure of the molecular system does not change during the photochemical process. Thus, a single-point calculation is sufficient. For the geometry optimization or MD simulation of the system, the complex electronic structure of retinal makes the use of a (modest) QM method necessary.

The calculation starts with a QM/MM calculation with approximative DFT, and the structure of the whole protein is optimized. The coordinates of QM atoms are written into a file, and so are the coordinates of all MM atoms together with the charges. These sets of data are fed to a highly correlated method, for the calculation of excitation energy.

XI. ENHANCING THE SAMPLING

At room temperatures, normal nanosecond length MD simulations have difficulty overcoming barriers to conformational transitions and may only sample conformations in the neighborhood of the initial structure.

A. Molecular dynamics as a way to the global minimum

Quotation from "A molecular dynamics primer" by Furio Ercolessi, University of Udine, Italy (`www.fisica.uniud.it/~ercolessi`).

Molecular dynamics may also be used as an optimization tool. Let us suppose that a set of N particles has many possible equilibrium configurations – this is truly the case with large (bio)molecules. The energy of these configurations is in general different, and one of them will be the lowest; each of the configurations, however, corresponds to a local minimum of the energy and is separated from every other by an energy barrier.

Finding the most energetically favorable structure – i.e. the global minimum of the energy function – within an approach based on traditional minimization techniques (steepest-descents, conjugate gradients, etc.) is tricky as these methods do not normally overcome energy barriers at all and tend to fall into the nearest local minimum. Therefore, one would have to try out several (many) different starting points, corresponding to different "attraction basins" in the energy landscape, and relax each of them to the bottom of the basin. The optimal structure would then be the one with the lowest energy, provided we were lucky enough to select it in the list of candidates.

1. Simulated annealing

Temperature in an MD (or Monte Carlo) simulation is the key to overcome the barriers: States with energy E are visited with a probability of $\exp[-E/k_BT]$. If T is sufficiently large, then the system will "see" the simultaneous existence of many different minima, still spending more time in the deeper ones. By decreasing T slowly to zero, there is a good chance that the system will pick up the deepest minimum and stay trapped there. This consideration is the principle of simulated annealing: The (molecular) system is equilibrated at a certain temperature and then (slowly) cooled down to $T = 0$. While this procedure does

not guarantee that the true global minimum will be reached, it often does so. And, since no a priori assumptions are made about the optimal structure, it often yields structures that would have been difficult to foresee by intuition alone.

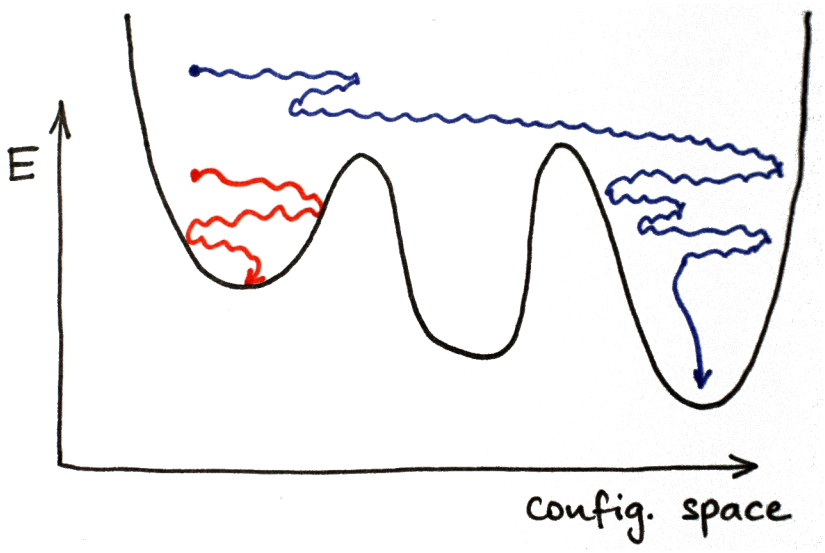

FIG. 65: Simulated annealing.

This method is often used to optimize the structure of molecular systems, but its validity is much more general: Given an objective function $Z(\alpha_1, \ldots, \alpha_N)$ depending on N parameters, one can regard each of these parameters as a degree of freedom, assign it a "mass", and let the system evolve with a molecular dynamics or Monte Carlo algorithm to perform simulated annealing. One of the early applications of this method can be found in a famous paper discussing an application to the problem of the traveling salesman (Kirkpatrick et al., Science 1983).

2. MD quenching

There is yet another possibility to make use of molecular dynamics not only to obtain the minima of the energy, but even to approximate their relative free energies (or equilibrium constants). An MD/quenching simulation consists of a usual MD trajectory, which is a basis for subsequent minimizations: In regular intervals, the structure from the simulation is subject to energy-minimization. In principle, we avoid the need to select starting structures for our minimizations – instead, we let the MD simulation take care of that.

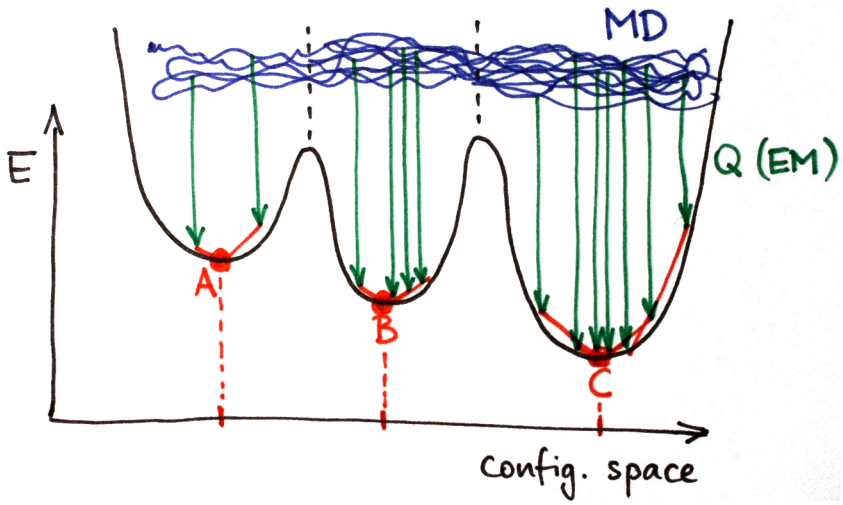

FIG. 66: MD quenching.

The obtained (possibly many) minimized structures can be processed e.g. by a cluster analysis to determine the set of unique optimal structures, their total energies and number of hits. For a small molecular system, we would observe few unique structures, each occuring many times; for larger systems, the number of unique structures would grow rapidly.

A potentially appealing feature of MD/quenching is the possibility to estimate the relative free energies of the observed structures. If the MD simulation subject to post-processing is long enough (i.e. if sufficient sampling of the configuration space is guaranteed) then the ratio of their occurence (number of hits, n_i) determines the equilibrium constant K, and thus the free energy ΔG:

$$\begin{aligned} K &= \frac{n_2}{n_1} \\ \Delta G &= -k_B T \log K = k_B T \log \frac{n_2}{n_1} \end{aligned} \tag{XI.1}$$

It is important to note that we consider whole regions of configuration space (as in Fig. X) rather than points to be individual structures. Therefore, we obtain no curves of free energy as a function of coordinate(s) but rather single values of free energy differences for certain pairs of "structures". There is an interesting, neraly philosophical question connected to this – is there something like "free energy surface" at all? Or, like obviously is the case with quenching, is it only meaningful to ask for discrete values of free energy differences?

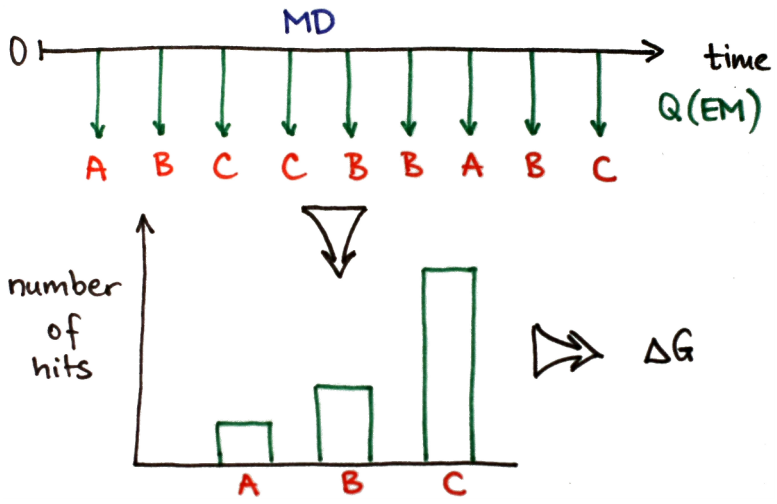

FIG. 67: MD quenching2.

B. Replica-exchange MD

Replica-exchange molecular dynamics (REMD, a.k.a. parallel tempering) is a method to accelerate the sampling of configuration space, which can be applied even if the configurations of interest are separated by high barriers. With REMD, several (identical) copies, or replicas of the molecular system of interest are simulated at the same time, with different temperatures. The essence of the method is that the coordinates together with velocities of the replicas may be switched (exchanged) between two temperatures. In practice, the probability of the replica exchange between temperatures $T_1 < T_2$ is determined in (regular) time intervals from the instantaneous potential energies U_1 and U_2 in the corresponding simulations as

$$P(1 \leftrightarrow 2) = \begin{cases} 1 & \text{if } U_2 < U_1, \\ \exp\left[\left(\frac{1}{k_B T_1} - \frac{1}{k_B T_2}\right) \cdot (U_1 - U_2)\right] & \text{otherwise.} \end{cases} \tag{XI.2}$$

Then, if $P(1 \leftrightarrow 2)$ is larger than a random number, the replicas in simulations at temperatures T_1 and T_2 are exchanged.

When using REMD, there usually one replica is simulated at the temperature of interest (often $T_1 = 300$ K) and several other replicas at higher temperatures ($T_1 < T_2 < T_3 < \ldots$). After, say, 1000 steps of MD, replica exchanges $1 \leftrightarrow 2$, $3 \leftrightarrow 4$ etc. are attempted, and after next 1000 steps the same is done for $2 \leftrightarrow 3$, $4 \leftrightarrow 5$ etc. so that only the replicas at "neighboring" temperatures can be exchanged. With such setup, the advantages of the

simulations at high temperatures – fast sampling and frequent crossing of energy barriers – combine with the correct sampling at all temperatures, above all at the (lowest) temperature of interest. Although the computational cost of REMD simulations is increased (because many simulations are running simultaneously), this additional investition of resources pays off with extremely accelerated sampling. Moreover, the simulations running at different temperatures are completely independent of each other between the points of attempted exchange, making this problem trivially (*embarassingly*) parallelizable. The first application of REMD was for a truly biophysical problem – folding of a protein (Sugita & Okamoto, Chem. Phys. Lett. 1999).

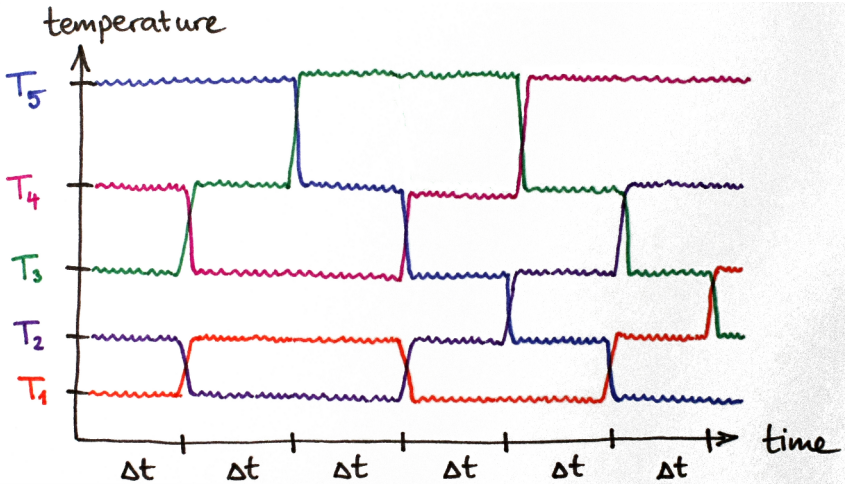

FIG. 68: Replica-exchange MD.

An important point with REMD is a suitable choice of temperatures T_i. This depends on (i) how frequent exchanges we wish (average probability $P(1 \leftrightarrow 2)$), (ii) the size of the system (the number of degrees of freedom N_{dof}) and (iii) the number of temperatures/simulations. For protein/water systems with all bond lengths constrained to their respective equilibrium values (so that $N_{\mathrm{dof}} \approx 2N$, N – number of atoms), the average probability is related to the difference of temperatures $T_2 - T_1 = \varepsilon T_1$ as

$$\overline{P(1 \leftrightarrow 2)} \approx \exp\left[-2\varepsilon^2 N\right] \tag{XI.3}$$

Using this relation, we can design the set of temperatures to suit our needs.

The REMD method can be likened to "super simulated annealing" without a need to restart. The systems at high temperatures can feed new local optimizers to the systems at

low temperatures, allowing tunneling between metastable states and improving convergence to a global optimum.

1. Replica-exchange umbrella sampling

There is an interesting application of the replica-exchange idea concerning biasing potentials rather than thermodynamic parameters (Okamoto et al., J. Chem. Phys. 2000). With the replica-exchange umbrella sampling approach (REUS), several copies of the molecular system are simulated with different biasing potentials – these are the separate umbrella-sampling simulations as presented in a previous chapter. As with the previously described REMD, an exchange of replicas with 'neighboring' umbrellas is attempted in regular intervals. Obiously, the criterion for the acceptance of a replica exchange has to be modified, and may read for instance

$$\Delta = \frac{1}{kT_1}\left(U_1(q_2) - U_1(q_1)\right) - \frac{1}{kT_2}\left(U_2(q_1) - U_2(q_2)\right) \tag{XI.4}$$

$$P(1 \leftrightarrow 2) = \begin{cases} 1 & \text{if } \Delta \leq 0, \\ \exp\left[-\Delta\right] & \text{otherwise.} \end{cases} \tag{XI.5}$$

where U_i is potential energy calculated with the energy function (including bias – umbrella) from simulation i, and q_i are the coordinates of all atoms from simulation i. With this setup, improved sampling of the configuration space and thus increased efficiency of the simulation may be expected.

It is even possible to do *multidimensional replica exchange* simulations, where the molecular system is replicated with multiple different simulation parameters – for instance, various temperatures *and* various biasing potentials.

C. Methods using biasing potentials

Using quotations by Helmut Grubmüller
(`www.mpibpc.mpg.de/home/grubmueller/projects/MethodAdvancements/ConformationalDynamics`

The energy landscapes occuring in large (bio)molecular systems feature a multitude of almost iso-energetic minima, which are separated from each other by energy barriers of various heights. Each of these minima corresponds to one particular structure ('conformational

substate'); neighboring minima correspond to similar structures. Structural transitions are barrier crossings, and the transition rate is determined by the height of the barrier.

Since in conventional MD simulations only nanosecond time scales can be covered, only the smallest barriers are overcome in simulations, and the observed structural changes are small. The larger barriers are traversed more rarely (however the transition process itself may well be fast), and thus are not observed in MD simulations.

Several approaches to remedy this drawback by way of modifying the potential energy surface of the molecular system have been proposed.

1. Conformational flooding

(Grubmüller, Phys. Rev. E 1995)

A method called 'conformational flooding' accelerates conformational transitions in MD simulations by several orders of magnitude and thereby actually can bring slow conformational transitions into the scope of simulations. From the ensemble generated by the (unbiased = normal) MD simulation, a localized artificial 'flooding potential' V_{fl} of certain (variable) strength can be constructed, meeting two requirements: (i) V_{fl} shall affect only the initial conformation and vanish everywhere outside of this region of conformational space, and (ii) it shall be well-behaved (smooth) and 'flood' the entire initial potential-energy well. A multivariate (n-dimensional) Gaussian function exhibits such a behavior:

$$V_{\mathrm{fl}} = E_{\mathrm{fl}} \cdot \exp\left[-\frac{E_{\mathrm{fl}}}{2k_{\mathrm{B}}T} \cdot \sum_{i=1}^{n} q_i^2 \lambda_i\right] \tag{XI.6}$$

where E_{fl} is the strength of the flooding potential. Here, the first n essential dynamic modes with eigenvalues λ_i will be flooded, with q_i being the coordinates along these modes.

This potential is included within subsequent 'flooding' (biased) simulations and rises the minimum of the initial conformation. Thereby, the barrier height is reduced, and the transitions are accelerated (following the theory of transition states). It is important to note that this is achieved solely by modifying the energy landscape within the minimum where the dynamics is already known and thus uninteresting; the barriers and all the other minima – which we are interested in – are not modified at all. The bottom-line is that 'conformational flooding' is expected to induce unbiased transitions, i.e. those which would be observed without the flooding potential, too, on a much longer time scale.

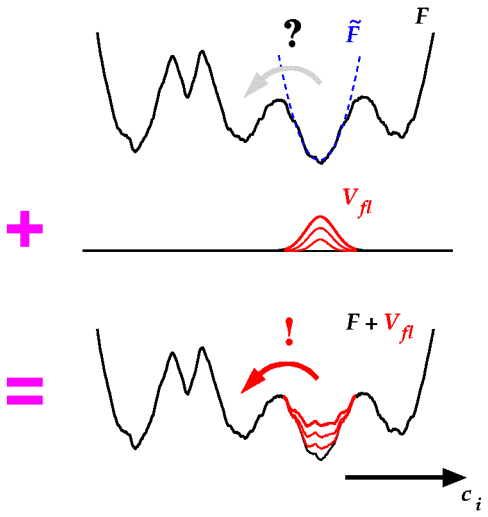

FIG. 69: Sketch of the conformational flooding (from the website of H. Grubmüller).

2. Metadynamics

Using quotation by Alessandro Laio (`people.sissa.it/~laio/Research/Res_metadynamics.php`)

The method is aimed at reconstructing the multidimensional free energy of complex systems (Laio & Parrinello, Proc. Natl. Acad. Sci. USA 2002). It is based on an artificial dynamics (metadynamics) performed in the space defined by a few collective variables S, which are assumed to provide a coarse-grained description of the system. The dynamics is biased by a history-dependent potential constructed as a sum of Gaussians centered along the trajectory of the collective variables. A new Gaussian is added at every time interval t_G, and the biasing potential at time t is given by

$$V_G(S(x),t) = \sum_{t'=t_G,2t_G,3t_G,\ldots} w \cdot \exp\left[\frac{(S(x)-s_{t'})^2}{2\cdot\delta s^2}\right] \qquad \text{(XI.7)}$$

where w and δs are the height and the width of the Gaussians, and $s_t = S(x(t))$ is the value of the collective variable at time t. In the course of time, this potential is filling the minima on the free energy surface, i.e. the biased energy surface (sum of the Gaussians and the free energy) as a function of the collective variable(s) S is becoming constant. So, the MD protocol exhibits a kind of memory via the changing potential-energy function – a concept that was introduced earlier under the name "local elevation" (Huber et al., J. Comp. Aided Molec. Design 1994).

This approach can be exploited to explore new reaction pathways and accelerate rare events, and also to estimate the free energies efficiently. The features of metadynamics:

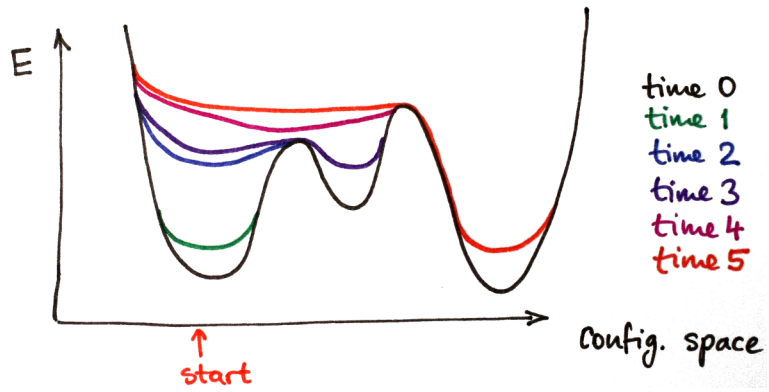

FIG. 70: Metadynamics.

- The system escapes a local free energy minimum through the lowest free-energy saddle point.

- The dynamics continues, and all the free-energy profile is filled with Gaussians. At the end, the sum of the Gaussians provides the negative of the free energy. This latter statement is correct if the dynamics along S is much slower than the dynamics along the remaining (transversal) degrees of freedom.

The crucial point of the method is to identify the variables that are of interest and that are difficult to sample, since the stable minima in the space spanned by these variables are separated by barriers that cannot be cleared in the available simulation time. These variables $S(x)$ are functions of the coordinates of the system; practical applications allow the definition of up to three such variables, and the choice depend on the process being studied. We can think for instance of the principal modes of motion obtained with principal component analysis (covariance analysis, essential dynamics). However, the choice of S may be far from trivial.

The metadynamics method may be also classified as a variant of the adaptive umbrella sampling approach.

D. Locally enhanced sampling

Quotation from the Amber website, by David A. Case (`www.ambermd.org`).

Locally enhanced sampling (LES) is a mean-field technique which allows selective application of additional computational effort to a portion of the system, increasing the sampling

of the region of interest (Elber & Karplus, 1990). The enhanced sampling is achieved by replacing the region(s) of interest with multiple copies. These copies *do not interact* with each other, and interact with the rest of the system in an *average way*. This average is an average force or energy from all of the individual copy contributions, not one force or energy from an average conformation of the copies.[50] A key feature is that the energy function is modified such that the energy is identical to that of the original system when all LES copies have the same coordinates.

During the simulation, the copies are free to move apart and explore different regions of conformational space, thereby increasing the statistical sampling. This means that one can obtain multiple trajectories for the region of interest while carrying out only a single simulation. If the LES region is a small part of the system (such as a peptide in solution, or a loop in a protein), then the additional computational effort from the added LES particles will be a small percentage of the total number of atoms, and the multiple trajectories will be obtained with a *small additional computational effort*.

Perhaps the most useful feature of the LES method is that it has been shown that the barriers to conformational transitions in a LES system are reduced as compared to the original system, resulting in more frequent conformational changes (Roitberg & Elber, 1991). This can be rationalized with a simple model: Imagine a protein side chain that has been replaced with 2 copies. At finite temperatures, these copies will have different conformations. Now consider the interaction of another part of the system with this region – previously, steric conflicts or other unfavorable interactions may have created high barriers. Now, however, the rest of the system sees each of these 2 copies with a scaling factor of $\frac{1}{2}$. Whereas one copy is in an unfavorable conformation, the other may not be, and the effective barrier with a distribution of copies is lower than with a single copy (as in normal MD).

Another way to consider the LES copies is that they represent an intermediate state between a normal simulation where each point in time represents a single structure, and a purely continuum model where the probability distribution of regions of interest are represented by a continuous function. The atoms outside a LES region interact with that region as if it were (in the limit of many copies) a continuum, with a probability scaling given to

[50] Note the difference! The forces from all copies are calculated and their average is then taken. *No average structure* or the like is calculated.

all interactions. Therefore, the most unfavorable interactions are reduced in magnitude as compared to the original system.

Another major advantage of LES over alternate methods to reduce barriers or improve sampling is that it is compatible with current state-of-the-art simulation techniques such as molecular dynamics in explicit aqueous solvation (problems for techniques such as Monte Carlo or genetic algorithms) and the particle–mesh Ewald technique for accurate treatment of long-range electrostatic interactions. Higher temperatures can increase rates of barrier crossing, but one is then faced with issues related to solvent behavior at higher temperatures, maintaining proper densities and pressures, stability of the molecule of interest at the elevated temperature, and so on. LES gives more direct control over which regions should be enhanced, and also provides other benefits such as improvement in statistical sampling discussed above.

XII. VARIOUS – COARSE GRAINING, HARD SPHERES, MONTE CARLO

A. United-atom force fields and coarse-grained models

In the studies of biomolecules, a proper and efficient treatment of the solvent is the key to the feasibility of the entire model. However, it may well happen that there are other components in the system that contain a large number of atoms – an example may be the lipid in the studies of transmembrane proteins. Even worse, the biomolecule itself may be exceedingly large – a very large protein or a long nucleic acid species. In such cases, it is necessary to modify the description of the biomolecule – to simplify the molecular model.

Early force fields (like Weiner 1984 and others) already used a similar idea. Within the *united-atom* force fields, each hydrogen atom was considered not individually, but rather condensed to the heavy atom to which it was connected. This way, the number of atoms was reduced considerably if compared with the *all-atom* force fields, which earned popularity in the 1990's. It is necessary to mention here that this approach works very well for non-polar C–H bonds, so that it is a very good approximation to consider a methyl group constituting one united atom. On the other hand, the substitution of a polar O–H group by a single particle is obviously a very crude approximation which will not work unless there are further correction terms in the force field. The united-atom force fields found their use in the modern computational chemistry e.g. in studies involving lipids, where each methylene group constitutes a united atom, cf. Fig. 71.

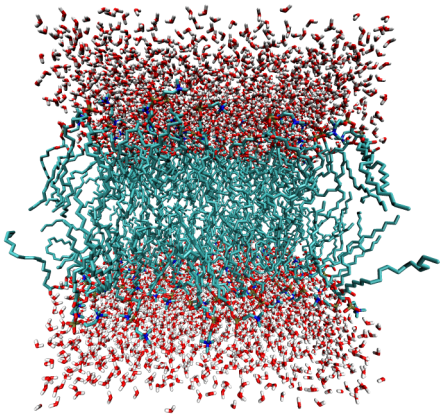

FIG. 71: A snapshot from the simulation of a lipid bilayer in water. The lipid (DOPC) is described with a united-atom force field – every CH_2 group is represented by a united atom. Downloaded from the website of R. Böckmann.

An advanced and sophisticated approach to cut the computational expense of simulations is the *coarse graining* (CG) of the problem. Quite naturally, a way to accelerate the evaluation of interactions is to reduce the number of particles involved. As it may not be always possible to reduce the number of atoms, an alternative idea is to consider particles composed of *several* atoms, so-called *beads*. Then, the number of inter-particle interactions will decrease, and in spite of the possibly more complex form of these interactions, the computational expense may be largely reduced as well. The necessary parameters of the force field are often obtained by fitting to all-atom force fields.

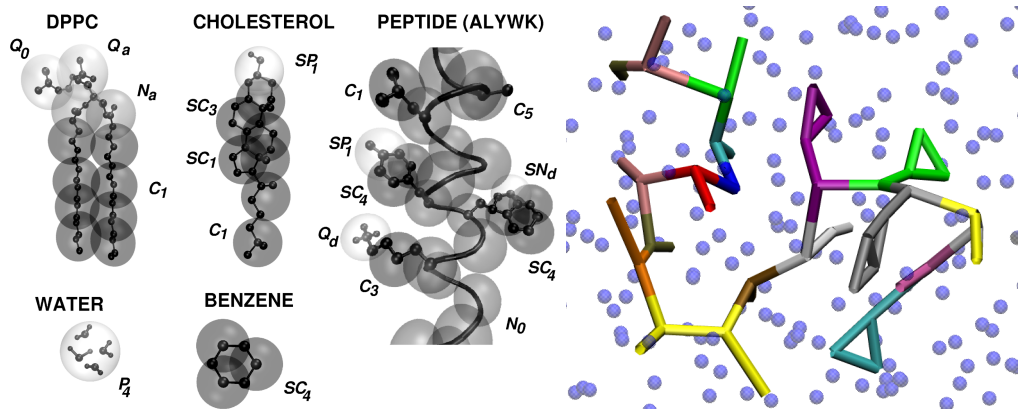

FIG. 72: Left: The CG force field MARTINI – mapping of beads onto molecular fragments. Right: A solvated peptide with MARTINI. Downloaded from the MARTINI website.

In the MARTINI force field, every bead represents 3 or 4 heavy atoms together with the connected hydrogen atoms, see Fig. 72. Coarse-grained simulations run faster than simulations with all-atom force fields for several reasons:

- smaller number of particles leading to fewer interactions that need to be evaluated
- it is possible to use a long integration time step due to large masses of beads, which can be as much as 25 fs with Martini (i.e. 100 fs effectively, see below)
- these force fields are often constructed for use with faster simulation algorithms – e.g. cut-off for electrostatics with Martini
- smaller number of degrees of freedom leads to smoother free energy surfaces and fewer barriers that any process needs to overcome. This acceleration is by a factor of 3

to 8 for Martini – not uniform (the same for every process), while a factor of 4 (for acceleration of diffusion in water) is usually used to calibrate the time scale.

Such CG force fields are particularly useful for simulations of large-scale conformational transitions, involving either exceedingly large molecular systems or excessive time scales, or both. The accessible length and time scales are typically 2 to 3 orders of magnitude larger compared with atomistic simulations. Another example is the VAMM force field for proteins, where every amino acid is represented by a single bead at C-α, see Fig. 73.

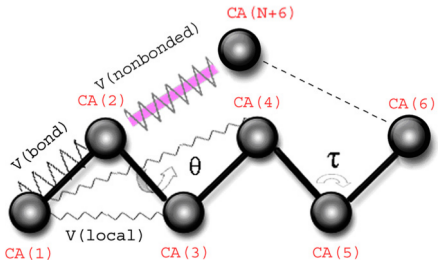

FIG. 73: The CG force field VAMM. Reprinted from Korkut & Hendrickson 2009.

B. MD simulation of hard bodies

The first MD simulation of a system in the condensed phase used the model of hard spheres (Alder & Wainwright, J. Chem. Phys. 1957). Representing a first step from the ideal gas model towards realistic molecules, this model has been a valuable tool above all in statistical thermodynamics, deriving e.g. equations of state and virial expansions.

1. The hard-sphere potential

The potential is a pairwise one. The potential energy of a system of two hard spheres with radius R equals zero for distances larger than the diameter of the spheres and rising above all bounds (infinity) for shorter distances when the spheres overlap:

$$V(r) = \begin{cases} 0 & \text{if } r > 2R \\ +\infty & \text{otherwise} \end{cases} \tag{XII.1}$$

The potential is *discontinuous* and thus not differentiable, and this is different from the potentials typically used in biomolecular simulation.

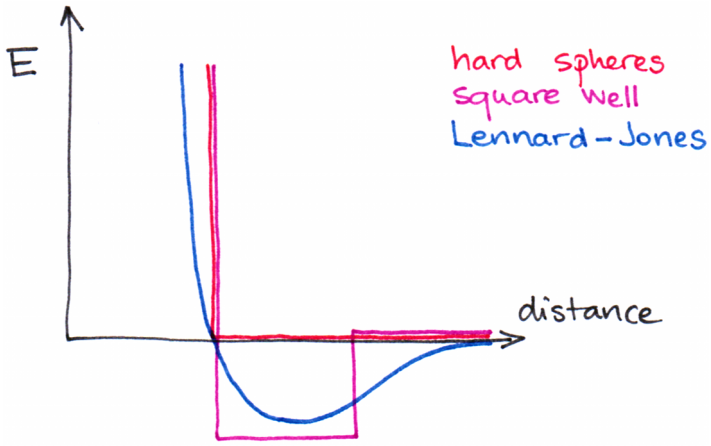

FIG. 74: The potentials of hard spheres, square well and Lennard-Jones.

If we wished to proceed further towards realistic description, however preserving the simplicity of the interaction model, we would probably opt for the so-called *square well model*, which features a region of negative potential energy (corresponding to attraction) starting at the contact distance $2R$. Clearly, such an approximation goes in the direction of the Lennard-Jones potential, which describes the behavior of nonpolar fluid very well.[51]

Hard-convex-body potential is another extension used in statistical thermodynamics. Still, the potential energy function is discontinuous – zero if the bodies do not intersect and infinity if they do. The enhancement is represented by the shape of the bodies, which is not spherical anymore but rather ellipsoidal or the like. Such a shape may better describe diatomic molecules for instance.

2. Simulation protocol

As stated in the previous chapters a few times, the integration of Newton's equations motion requires the used (pair) potential to be continuous and possibly smooth (i.e. with continuous first derivative). If this is not the case, then the atoms will experience sudden 'jumps' in forces, leading to unstable simulations and wrong sampling of the configuration space, see Fig. 75.

The situation with the hard-body potential is even worse, as there is an infinitely high

[51] This is probably the reason why physical chemists like argon so much. The simple LJ potential describes argon extremely accurately.

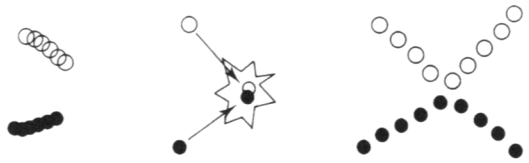

FIG. 75: If we attempted to simulate hard spheres with an integrator, we would see an explosion caused by a sudden occurence of an overlap of atoms, much the same as in the case of a simulation with continuous potential and a way too large time step (center). However, with hard spheres, an arbitrarily short time step would be still too long.

jump of potential energy at the edge of the body (particle). What would a simulation of hard spheres with (say) the Verlet integrator look like? There are no forces in any initial configuration, and so the spheres move with their initial velocities until, all of a sudden, two spheres start to overlap. At that very moment, the energy and the forces are infinite, and the simulation crashes.

The simulation protocol for a system of particles interacting with a hard-body potential has to be adjusted to the discontinous character of this potential. The spheres (bodies) move along straight lines between collisions, which are perfectly elastic and instantaneous. A simulation of such a system proceeds as follows:

1. Identify the next pair of spheres (bodies) to collide, and calculate when this collision will occur.

2. Calculate the positions of all spheres at the collision time, using the principle of conservation of linear momentum and kinetic energy.

3. Determine the new velocities of the two spheres after collision.

4. Repeat from start.

Obviously, no further approximations are involved in this protocol, and a simulation will be exact within the model of hard spheres. (This is different with continuous potentials, where approximations have to be made, usually via a stepwise integration of the equations of motion.)

The potential energy is constant (zero) throughout the simulation. Thus, the conservation of total energy forces the conservation of kinetic energy, meaning that in any simulation with hard spheres, the temperature is actually constant.

C. Monte Carlo approach

In many (if not most) of the applications of molecular dynamics, the main objective is not to study how the molecular system evolves in time, but rather to generate as many configurations of the system as possible in order to sample the configuration space and estimate some thermodynamic quantites. MD is not the only possibility to do this, and we are actually free to design a method to generate the needed configurations as long as these sample the correct (e.g. canonical ensemble).

Another possibility are the Monte Carlo methods (MC). Actually, an MC technique was the first technique used to perform a computer simulation of a molecular system. The not-too-chemically sounding name comes from the crucial role that random numbers play in the MC algorithm.

1. *Monte Carlo integration*

As mentioned above, one of the major goals if molecular simulations is to calculate the thermodynamic properties. Formally, this is done by the integration over the entire configuration space. Now then, how could we use a method based on randomness to integrate a function?

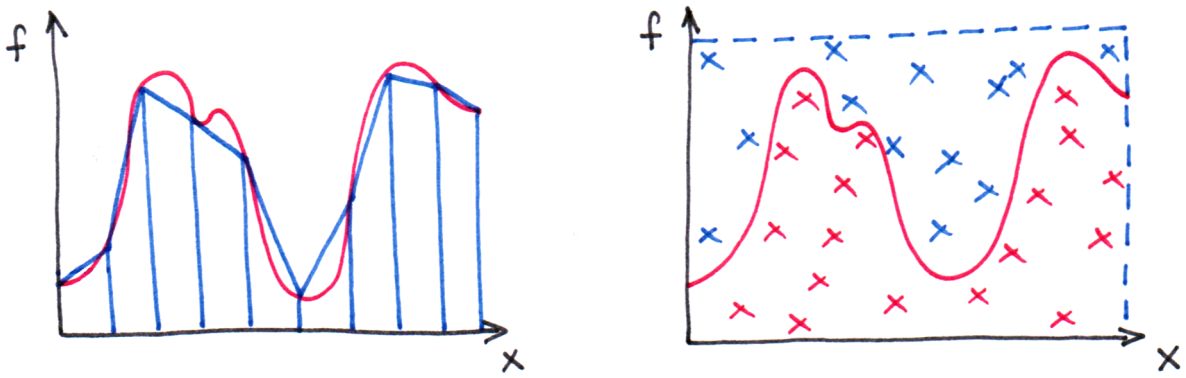

FIG. 76: Integration with the trapezoidal rule (left) and with Monte Carlo (right).

An example is shown in Fig. 76 – the task is to estimate the area under the curve, or to integrate the function. This could be done by the application of the trapezium rule. However, this method (as well as all the other commonly used ones) comes into trouble if we have to integrate a function of many variables, as is always the case in the studies of

molecular systems. Here, we can make use of an alternative idea: Generate N randomly placed points within a rectangle, and count how many points (n) lie under the curve. Then, the ratio n/N approximates the ratio of area under the curve to the area of the rectangle.[52]

Importantly, it is straightforward to extend this idea to a problem in many dimensions – and we can make use of this in studies of molecular systems. Conveniently, the integration will be made even more straightforward if we are able to generate the configurations with the right probability, i.e. sampling the correct thermodynamic (e.g. canonical) ensemble. Such *importance sampling* will make it possible to average the thermodynamics quantity trivially over the ensemble of generated configurations.

2. Metropolis' method

A typical MC simulation of a molecular system generates a sequence of configurations in an iterative way – in every iteration, one configuration is produced. Usually, a new configuration is constructed from the current one by randomly shifting a single randomly chosen atom (or, in general, particle). In practice, the new set of Cartesian coordinates is calculated with random numbers $\xi \in (0, 1)$ as

$$\begin{aligned} x_{\text{new}} &= x + (2\xi - 1) \cdot \delta r \\ y_{\text{new}} &= y + (2\xi - 1) \cdot \delta r \\ z_{\text{new}} &= z + (2\xi - 1) \cdot \delta r \end{aligned} \tag{XII.2}$$

where δr is the maximum allowed displacement.

Then, a test is performed to inspect if this configuration shall be accepted or not. To do this, potential energy of the entire molecular system is calculated. The calculation can be optimized by realizing that only a small part of the system (a single particle) has moved since the previous iteration. Consequently, only a small part of the usually considered pair interactions changes.

The acceptance probability of the trial configuration is obtained from the current potential

[52] Apply the Monte Carlo idea to calculate π as follows: Generate pairs of random number between 0 and 1 (x, y). Count the pairs for which $x^2 + y^2 < 1$, i.e. the point (x, y) lies within the circle centered at (0,0) with a radius of 1. The ratio of this number to the total number of pairs approximates the value of $\pi/4$.

energy U and that of the trial configuration U_{new} as

$$P = \begin{cases} 1 & \text{if } U_{\mathrm{new}} < U \\ \exp\left[-\frac{U_{\mathrm{new}}-U}{k_{\mathrm{B}}T}\right] & \text{otherwise} \end{cases} \tag{XII.3}$$

For $P < 1$, a (pseudo)random number is drawn from the interval (0,1). The trial configuration is accepted if P is larger than this random number. If it is not the case, the trial configuration is discarded and a new one is generated by modifying the coordinates of the current configuration.

The percentage of accepted configurations (among all the generated) is governed by the maximum allowed displacement δr, which is an adjustable parameter. It is usually chosen so that $\frac{1}{3}$ to $\frac{1}{2}$ of all configurations are accepted. Such acceptance ratio was shown to lead to the most efficient sampling of the configuration space. If δr is too small, then most configurations are accepted though, but the configurations are very similar and the sampling is slow. On the other hand, if δr is too large, then too many trial configurations are rejected. Often, δr is adjusted in the course of the simulation in order to reach a certain target acceptance ratio.

There are some modifications possible to the described recipe. Instead of selecting the atom to move randomly, it is possible to move the atoms sequentially, in a preset order. This way, one less random number per iteration has to be obtained. Alternatively, several atoms can be moved at once, instead of a single atom. With an appropriate maximum allowed displacement, this procedure may sample the configuration space very efficiently.

3. Intermezzo: generators of pseudorandom numbers

A Monte Carlo algorithm requires several random numbers to be obtained in every iteration, and since many steps have to be performed in a typical simulation (where many may mean millions or so), it is necessary to have a reliable and efficient source of random numbers. It would be most convenient to be able to 'calculate' random numbers in some way. This is actually a paradoxical requirement: computers are intrinsically deterministic devices, which are designed to deliver results that are determined by the input.

However, there are ways to generate sequences of 'pseudorandom' numbers, which are actually not random in the true meaning of the word. Still, they are independent enough of

each other and have the right statistical properties, which makes them useful for MC.

Most commonly used are the *linear congruential generators*, which produce sequences of pseudorandom numbers. A following number in the sequence ξ_{i+1} is obtained by taking the previous number ξ_i, multiplying by a constant (a), adding another constant (b) and taking the remainder when dividing by yet another constant (m). Obviously, an initial value ('seed') has to be given to the generator (the system time on the computer is often used). If 'real' values are requested rather than integers, the obtained number is divided by the modulus m (to get to the interval (0,1)).

$$\begin{aligned} \xi_0 &= \text{seed} \\ \xi_{i+1} &= (a \cdot \xi_i + b) \bmod m \end{aligned} \tag{XII.4}$$

Here, it is essential to choose 'good' values of a, b and m. If they are chosen carefully, then the generator will produce all possible values $0, \ldots, m-1$ and the sequence does not start to repeat itself until m numbers have been generated. If they are not, the sequence starts to repeat much earlier, and there is not much randomness in there at all. A disadvantage of these generators is that the generated points in an N-dimensional space are not distributed uniformly in the space but rather lie on at most $\sqrt[N]{m}$ $(N-1)$-dimensional planes (i.e. on straight lines if we have a 2D space). If the generator is poor, the number of these planes is much smaller than $\sqrt[N]{m}$.[53]

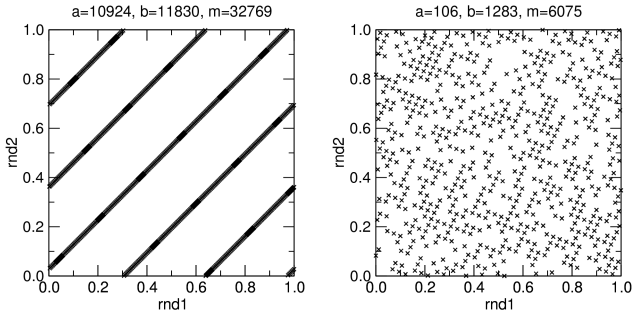

FIG. 77: A bad and a good generator of pseudorandom numbers. Each point (rnd1,rnd2) is a pair of consecutive numbers in the generated sequence.

In spite of the mentioned disadvantages, linear congruential generators are often used in MC simulations because of their extreme simplicity and thus computational efficiency. The

[53] An example of such generator is RANDU: ξ_0 is odd and $\xi_{i+1} = 65539 \cdot \xi_i \bmod 2^{31}$. All generated values are odd, the period is only 2^{29} and the points $(\xi_i, \xi_{i+1}, \xi_{i+2})$ cumulate on as few as 15 planes in space.

classes of pseudorandom number generators of higher quality include the linear feedback shift register generators (LFSR) or Mersenne twister (MT). LFSR uses several bits from the current number to generate a new sequence of bits constituting a newly generated number, and it does not suffer from the cumulation of the generated numbers on hyperplanes.
MT is the current state of the art among generators and outperforms the previously mentioned e.g. by an extremely long period of $2^{19937} - 1$ and no cumulation of numbers on hyperplanes in spaces with up to 623 dimensions. In a modified form, it is even suitable for cryptographic applications.

Alternative generators – from WIKIPEDIA: In Unix-like operating systems (with Linux being the first), `/dev/random` (or `/dev/urandom`) is a special file that serves as a random number generator or as a pseudorandom number generator. It allows access to environmental noise collected from device drivers and other sources.

4. Monte Carlo simulation of molecules

The easiest implementation of MC is for systems of monoatomic molecules, because it is only necessary to deal with the translational degrees of freedom. In polyatomic molecules, the implementation is more complex, and the situation is most difficult if there is much conformational flexibility in the molecules. Then, the internal degrees of freedom have to be free to vary, but this may often lead to an overlap of atoms accompanied by energy growing steeply. The ratio of acceptance of configurations would be extremely low.

It is still quite easy to simulate rigid molecules with MC. Apart from their position in space, their orientation has to be varied. This is accomplished by a rotation along one of the Cartesian axes (x, y or z) by a randomly chosen angle. There is some trigonometry to do to obtain the position of the molecule in the trial configuration.

5. Monte Carlo simulation of polymers

Many approximative models of polymers have been developed that are suitable for MC simulation. A class of convenient representations of polymers is that of a chain of monomer units, which are elementary particles (without further internal structure).

Lattice models are very simple and thus useful for very efficient studies of polymers. Here,

monomer units connected with a bond can occupy neighboring lattice points in a cubic or tetrahedral lattice (Fig. 78). The used expressions for potential energy are usually very

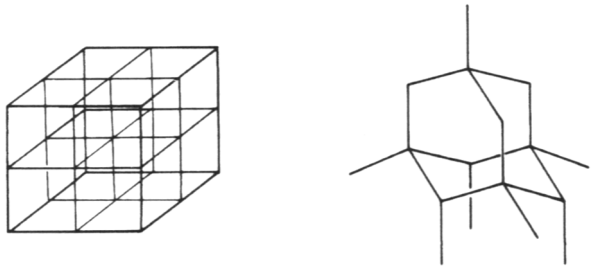

FIG. 78: Monte Carlo of a polymer – cubic (left) and diamond-like (right) lattices.

simple, which is partially forced by the simple structure of the model but also required to evaluate the energy rapidly and to sample the configuration space efficiently. An example of a more realistic and thus more complex lattice model is the 'bond fluctuation' model, where the lattice is finer-grained with respect to the bond length and the bonds between the particles (which actually stand for several covalent bonds each) are not constrained to lie on the lattice edges (Fig. 79).

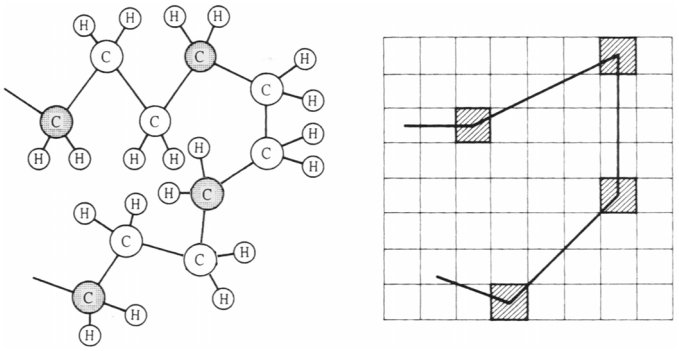

FIG. 79: Monte Carlo of a polymer – the bond fluctuation model. A single 'effective' bond in the model (right) consist of three covalent bonds along the chain of the real polymer molecule (left).

The simplest type of simulation of such a polmer chain is a *random walk*. Here, the chain grows in a random direction until the desired length is achieved. The first implementation does not consider the excluded volume of the previous segments, and the chain is free to cross itself. It is possible to evaluate various structural properties with this model, by averaging the results over many 'simulations.' For instance, the end-to-end distance R_n and the radius

of gyration s_n are obtained for a chain composed of n bonds with length l as

$$\begin{aligned} \left\langle R_n^2 \right\rangle_0 &= n \cdot l^2 \\ \left\langle s^2 \right\rangle_0 &= \left\langle R_n^2 \right\rangle / 6 \end{aligned} \tag{XII.5}$$

While the missing description of excluded volume may seem to be a serious flaw at the first sight, this may not be always the case. In the so-called theta state, the effects of excluded volume and attractive interactions within the polymer and between the polymer and the solvent exactly cancel (also, the second virial coefficient vanishes), and the expressions derived with the simple random walk are actually valid. (The calculated parameters are often designated with the subscript '0').

The excluded volume can be taken into account by not allowing the chain to extend to the already occupied lattice points – *self-avoiding walk* (Fig. 80). This model was used to generate *all* possible configurations of a polymer of given length, in order to evaluate the partition function leading to all thermodynamic properties. The 'potential energy' may be calculated with a reasonable model of interaction of the nearby monomer units. Also, it is possible to consider copolymers consisting of two different types of monomer units. Extreme attention has been paid to the structural properties again; an example result is the end-to-end distance in a limit of large number of elements of

$$\left\langle R_n^2 \right\rangle \approx n^{1.18} \cdot l^2 \tag{XII.6}$$

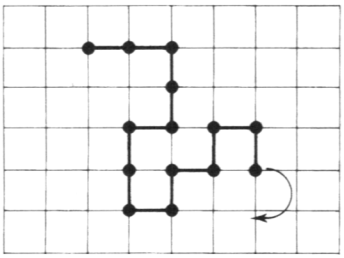

FIG. 80: Monte Carlo of a polymer – self-avoiding walk.

While it need not be difficult to generate a configuration of the polymer chain, it can be nearly impossible to modify this configuration e.g. with a MC engine, especially for densely packed polymers. A widely used algorithm in MC simulations, which is not limited to lattice models, is the *slithering snake* model. Here, one end of the polymer chain is randomly chosen as the head, and an attempt is made to connect a new monomer unit to it. If the attempt

is successful, one monomer is removed from the other end. The whole procedure is then repeated.

A natural way to improve the lattice models is to leave the lattice. The simplest of such 'continuous' polymer models consists of a string of connected beads (particles), which are freely connected and interacting with each other with a spherically symmetric potential (like Lennard-Jones). Note that the beads do not generally correspond to monomer units and so the links are not the chemical bonds between monomers. The links may be either of fixed length or free to vary with a harmonic potential.

The most unrealistic property of such a model is continuous variation of link angles. The *freely rotating chain model* improves this behavior by holding the link angles fixed while allowing free rotation about the links (i.e. continuous variation of 'dihedral angles'). Obviously, this will affect the overall structure of the polymer chain compared to the freely connected one; the characteristic ratio

$$C_n = \frac{\langle R_n^2 \rangle}{n \cdot l^2} \tag{XII.7}$$

indicating the extension of the chain will converge to the value of

$$C_\infty = \frac{1 - \cos\theta}{1 + \cos\theta} \tag{XII.8}$$

with bond angle θ. For instance, $C_\infty \approx 2$ for a tetrahedral bond angle of 109°.

The *rotational isomeric state model* (RIS) by Flory (1969) improves the description by allowing every link to adopt only one of a defined set of rotational states (i.e. dihedral angles). These states usually correspond to minima of potential energy, for instance the trans, gauche(+) and gauche(-) conformations for a polyalkane chain. An elegant feature of the model is that it uses various matrices to described conformation-dependent properties. RIS is the best known one of the 'approximative' ways to describe polymer chains. It can be conveniently combined with MC simulation to estimate a wide range of properties. In such a simulation, conformations of the chain are generated with probability distributions corresponding to their statistical weights, which are a component of the RIS model (in a matrix form). With u_{ab} being the statistical weight of dihedral state b following a link in the dihedral state a, the matrix of statistical weights for an example of polyalkane chain may

look like this:

$$U \equiv \begin{pmatrix} u_{tt} & u_{tg^+} & u_{tg^-} \\ u_{g^+t} & u_{g^+g^+} & u_{g^+g^-} \\ u_{g^-t} & u_{g^-g^+} & u_{g^-g^-} \end{pmatrix} = \begin{pmatrix} 1.00 & 0.54 & 0.54 \\ 1.00 & 0.54 & 0.05 \\ 1.00 & 0.05 & 0.54 \end{pmatrix} \tag{XII.9}$$

Starting on one end of the chain, a conformation is generated by calculating the dihedral angles sequentially, until the whole chain is done. The probability of each dihedral angle is determined by the a priori probabilities of the dihedral states and on the state of the previous dihedral angle; a Monte Carlo engine is then used to select one of the values.

In a typical study, a large number of such chain will be grown, and the properties of interest will be calculated for each of them and averaged. The RIS-MC approach can be used to estimate properties like pair correlation functions (for atoms within the polymer chain), scattering functions and the force–elongation profiles.

Black-and-white figures were reprinted from Leach, Molecular Modelling.